Interactions between non-prion and prion domains of Rnq1 direct formation of amyloid vs liquid-like aggregates and create transmission barriers

Short title:

Interactions between prion and non-prion domains of Rnq1

Sangeun Park[1], Dania M. Maldonado[1], Michele L. Kadnar[2], Monica Andrade[2, #a], Anna P. Fomitchova[2, #b], Susan W. Liebman[1], Irina L. Derkatch[1,2,*]

[1] Department of Pharmacology, University of Nevada Reno, Reno, Nevada, United States of America

[2] Department of Microbiology, New York University School of Medicine, New York, New York, United States of America

[#a] Current address: Department of Biological and Vision Sciences, College of Optometry, State University of New York, New York, New York, United States of America

[#b] Current address: New York Medical College / New York Metropolitan Hospital, New York, New York, United States of America

* Corresponding Author:

E-mail: iderkatch@unr.edu

Abstract

Prions are self-propagating protein conformations usually existing as amyloid aggregates. [*PIN*$^+$], a prion form of the Rnq1 protein occasionally found in wild and laboratory yeast strains, facilitates both the *de novo* formation and destabilization of other yeast prions, and affects aggregation and toxicity of human misfolding disease proteins expressed in yeast. Rnq1 contains a short N-terminus with no confirmed function (the non-prion domain, NPD) and a C-terminus that carries four QN-rich regions and is sufficient for [*PIN*$^+$] formation and maintenance (prion domain, PD). In the current study, a genetic screen identified the NPD T27P mutation that blocks transmission of the [*PIN*$^+$] prion state from wild type Rnq1 (Rnq1$_{WT}$) to mutant Rnq1$_{T27P}$. The mutation doesn't prevent Rnq1$_{T27P}$ from switching to a prion state when overexpressed *in vivo*, or from forming amyloid fibers *in vitro*. Furthermore, like [*PIN*$^+_{WT}$], the newly formed [*PIN*$^+_{T27P}$]s promote the *de novo* appearance of the Sup35-based prion [*PSI*$^+$]. We conclude that the NPD mutation creates a barrier for prion transmission from [*PIN*$^+_{WT}$] to Rnq1$_{T27P}$. Because fluorescence microscopy shows that Rnq1$_{T27P}$ efficiently joins [*PIN*$^+_{WT}$] aggregates, the barrier is likely due to the inability of Rnq1$_{T27P}$ to propagate the specific [*PIN*$^+_{WT}$] conformational variant. Indeed, the analysis of [*PIN*$^+_{T27P}$]s resulting from rare transmission events from [*PIN*$^+_{WT}$] indicates that these [*PIN*$^+_{T27P}$]s must undergo conformational adaptation to yield more stable prion variants. Deletion analysis revealed that T27P constrains prion conformations through the first two QN-rich regions within the PD. The finding that Rnq1$_{T27P}$-YFP readily forms non-amyloid liquid-like droplets, which Rnq1$_{WT}$-YFP does not form, supports the idea that the NPD affects aggregation properties of the PD. We propose that these aggregation properties are essential for Rnq1's functions, such as controlling aggregation of other proteins. This provides new insight into the role of heterologous proteins and transmission barriers in the origins of protein misfolding diseases.

Keywords: yeast, prion, prion variant, prion strain, amyloid, liquid-like droplets, transmission barrier, Rnq1, [*PIN*$^{+}$], [*RNQ*$^{+}$], Sup35, [*PSI*$^{+}$].

Abbreviations: NPD – non-prion domain, PD – prion domain, WT – wild type, GuHCl- guanidine hydrochloride, 5-FOA - 5-fluoroorotic acid, aa – amino acid, YFP – Yellow Fluorescent Protein, CFP – Cyan Fluorescent Protein, EV – empty vector, TEM – transmission electron microscopy, ThT - thioflavin T, Hex - 1,6 hexanediol –, RT - room temperature, HFIP - 1,1,1,3,3,3 hexafluoroisopropanol.

Author Summary

Proteins must fold into the right shapes to work properly. Sometimes they fold incorrectly and stick together, forming long fiber aggregates that damage cells. This kind of “protein misfolding” causes human diseases such as Alzheimer’s. Certain yeast proteins behave similarly, making them useful to study this process. We investigate a yeast protein called Rnq1, which has a region that helps it misfold into fibers. These fibers can also cause other, unrelated proteins to misfold. We found that a mutation in a different part of Rnq1— outside the aggregation region — reduces the ability of non-mutant Rnq1 fibers to convert mutant Rnq1 into growing fiber aggregates. We also identified which section of the aggregation region is affected by this mutation. Interestingly, although the rarely converted mutant aggregates grow poorly at first, they can eventually “adapt” into a shape that grows better. The same mutation also pushes Rnq1 to form liquid-like droplets instead of fibers. Our findings show that the non-aggregating part of Rnq1 controls how Rnq1 aggregates, and, consequently, the appearance and elimination of aggregates formed by other proteins. Our work also helps explain how barriers to misfolded protein growth can be overcome, which is relevant to understanding human protein misfolding diseases.

73 # Introduction

74 The prion hypothesis postulates that some proteins can acquire stable unconventional
75 conformations and pass these conformations to newly synthesized molecules with the same
76 primary sequence. Amyloid, the β-sheet-rich fibers with protein molecules stacked on top of one
77 another, is the structural basis for most prions and prion-like self-propagating protein
78 conformations (Chuang et al., 2018; Dobson, 2017; Ke et al., 2020). Prions and amyloids
79 attracted attention due to their connection to the so-called protein misfolding diseases that are
80 associated with the formation of amyloid aggregates. The list of such diseases is expanding
81 quickly from *bona fide* prion diseases, such as scrapie in sheep, mad cow disease in cattle, and
82 Creutzfeldt-Jakob disease (CJD) in humans, which prompted the development of the paradigm
83 of protein-based inheritance, to much more common neurodegenerative diseases, such as
84 Alzheimer's and Parkinson's, as well as type 2 diabetes and, possibly, cancer (Ayers et al., 2020;
85 Joshi and Ahuja, 2023).

86 Many protein misfolding diseases can be both sporadic, usually with a later age of onset,
87 and hereditary, e.g. due to mutations in amyloid-forming proteins. This underscores the
88 importance of uncovering the cellular mechanisms that drive and inhibit protein misfolding, as
89 well as the control of conformational changes within specific aggregation-prone proteins that lead
90 to disease-related aggregation. Prion diseases can also be infectious. Luckily, protective
91 measures were stepped up in recent decades to prevent iatrogenic human to human
92 transmission. Animal to human transmission is usually prevented by transmission barriers when
93 differences in primary sequences of protein homologs from different species make interspecies
94 transmission of the prion state inefficient (Beringue et al., 2008). However, as we learned from
95 the appearance of a novel human disease resulting from a cross of the transmission barrier
96 between cattle and humans, variant Creutzfeldt-Jakob disease (vCJD), such barriers may not be

97 strong enough (Houston and Andreoletti, 2019). An important aspect of the problem is possible
98 rapid adaptation of prion conformations in a new host after rare across-the-barrier transmission
99 events (Weissman, 2012). Also, across-the-barrier transmission leads to forms of disease with
100 distinct clinical manifestations compared to sporadic and hereditary diseases, like in the case of
101 sporadic CJD and vCJD transmitted from cattle (Igel-Egalon et al., 2018).

102 Prion research has been greatly facilitated by the discovery of naturally occurring prions
103 in the yeast *Saccharomyces cerevisiae* (Wickner, 1994; Liebman and Chernoff, 2012;
104 Zhouravleva et al., 2023). The same underlying amyloid structure of yeast prions and human
105 disease-related aggregation-prone proteins, as well as evolutionary conservation of genes
106 makes yeast an excellent model for studying protein aggregation and mechanisms that control it.
107 Many yeast prions carry long terminally located QN-rich domains that are unfolded in soluble
108 proteins but are required and sufficient for taking on prion conformations and maintaining them.
109 Hence their name – prion domains (PDs). Similar QN-rich or expanded polyQ domains also drive
110 aggregation of some human disease proteins (Fuenteabla et al., 2010; Lieberman et al., 2019).
111 [*PSI*$^+$], the prion form of a translation termination factor Sup35 (eRF3), is the most extensively
112 studied yeast prion, and many important findings come from the [*PSI*$^+$] prion research (Liebman
113 and Chernoff, 2012). One such finding is prion-prion interactions (Derkatch and Liebman, 2007).
114 Initially, it was postulated that overexpression of a prion-forming protein should induce the *de*
115 *novo* appearance of its respective prion conformation because increased protein concentration
116 makes switching to a prion state more likely (Wickner, 1994). It was further postulated that if a
117 prion is lost or cured from the cell, it should re-appear in the cell's progeny either rarely
118 spontaneously or frequently upon overexpression of the prion-forming protein (*ibid.*). Initial data
119 for [*PSI*$^+$] appeared to support these postulates (Derkatch et al., 1996). However, once [*PSI*$^+$]
120 was eliminated by the addition to yeast culture media of low concentrations of guanidine
121 hydrochloride (GuHCl), a generic yeast prion curing agent, efficient induction of [*PSI*$^+$] by Sup35

122 overexpression was no longer possible. This was because the treatment also cured the
123 previously unknown [*PIN*$^+$] prion required for induction of [*PSI*$^+$] (Derkatch et al., 1997).
124 [*PIN*$^+$] is formed by the Rnq1 protein (Sondheimer and Lindquist, 2000; Derkatch et al.,
125 2001). Rnq1 consists of a short N-terminal domain with no confirmed function (the non-prion
126 domain, NPD, aa 1-132; Fig 1A) and a C-terminal QN-rich domain sufficient for [*PIN*$^+$] formation
127 and maintenance (prion domain, PD; aa 132-405). The prion domain of Rnq1 is complex. It
128 carries four discrete QN-rich regions. None of these alone is essential for [*PIN*$^+$] prion
129 maintenance, and any two are sufficient (Kadnar et al., 2010). Also, bacterially expressed
130 purified Rnq1 fragments carrying NPD with only QN2, QN3 or QN4 form amyloid fibers *in vitro*
131 (*ibid.*). The QN1 region is very short and does not form amyloid when attached to the Rnq1 NPD,
132 but synthetic QN1 peptide does form amyloid fibers (*ibid.*). The [*mini-PIN*$^+$]s formed by Rnq1
133 fragments with different combinations of QN-rich domains are all able to promote the *de novo*
134 formation of [*PSI*$^+$] upon Sup35 overproduction, *i.e.* no specific QN-rich region of Rnq1's PD is
135 essential for this prion-prion interaction (*ibid.*).
136 Beyond promoting the *de novo* formation of [*PSI*$^+$], [*PIN*$^+$] is involved in other prion-prion
137 interactions, both positive and negative. For example, [*PIN*$^+$] also facilitates the *de novo*
138 appearance of the [*URE3*] and [*SWI*$^+$] prions with QN-rich PDs, even though the presence of
139 [*PIN*$^+$] is not a requirement (Bradley et al., 2002; Du et al., 2017), as well as some artificial prions
140 (Borkhsenius et al., 2002) and the [HET-s]$_Y$ prion formed in yeast by the *Podospora anserine*
141 prion-forming protein Het-s with a non-QN-rich PD (Taneija et al., 2007). [*PIN*$^+$] also interacts
142 with non-prion aggregation-prone proteins, such as human Huntington's and Machado-Joseph
143 disease-associated proteins with expanded polyQ stretches (Osherovich and Weissman, 2001;
144 Meriin et al., 2002) and TDP-43 associated with amyotrophic lateral sclerosis, frontotemporal
145 dementia and limbic-predominant age-related encephalopathy (Park et al., 2017). An example of
146 negative interactions is the mutual inhibition of stable inheritance by certain [*PSI*$^+$] and [*PIN*$^+$]

147 prion variants: some weak [*PSI*$^+$] variants are very unstable in the presence of some “single dot”
148 [*PIN*$^+$] variants, while some strong [*PSI*$^+$] variants destabilize some “single dot” [*PIN*$^+$]s (Bradley
149 and Liebman, 2003; Mathur et al., 2009; Villali et al., 2020). Yet another type of interaction is a
150 dramatic enhancement by [*PIN*$^+$] of the [*SWI*$^+$]-associated nonsense suppression in the strains
151 lacking Sup35 PD (aka [*NSI*$^+$], Nizhnikov et al., 2016).

152 Like other prions, [*PIN*$^+$] depends on chaperone proteins for its maintenance. Some of
153 these interactions are common with most other prions. For example, lack of the Hsp104
154 disaggregase cures [*PIN*$^+$], as well as [*URE3*], [*PSI*$^+$], and [*SWI*$^+$] (Chernoff et al., 1995; Derkatch
155 et al., 1997; Moriama et al., 2000; Du et al., 2008), likely because Hsp104 promotes
156 conformational changes in prion aggregates and is needed to break growing prion aggregates to
157 create smaller seeds that can be transmitted to daughter cells (Chernoff et al., 1995; Wegrzyn et
158 al., 2001; Sapute-Krishnan et al., 2007). However, some prion-chaperone interactions are
159 specific for a particular prion: the same chaperone can affect the formation of one prion but not
160 others, and some chaperones have opposite effects on different prions (Barbitoff et al., 2022).
161 [*PIN*$^+$] has a highly specific interaction with Sis1, an Hsp40 co-chaperone of Hsp70 chaperones:
162 not only does [*PIN*$^+$] critically depend on Sis1 for maintenance (Sondheimer et al., 2001), but
163 Sis1 is present in [*PIN*$^+$] aggregates in equimolar amounts with Rnq1 (Lopez et al., 2003). In
164 Sis1, the region critical for [*PIN*$^+$] maintenance is within the G/F region that is not needed for the
165 maintenance of other prions (Lopez et al., 2003). In Rnq1, the major site for interaction with Sis1
166 is located not in the PD, but in the NPD, in the LGKLALI sequence (Douglas et al., 2008).

167 Strikingly, most prion-forming proteins, including PrP in mammals and Rnq1, Sup35, and
168 Ure2 in yeast, can form not just one but multiple prion variants (or prion strains) that differ in
169 numerous prion-associated phenotypes (Bessen and Marsh, 1992; Bessen et al., 1995; Derkatch
170 et al., 1996; Bradley et al., 2002; Schlumpberger et al., 2001). These prion variants manifest
171 different conformations of prion-forming proteins in prion aggregates thus leading to differences

172 in aggregate size, sensitivity to cellular chaperones and interactions with other prions *in vivo*, as
173 well as in stability of corresponding amyloids *in vitro* (see above). Extensive studies of mutations
174 within the Sup35 PD demonstrate that its primary sequence affects its conformational flexibility in
175 terms of what [*PSI*$^{+}$] strains the mutant protein can maintain (DePace, 1998; Chang et al., 2008;
176 Bateman and Wickner, 2013).

177 Here we show that in Rnq1 the NPD is involved in determining the conformational
178 flexibility of its PD and its ability to form particular amyloid variants and non-amyloid aggregates.
179 Our findings are consistent with the hypothesis that the cellular function of the Rnq1 NPD is to
180 regulate the aggregation of its PD and, through this aggregation, to control aggregation and
181 disaggregation of other prions and prion-like aggregates.

182

183 Results

184 Genetic screen for *RNQ1* mutations leading to a Pin^{-} phenotype

185 Our goal was to investigate the structure-function organization of the Rnq1 protein in terms of its
186 ability to maintain the [*PIN*$^{+}$] prion and to facilitate the induction of the heterologous [*PSI*$^{+}$] prion.
187 Our approach was to screen for *RNQ1* mutant alleles (*RNQ1*$_{MUTANT}$) that, when substituted for
188 wild type *RNQ1 (RNQ1*$_{WT}$) in a [*PIN*$^{+}$] strain (Pin^{+} phenotype), lead to a Pin^{-} phenotype. The Pin
189 phenotype was scored by examining the *de novo* appearance of the [*PSI*$^{+}$] prion upon transient
190 high-level expression of the PD of the [*PSI*$^{+}$] prion forming protein Sup35 fused to YFP,
191 Sup35NM-YFP. The Pin^{+} *vs* Pin^{-} phenotype was assigned, respectively, when [*PSI*$^{+}$] appearance
192 was detected *vs* not detected.

193 The screen is schematically shown in Fig 1B. **First**, *CEN LEU2* plasmids carrying PCR-
194 mutagenized *RNQ1* driven by its native non-mutagenized promoter and followed by its native
195 non-mutagenized terminator sequence were transformed into a [*PIN*$^{+}$][*psi*$^{-}$] strain where the

196 chromosomal copy of *RNQ1* was deleted and [*PIN*$^+$] was maintained by a similar *RNQ1*$_{WT}$
197 plasmid (*CEN URA3*). The strain also carried the *CEN HIS3* plasmid with the *SUP35NM-YFP*
198 [*PSI*$^+$] inducing construct controlled by the *GAL* promoter, and the *ade1-14* mutation allowing for
199 [*PSI*$^+$] detection. Transformants were selected on and then patched onto synthetic media
200 selective for all plasmids, thus allowing for ~20 generations of co-expression of Rnq1$_{WT}$ and
201 Rnq1$_{MUTANT}$. **Second**, after two passages on media selective for only the mutagenized *RNQ1*
202 and [*PSI*$^+$] inducing plasmids, the *RNQ1*$_{WT}$ maintainer plasmid was shuffled out on media
203 supplemented with 5-FOA and selective for the other two plasmids. **Third**, [*PSI*$^+$] was induced by
204 high-level expression of Sup35NM-YFP on SGal-LeuHis media. **Fourth**, cells carrying [*PSI*$^+$]
205 were selected on non-inducing media lacking adenine and not selective for plasmids. Selection
206 of [*PSI*$^+$] cells on adenineless media is based on nonsense suppression of the *ade1*-14 (UGA)
207 mutation due to the recruitment of the Sup35 protein, a translation termination factor, into the
208 [*PSI*$^+$] prion aggregates. For Pin$^+$ cultures, thick, even if heterogeneous, growth was observed
209 over the entire patch. For the presumptive Pin$^-$ cultures, either no growth or rare Ade$^+$ colonies
210 were observed on media lacking adenine. In such cultures, the Pin$^-$ phenotype was confirmed by
211 colony purifying yeast from the inducing SGal-LeuHis media onto YPD, where [*PSI*$^+$] Ade$^+$ cells
212 form pink or white colonies that are clearly distinct from red Ade$^-$ colonies formed by [*psi*$^-$] cells.
213 Finally, the Pin$^-$ phenotype was confirmed by fluorescence microscopy of cells grown on the
214 [*PSI*$^+$] inducing galactose media using the YFP-tagged Sup35NM as a reporter for the lack of
215 Sup35 aggregation. In Pin$^+$ cultures the appearance of [*PSI*$^+$] is visualized as ring- or dot-like foci,
216 while in [*psi*$^-$] cells Sup35NM fluorescence is evenly distributed (Patino and Lindquist, 1996;
217 Zhou et al., 2001). To confirm that the Pin$^-$ phenotype was due to a mutation in the shuffled-in
218 *RNQ1* gene, *RNQ1*$_{MUTANT}$ plasmids were isolated from each candidate mutant, individually re-
219 transformed back into the yeast strain used for the original screen, and tested according to the

220 same scheme (see Materials and Methods for additional approaches used to improve the
221 candidate pool).
222 Approximately 12,000 yeast transformants were screened and 54 were either firmly Pin$^-$,
223 or their Pin phenotype was dramatically reduced. 53 of these carried plasmids with either
224 nonsense or frameshift *RNQ1* mutations. All nonsense mutations and most frameshifts were
225 located in the N-terminal part of *RNQ1*, either within its NPD, or before the end of the second
226 QN-rich domain within the PD (QN2, see Fig 1A). All five unique frameshift mutations that were
227 located downstream of QN2 led to long C-terminal extensions due to out-of-frame translation.
228 The only missense mutant that passed the screen carried the T27P (ACA ⇨ CCA) mutation in
229 the beginning of the Rnq1 NPD (Fig 1A; also see Fig 2B).
230 Identification in the screen of constructs synthesizing only the NPD or part of it was
231 expected because of the requirement of the PD of Rnq1 for the maintenance of the [*PIN*$^+$] prion
232 (Vitrenko et al., 2007a; Kadnar et al., 2010). The fact that no nonsense mutations were detected
233 beyond the second QN-rich region can be explained based on our earlier deletion analysis of
234 Rnq1 (Kadnar et al., 2010): the QN-rich regions within Rnq1 PD are redundant in their ability to
235 acquire the [*PIN*$^+$] prion state from Rnq1$_{WT}$ and maintain the Pin$^+$ phenotype (i.e. allow for [*PSI*$^+$]
236 induction). Specifically, the N-terminal Rnq1 fragments including at least QN1 and entire QN2
237 were sufficient to maintain Pin$^+$, so mutants retaining these regions were not expected to pass
238 the screen. However, deletion analysis also indicated that the C-terminal location of the QN2
239 region in the truncated construct carrying only QN1 and QN2 was important for the transfer of
240 [*PIN*$^+$] from Rnq1$_{WT}$ (*ibid*), so the identification of frameshifts leading to long extensions
241 downstream of QN2 is also not surprising. Finally, the fact that we have not identified PD-located
242 missense mutations can also be explained by the structural redundancy of the Rnq1 PD: a single
243 mutation that would just inactivate one of the four QN-rich regions is unlikely to block [*PIN*$^+$]
244 propagation or the ability of the mutant to promote [*PSI*$^+$] induction.

245 **The inability to induce nonsense suppression in cultures where Rnq1$_{T27P}$ was**
246 **substituted for Rnq1$_{WT}$ is due to the dramatic reduction in the ability to induce**
247 **[*PSI*$^+$]**

248 For all experiments described here and below, we used plasmids with the T27P mutation
249 introduced by site-directed mutagenesis, to exclude the possibility that additional mutations in the
250 regions we did not sequence outside of the *RNQ1* gene may have contributed to the Pin$^-$
251 phenotype during the screen. We also reasonably excluded the possibility that the absence of
252 [*PIN*$^+_{T27P}$] in most post-shuffle Rnq1$_{T27P}$ cells was due to insufficient Rnq1$_{T27P}$. Although there is
253 an ~2-fold difference in protein abundance between Rnq1$_{T27P}$ and Rnq1$_{WT}$ (Fig 2A) this is unlikely
254 to be the main reason for the prion loss because (i) [*PIN*$^+_{WT}$] is 100% stable in diploids
255 heterozygous for *RNQ1* deletions (Derkatch et al., 2001) and (ii) a similar reduction in
256 abundance compared to full-length Rnq1$_{WT}$ does not destabilize mini-[*PIN*$^+$]s maintained by
257 Rnq1 fragments (Kadnar et al., 2010).

258 The goal for further experiments was to understand what leads to the loss of the Pin$^+$
259 phenotype of the *rnq1-Δ* yeast cultures expressing Rnq1$_{T27P}$ after the elimination of Rnq1$_{WT}$. As
260 can be seen on Fig 2B, the cultures expressing Rnq1$_{T27P}$ were almost Pin$^-$ compared to the
261 positive control expressing Rnq1$_{WT}$. However, compared to the negative control where Rnq1$_{WT}$
262 was substituted with the empty vector (EV), there were occasional Ade$^+$ colonies on adenineless
263 media on the Rnq1$_{T27P}$ patches. Out of 24 such Ade$^+$ microcolonies from six independent
264 Rnq1$_{T27P}$ transformants, 23 were [*PSI*$^+$] according to the GuHCl test. The fluorescence analysis
265 of Ade$^+$ cultures that retained the *GAL-SUP35NM-YFP* plasmid revealed dot-like foci in most
266 fluorescent cells in all eight cultures examined, and these foci were indistinguishable from [*PSI*$^+$]
267 foci in the control Rnq1$_{WT}$ cultures. Thus, the Ade$^+$ colonies in the cells expressing Rnq1$_{T27P}$ after

268 shuffle were due to [*PSI*$^+$]s, so [*PSI*$^+$] induction was not blocked completely due to the T27P
269 mutation.

270 We then asked whether the [*PSI*$^+$] induction was indeed ~50-100-fold less frequent in the
271 Rnq1$_{T27P}$ *vs* the Rnq1$_{WT}$ cultures, as it appeared, or alternatively it was close to normal levels but
272 most newly forming [*PSI*$^+$]s were not detected in the assay based on the ability of [*PSI*$^+$] cells to
273 grow on adenineless media. This could happen for five reasons. (1) Most [*PSI*$^+$] variants forming
274 in cells carrying [*PIN*$^+_{T27P}$] are "very weak" and unable to ensure robust growth on adenineless
275 media. Indeed, some [*PIN*$^+$] variants promote induction of predominantly weak [*PSI*$^+$]s (Sharma
276 and Liebman, 2013). (2) Most [*PSI*$^+$]s promoted by [*PIN*$^+_{T27P}$] are highly unstable and are lost
277 during the first few cell divisions. Indeed, some [*PSI*$^+$] variants are permanently unstable
278 (Sharma and Liebman, 2012), and some [*PIN*$^+$] variants are known to destabilize weak [*PSI*$^+$]s
279 they induce (Bradley and Liebman, 2003). (3) In [*PIN*$^+_{T27P}$] cells, most newly forming Sup35
280 aggregates do not mature into [*PSI*$^+$] or are lost in the absence of Sup35 overexpression. Such
281 [*PSI*$^+$] variants have been described by Salnikova et al. (2005). (4) Most [*PSI*$^+$]s in [*PIN*$^+_{T27P}$]
282 cultures are extremely toxic and lead to cell death on the Sup35NM-YFP inducing media, prior to
283 transfer to adenineless media where Sup35NM-YFP is no longer expressed. Indeed, growth of
284 [*PSI*$^+$] cells is inhibited by Sup35 overexpression in a [*PSI*$^+$] variant-specific manner (Derkatch et
285 al., 1996). (5) Most [*PSI*$^+$]s induced in [*PIN*$^+_{T27P}$] are toxic even in the absence of Sup35NM-YFP
286 expression. Such "killer" [*PSI*$^+$]s have also been described (McGlinchey et al., 2011).
287 Experiments discussed below essentially exclude all these possibilities.

288 To assess the strength of [*PSI*$^+$] variants induced in cells expressing Rnq1$_{WT}$ and
289 Rnq1$_{T27P}$, yeast scraped up from patches incubated on SD-Ade media at 20^{0}C for ~25 days after
290 [*PSI*$^+$] induction were colony purified on YPD, and individual colonies were randomly picked for
291 further analysis. Incubation at low temperature promotes nonsense suppression in weaker [*PSI*$^+$]
292 variants (Derkatch et al., 1996) and prolonged incubation, in our experience, allows even the

293 weakest [*PSI*$^+$]s to form microcolonies. We found that similar arrays of [*PSI*$^+$] variants were
294 induced in the presence of Rnq1$_{WT}$ and Rnq1$_{T27P}$, with no prevalence for weak [*PSI*$^+$]s in the
295 Rnq1$_{T27P}$ cultures. Specifically, moderate [*PSI*$^+$]s constituted 85% and 91%, weak [*PSI*$^+$]s – 6%
296 and 6%, and strong [*PSI*$^+$]s – 10% and 3% for Rnq1$_{WT}$ and Rnq1$_{T27P}$, respectively (Table S1).
297 The slightly smaller percentage of strong [*PSI*$^+$] variants induced in Rnq1$_{T27P}$ cells was not
298 statistically significant (p>0.1) and could not explain the large difference in the Pin phenotype.
299 Furthermore, the dramatically reduced Pin$^+$ phenotype in the Rnq1$_{T27P}$ after-shuffle
300 cultures was not due to extremely weak (essentially Ade$^-$) or highly unstable [*PSI*$^+$] variants. To
301 test this, yeast were colony purified directly from the [*PSI*$^+$] inducing galactose media onto YPD.
302 Only ~0.7% of >5,000 colonies originating from 12 independent *RNQ1$_{T27P}$* transformants were
303 white or pink, and most of these colonies were [*PSI*$^+$] based on the GuHCl test and, also, the
304 Sup35 aggregation test for those that retained the *SUP35NM-YFP* plasmid. The color of pink
305 colonies and their ratio to white colonies was similar to that in the positive control cultures with
306 *RNQ1$_{WT}$* shuffled-in where white and pink (and [*PSI*$^+$]) colonies constituted ~20%. In the negative
307 control cultures with EV shuffled-in, the rare (<0.1%) non-red colonies were usually white and not
308 [*PSI*$^+$]. This is consistent with results shown in Fig 2B. Importantly, no dark pink colonies
309 indicative of very weak [*PSI*$^+$] were detected in Rnq1$_{T27P}$ cultures, and analysis of all slightly
310 lighter shade of red colonies (~30) showed that they were not [*PSI*$^+$]. In addition, fluorescence
311 microscopy of ~40 typical red colonies retaining *GAL-SUP35NM-YFP* did not reveal any [*PSI*$^+$]s.
312 Finally, no increase of the proportion of sectored white/red or pink/red [*PSI*$^+$] colonies was
313 detected for Rnq1$_{T27P}$ compared to Rnq1$_{WT}$. The fact that newly forming [*PSI*$^+$]s are frequently
314 unstable is well-known, so the presence of some sectored colonies was expected (Sharma and
315 Liebman, 2012). All potentially sectored colonies in Rnq1$_{T27P}$ cultures yielded stable [*PSI*$^+$]s upon
316 further analysis. Altogether, these experiments exclude possibilities (1) and (2) from the list
317 above.

318 Fluorescence microscopy of aggregate formation upon high expression of Sup35NM-YFP
319 was used to record the initial steps of [*PSI*$^+$] formation. In the after-shuffle Rnq1$_{T27P}$ cultures only
320 ~2.5% cells had aggregates (Table 1; Fig 2C). This is significantly less compared to Rnq1$_{WT}$
321 (~57%) and significantly more compared to EV (<0.01%). Both ring-, line- and dot-shaped foci
322 were detected in the *RNQ1$_{T27P}$* carrying cells, and these foci were not distinguishable from those
323 in cells with *RNQ1$_{WT}$*. The presence of dot-like foci indicative of mature [*PSI*$^+$] and occasional
324 mother-daughter pairs with aggregates in both cells indicated that newly forming Sup35
325 aggregates were heritable in the Rnq1$_{T27P}$ expressing cells. Also, there was no indication of
326 increased cell toxicity in cells co-expressing Rnq1$_{T27P}$ and Sup35NM-YFP: no abnormally shaped
327 elongated cells, no increase in the proportion of non-fluorescent cells, and no growth inhibition
328 compared to the Rnq1$_{WT}$ control (Fig S1). Finally, in the [*PSI*$^+$]s induced in the Rnq1$_{T27P}$
329 expressing cells, maintenance of the *LEU2 RNQ1$_{T27P}$* and *HIS3 GAL-SUP35NM-YFP* plasmids
330 was not reduced compared to the maintenance of *LEU2 RNQ1$_{WT}$* and *HIS3 GAL-SUP35NM-YFP*
331 in the [*PSI*$^+$]s induced in the Rnq1$_{WT}$ cells (see description of [*PSI*$^+$] isolation above and Table
332 S1). Together, these experiments exclude possibilities (3), (4), and (5) above.
333 In summary, the cultures expressing Rnq1$_{T27P}$ have a dramatically reduced but otherwise typical
334 Pin$^+$ phenotype.

335 **Table 1. Analysis of Sup35NM-YFP aggregation in *RNQ1$_{T27P}$* cells after shuffling out the**
336 ***RNQ1$_{WT}$* plasmid indicates low-level [*PSI*$^+$] induction.**

Construct after plasmid shuffle	% cells with Sup35NM-YFP aggregates		
	Average	SD	SEM
RNQ1$_{WT}$	56.8	± 14.5	± 3.0
RNQ1$_{T27P}$	2.6	± 3.1	± 0.8
EV	0	NA	NA

337

338 Table 1 Legend. Aggregation of Sup35NM-YFP was analyzed in YID146 cells after
339 substituting the *RNQ1*$_{T27P}$ *LEU CEN* or indicated control constructs for *URA3 CEN*
340 *RNQ1*$_{WT}$ (see Fig 1B and text). To induce the expression of Sup35NM-YFP, yeast
341 passaged on FOA media to eliminate the *URA3 CEN RNQ1*$_{WT}$ plasmid were replica
342 plated onto the SD-LeuHis and then SGal-LeuHis media and incubated for ~48 hours
343 at 30^{0}C. For *RNQ1*$_{WT}$ and *RNQ1*$_{T27P}$, at least 11 vision fields were scored for each
344 construct, ~500 cells total per construct. For EV, no aggregates were detected in
345 ~1,000 cells scored. Based on T-test, differences are statistically significant between
346 Rnq1$_{T27P}$ *vs* Rnq1$_{WT}$ ($p<10^{-13}$), Rnq1$_{T27P}$ *vs* EV ($p<0.005$), and Rnq1$_{WT}$ *vs* EV ($p<10^{-14}$).
347 Qualitative assessment of aggregation in >10,000 cells in the cultures used for
348 quantification further confirmed the difference between the *RNQ1*$_{T27P}$ and EV: bright
349 ring- or dot-aggregates were readily detected in Rnq1$_{T27P}$ expressing cells, but no ring
350 aggregates were detected in EV cells, where there were only a few dot foci, mostly
351 atypically large. Also, similar observations were made upon qualitative assessments
352 after a shorter (overnight) incubation on SGal-LeuHis and after two passes on this
353 medium for over 4 days.

354

355 **Overexpression of Rnq1$_{T27P}$ induces a heritable Pin$^+$ phenotype indicative of the**
356 **formation of [*PIN*$^+$*$_{T27P}$*]**

357 In general, the *de novo* appearance of prions can be induced by their transient overexpression,
358 and the process of prion aggregate formation can be monitored by microscopy by attaching a
359 fluorescent tag to a prion forming protein (Zhou et al., 2001). However, Rnq1$_{WT}$ does not form *de*
360 *novo* [*PIN*$^+$] aggregates upon overexpression when attached to a C-terminal GFP family tag

361 (Derkatch et al., 2001), so a negative result for $Rnq1_{T27P}$ would not be informative. Thus, the *de*
362 *novo* induction of [PIN^{+}_{T27P}] and [PIN^{+}_{WT}] was attempted by overexpressing, respectively, the
363 **untagged** $Rnq1_{T27P}$ and $Rnq1_{WT}$ driven by the inducible *CUP* promoter and scoring for the Pin^{+}
364 phenotype by [PSI^{+}] induction upon high-level expression of Sup35NM-YFP.
365 For the first experiment (Fig 3A), the *CEN URA3* plasmids carrying either the *CUP-*
366 $RNQ1_{T27P}$ or $CUP\text{-}RNQ1_{WT}$ inserts, or just the empty *CEN URA3* vector, were introduced into a
367 [pin^{-}][psi^{-}] *rnq1-Δ* strain already carrying the *HIS3 GAL-SUP3NM-YFP* [PSI^{+}] inducing construct.
368 Transformants were patched on SD-UraHis media where plasmid-borne constructs were not
369 expressed. Then yeast cultures were replica plated onto the SGal-UraHis supplemented with
370 50μM $CuSO_4$ where $Rnq1_{T27P}$ or $Rnq1_{WT}$ were overexpressed together with Sup35NM-YFP, or
371 on control media where neither or only one of the two constructs was expressed (SD-UraHis,
372 SD-UraHis+50μM $CuSO_4$, and SGal-UraHis). Induction of [PSI^{+}] was scored on adenineless
373 media to which yeast were replica plated from either SGal-UraHis+50μM $CuSO_4$ or control
374 media. Indeed, heterogeneous growth on adenineless media indicative of [PSI^{+}] induction was
375 observed following co-overexpression of Sup35NM-YFP with either $Rnq1_{T27P}$ or $Rnq1_{WT}$, with no
376 obvious effect of the T27P mutation on the efficiency of [PSI^{+}] induction (Fig 3A). The *de novo*
377 formation of [PSI^{+}] was also confirmed by fluorescent microscopy: in cells from the SGal-
378 UraHis+50μM $CuSO_4$ media we observed ring-, line- and dot-shaped Sup35NM-YFP foci
379 indistinguishable in appearance between the $Rnq1_{T27P}$ and $Rnq1_{WT}$ expressing cultures (data not
380 shown). The limitation of this experiment was that it did not allow us to test if the Pin^{+} phenotypes
381 induced by the overexpression of $Rnq1_{T27P}$ and $Rnq1_{WT}$ were heritable, indicative of the
382 formation of, respectively, [$PIN_{T27P}{}^{+}$] and [PIN^{+}_{WT}], or only non-propagating aggregates were
383 formed by one or both constructs.

384 For the second experiment (Fig 3B), the [*pin*$^-$][*psi*$^-$] *rnq1-Δ* strain carrying the *HIS3 CEN*
385 *GAL-SUP3NM-YFP* plasmid was co-transformed with *URA3 CEN CUP-RNQ1*$_{T27P}$ (to be the
386 inducer of the [*PIN*$^+_{T27P}$] prion state) and the *LEU2 CEN* plasmid carrying *RNQ1*$_{T27P}$ under its
387 original promoter (to be the maintainer of this prion state after induction). Control samples were
388 co-transformed with corresponding *RNQ1*$_{WT}$ plasmids (*URA3 CEN CUP-RNQ1*$_{WT}$ and *LEU2*
389 *CEN RNQ1*$_{WT}$), or with empty vectors (*URA3 CEN* and *LEU2 CEN*). The Pin phenotype was
390 scored for by growth on adenineless media after overexpression of Rnq1$_{T27P\ (or\ WT)}$ and *GAL-*
391 *SUP3NM-YFP* induction but with 0 (co-overexpression), 1, 2, 3, or 4 passages on the non-
392 inducing glucose no-copper plasmid-selective media between the Rnq1$_{T27P\ (or\ WT)}$ overexpression
393 and *GAL-SUP3NM-YFP* induction. The efficiency of [*PSI*$^+$] induction was slightly but reproducibly
394 higher in the Rnq1$_{T27P}$ expressing cells compared to Rnq1$_{WT}$ in the nonsense suppression test for
395 most of ~50 co-transformants tested for each set of plasmids, but no statistically significant
396 difference was detected when aggregation was assessed by fluorescent microscopy (not
397 shown). As can be seen in Fig 3B, the Pin$^+$ phenotype of both Rnq1$_{T27P}$ and Rnq1$_{WT}$ expressing
398 cultures became slightly weaker upon subsequent passages on media not supplemented with
399 $CuSO_4$. This is expected considering that newly forming prions are frequently unstable (shown
400 before for spontaneous [*PIN*$^+_{WT}$]s by Derkatch et al. (2000) and newly induced [*PSI*$^+$]s by Zhou
401 et al. (2001)). Important is the retention of the robust Pin$^+$ phenotypes after ~30 generations (4
402 passages) on the no-copper media where Rnq1$_{T27P}$ and Rnq1$_{WT}$ were no longer overexpressed,
403 which is indicative of the formation of heritable [*PIN*$_{T27P}$$^+$] and [*PIN*$^+_{WT}$] prions (for comparison,
404 growth for a similar number of generations on 5mM GuHCl media that inhibits prion propagation
405 is sufficient to completely cure [*PIN*$^+$]). Also important is that Rnq1$_{T27P}$ is not deficient in acquiring
406 such a heritable [*PSI*$^+$]-inducing state compared to Rnq1$_{WT}$.
407

408 **Rnq1$_{T27P}$ forms amyloid fibers *in vitro***

409 Another way to assess the aggregation properties of Rnq1$_{T27P}$ was to test the ability of the
410 bacterially expressed and purified protein to form amyloid fibers *in vitro*. Previously, we found
411 that the fragments of Rnq1$_{WT}$ encompassing the NPD and one or two QN-rich regions of the PD
412 readily formed Thioflavin T (ThT)-binding amyloid fibers with reproducible kinetics and
413 concentration dependence (Kadnar et al., 2010). However, the same assay was much less
414 reproducible for the full-length Rnq1 even though full-length Rnq1 amyloid fibers could be
415 detected by transmission electron microscopy (TEM) similar to fibers formed by shorter Rnq1$_{WT}$
416 fragments (Vitrenko et al., 2007b; Kadnar et al., 2010).

417 Since shorter Rnq1 fragments work better for the ThT-binding assay, the ΔB1C2D3$_{T27P}$
418 construct that carries the Rnq1 NPD, the QG dipeptide repeats, the E helical region and QN4
419 was made and tested alongside the ΔB1C2D3$_{WT}$ (see Fig 1A for the map of the Rnq1 regions).
420 Both proteins ran according to their expected size on SDS-PAGE gels, although ΔB1C2D3$_{T27P}$
421 ran slightly higher than ΔB1C2D3$_{WT}$ (Fig 4A). The same change in mobility was observed for
422 proteins carrying the T27P mutations when they were isolated from yeast, indicative of a
423 conformational alteration due to the mutation even in the soluble state (see Fig 2A). Incubation of
424 both proteins in ThT resulted in a shift of the ThT excitation spectrum and increase of ThT
425 fluorescence at 483 nm, indicative of amyloid formation (Fig 4B). Sigmoidal fluorescence kinetics
426 was consistent with the presence of a rate-limiting nucleation step followed by a fiber growth
427 phase for both ΔB1C2D3$_{T27P}$ and ΔB1C2D3$_{WT}$. The length of the lag phase was concentration
428 dependent. Although there was considerable variation between duplicate samples, all showed
429 sigmoidal kinetics and, at equal protein concentrations, the lag phase was similar for the
430 ΔB1C2D3$_{T27P}$ and ΔB1C2D3$_{wt}$ samples.

431 For TEM, full-length Rnq_{T27P} was used and compared to full-length $Rnq1_{WT}$. Fibers were
432 assembled in the presence of ThT for ~70 hours and an increase of ThT fluorescence was
433 confirmed. TEM revealed >1μm-long non-branched fibers consisting of laterally associated
434 thinner fibrils for both $Rnq1_{T27P}$ and $Rnq1_{WT}$ (Fig 4C). However, the Rnq_{T27P} fibers were less
435 twisted and wider than the $Rnq1_{WT}$ fibers (30 – 50nm *vs* ~ 20nm) indicating a difference in
436 conformation due to the mutation in the amyloid state.
437

438 **The T27P mutation creates a barrier for the transmission of the prion state from**
439 **[*PIN*$^{+}_{WT}$] to $Rnq1_{T27P}$**

440 Next, we tested if the T27P mutation affects the transmission of the prion conformation from
441 $Rnq1_{WT}$ to $Rnq1_{T27P}$. If the transmission block were absolute, all post-shuffle cells expressing
442 $Rnq1_{T27P}$ would be [*pin*$^{-}$]. The incomplete Pin^{-} phenotype observed in our experiments is
443 consistent with either the [*PIN*$^{+}_{T27P}$] prion being absent in most but not all post-shuffle $Rnq1_{T27P}$
444 cells, or with the prion state being transmitted and maintained in $Rnq1_{T27P}$ cells but the mutation
445 making [*PIN*$^{+}_{T27P}$] extremely weak in its ability to induce [*PSI*$^{+}$]. To distinguish between these
446 possibilities, we changed the protocol from the one where the Pin state of the entire post-shuffle
447 cultures was scored (e.g. in Fig 2B) to a protocol testing the Pin phenotype of individual cells in
448 these cultures (see scheme in Fig 5A). The key difference (circled in red) is that now post-shuffle
449 cultures were colony purified before being tested for the Pin phenotype.

450 We found that only 1.5 – 2% of the colonies from the $Rnq1_{T27P}$ post-shuffle cultures
451 remained Pin^{+}, whereas the remaining 98 – 98.5% were clearly Pin^{-} (Table 2; also see a sample
452 plate in Fig 5B, but note that this plate was chosen to show the presence of Pin^{+} patches while
453 many plates had no Pin^{+} patches). We additionally confirmed that these Pin^{+} isolates did not
454 retain the *URA3 RNQ1*$_{WT}$ plasmid. Also, as expected, the Pin^{+} phenotype depended on the

455 presence of the *LEU2 RNQ1*$_{T27P}$ plasmid. In the positive control Rnq1$_{WT}$ post transmission
456 cultures, all but one colony were found to be Pin$^+$. This is consistent with the >99.5% [*PIN*$^+_{WT}$]
457 stability in the original yeast strain before transformation with any plasmids and plasmid shuffle.
458 In the negative control post-transmission cultures carrying just the EV, all but one colony were
459 found to be Pin$^-$ (see Table 2 note). The difference between the frequency of Pin$^+$ cells in the
460 Rnq1$_{T27P}$ and EV cultures was statistically significant in all experiments ($p<0.05$). Finally, the 1.5
461 – 2% Pin$^+$ cells detected in the Rnq1$_{T27P}$ post-transmission cultures were not due to *de novo*
462 [*PIN*$^+_{T27P}$] appearance. This is because [*PIN*$^+_{T27P}$] does not form in *rnq1-Δ* cells without Rnq1$_{T27P}$
463 overexpression (see Fig 3B bottom row). Also, when the *LEU2 CEN RNQ1*$_{T27P}$ or EV plasmids
464 were introduced into the [*pin*$^-$][*psi*$^-$] *rnq1-Δ* strain carrying *HIS3 GAL-SUP3NM-YFP*, no Pin$^+$
465 transformants were obtained among ~1,000 individual transformants tested, and the frequency of
466 Ade$^+$ colonies following attempted [*PSI*$^+$] induction was no greater in the *RNQ1*$_{T27P}$ transformants
467 compared to EV even after several passages on plasmid-selective media.
468

469 **Table 2. Only a small proportion of cells remain Pin$^+$ in the *RNQ1*$_{T27P}$ expressing cultures**
470 **after shuffling out the *RNQ1*$_{WT}$ plasmid.**

Experiment	Construct after plasmid shuffle	Total tested	Pin$^+$	Average Pin$^+$ (%)	SEM (%)	T-test
# 1	*RNQ1*$_{WT}$	435	435	100	± 0	
	RNQ1$_{T27P}$	286	7	2.23	± 0.79	
	EV	197	0	0	± 0	p=0.019
# 2	*RNQ1*$_{WT}$	420	419	99.76	± 0.23	
	RNQ1$_{T27P}$	796	15	1.49	± 0.53	
	EV	504	1*	0.19	± 0.19	p=0.038

471

472 Table 2 Legend. Shown are results of two independent experiments. For each experiment,
473 colonies from at least 11 post-shuffle $Rnq1_{T27P}$ cultures were tested. T-tests are only shown
474 for $Rnq1_{T27P}$ *vs* EV (for both experiments $p<0.05$); for all other combinations $p<1.0e^{-25}$.
475 * The only Pin^+ clone obtained in the EV control in Experiment 2 appears to be a non-Rnq1-
476 based prion.

477

478 Taken together, these findings support the idea of a transmission barrier between $Rnq1_{WT}$
479 and $Rnq1_{T27P}$. If this were true, the proportion of Pin^+ cells in the initial post-shuffle cultures
480 (Table 2) would be determined by both the frequency of the transmission of the prion state from
481 $Rnq1_{WT}$ to $Rnq1_{T27P}$ and the stability of the resulting [PIN^+_{T27P}] prion.

482 Because the phenotype of the $Rnq1_{T27P}$ Pin^+ isolates varied in strength (compare the two
483 $Rnq1_{T27P}$ Pin^+ patches on Fig 5B) and was moderately to significantly reduced relative to $Rnq1_{WT}$
484 after shorter incubation times or if grown on SD-Ade at 30^0C (not shown), we hypothesized that
485 the newly forming [PIN^+_{T27P}]s were unstable, so the Pin^+ $Rnq1_{T27P}$ patches contained both
486 [PIN^+_{T27P}] and [pin^-_{T27P}] cells and the strength of the Pin^+ phenotype reflected the proportion of the
487 [PIN^+_{T27P}] cells. To test this, four Pin^+ $Rnq1_{T27P}$ isolates were colony purified from the patches
488 made on the SD-LeuHis plasmid-selective media prior to testing for the Pin^+ phenotype (circled
489 in green in Fig 5A) onto SD-LeuHis, and then individual colonies were patched on the same
490 media and tested for the retention of [PIN^+_{T27P}] by [PSI^+] induction. Indeed, in all four Pin^+
491 $Rnq1_{T27P}$ isolates both Pin^+ and Pin^- cells were present, indicative of prion instability. Also, as
492 hypothesized, the strength of the Pin^+ phenotype in the original patch correlated with the fraction
493 of the Pin^+ cells found (Table 3).

494

495

496 **Table 3. In the post-shuffle Pin$^+$ Rnq1$_{T27P}$ isolates the [*PIN*$^+_{T27P}$] prion is mitotically**
497 **unstable and the strength of the Pin$^+$ phenotype correlates with fraction of cells retaining**
498 **the prion.**

Strength of Pin$^+$ in the original isolate (Round 1)	% Pin$^+$ cells (Round 2)	Average ± SD
Very weak	3.3	18.4 ± 12.3
Weak	14.3	
Moderate	27.3	
Moderate	28.6	

499

500 Table 3 Legend. See text and Fig 5A for experimental design (green circle indicates a step
501 at which Pin$^+$ isolates were colony purified). The strength of the Pin$^+$ phenotype in post-
502 shuffle Rnq1$_{T27P}$ isolates was determined by growth on SD-Ade and SEt-Ade media at
503 30^{0}C and SD-Ade media at 20^{0}C after [*PSI*$^+$] induction. "Moderate", "weak" and "very weak"
504 corresponds to the Pin$^+$ phenotypes compared to similarly obtained post-shuffle Rnq1$_{WT}$
505 isolates where the Pin$^+$ phenotype is considered "strong" and 100% cells retained the
506 prion. Shown are percentages of Pin$^+$ colonies obtained by colony purification of the
507 original Pin$^+$ Rnq1$_{T27P}$ isolates, as described in Results.

508

509 This is reminiscent of what happens when PrP^{Sc} prions cross the inter-species prion
510 transmission barriers (reviewed in Baskakov, 2014) and when Rnq1 fragments encompassing
511 different QN regions of the PD cross intraspecies transmission barriers in yeast (Kadnar et al.,
512 2010). In these cases, crossing the barrier usually leads to poorly propagating prion variants, and
513 stable prion variants are only detected in later passages either after selection and/or
514 conformational adaptation. Thus, we asked if the unstable [*PIN*$^+_{T27P}$] prions that formed during

515 co-expression of Rnq1$_{T27P}$ with Rnq1$_{WT}$ in [*PIN*$^{+}_{WT}$] cells would eventually mature into more stable
516 ones. The stability of [*PIN*$^{+}_{T27P}$] was first scored in 13 Pin^{+} Rnq1$_{T27P}$ post-shuffle isolates as
517 described above (Fig 5A, green circle), but this time Pin^{+} isolates were chosen randomly and ~84
518 colonies were scored for each isolate to estimate the stability more accurately (Round 2 in Fig
519 5C). Then, 21 [*PIN*$^{+}_{T27P}$] patches obtained in this round were again colony purified from pre-
520 induction SD-LeuHis and patched on SD-LeuHis for Round 3 of [*PIN*$^{+}_{T27P}$] stability analysis. This
521 was repeated with 42 Round 3 [*PIN*$^{+}_{T27P}$] patches for Round 4 analysis (Fig 5C). The number of
522 cell divisions between each round was equal and estimated to be ~19. As can be seen, while
523 [*PIN*$^{+}_{T27P}$] remained highly unstable in both Round 2 and Round 3 analyses, for some [*PIN*$^{+}_{T27P}$]
524 isolates in Round 3 stability increased significantly, with over 60% of cells retaining [*PIN*$^{+}_{T27P}$],
525 which was reflected by a moderate increase of the average stability in this round compared to
526 Round 2. In Round 4, however, no dramatic increase in stability was observed, suggesting that,
527 when [*PIN*$^{+}_{T27P}$] undergoes maturation without selection, prion variants characterized by different
528 stabilities can be formed and maintained.

529 To identify such prion variants, we repeated the analysis of post-shuffle [*PIN*$^{+}_{T27P}$]
530 stability, this time choosing only three independently obtained [*PIN*$^{+}_{T27P}$]s but keeping pedigree
531 data as separate sets and extending analysis beyond Round 4. In Pedigree 1 [*PIN*$^{+}_{T27P}$] was
532 extremely unstable early on but yielded an almost 100% stable [*PIN*$^{+}_{T27P}$] prion in Round 4, and
533 this prion remained stable in Round 5 (430/431 Pin^{+} in 12 [*PIN*$^{+}_{T27P}$] patches tested; Fig 5D). This
534 [*PIN*$^{+}_{T27P}$] prion depended on the maintenance of the *RNQ1*$_{T27P}$ plasmid, was GuHCl-curable, and
535 promoted the induction of a typical array of [*PSI*$^{+}$] variants at a frequency of a "strong" [*PIN*$^{+}_{WT}$].
536 Such stable [*PIN*$^{+}_{T27P}$]s were occasionally detected in other experiments.

537 In Pedigree 2, [*PIN*$^{+}_{T27P}$] remained very unstable in Round 4 and this very low stability
538 was maintained in Rounds 5 and 6, indicative of the establishment of a prion variant not prone to
539 subsequent changes in heritability (Fig 5D). In Pedigree 3 [*PIN*$^{+}_{T27P}$] reached a moderate level of

540 stability, significantly higher than in Pedigree 2 ($p<0.01$; Fig 5D), and remained moderately stable
541 in most cultures in Rounds 5 and 6 but yielded occasional isolates with significantly lower or
542 higher heritable stability (red and green asterisks on Fig 5D), indicative of the establishment of a
543 prion variant that is capable of further conformational adaptation. Altogether, we interpret these
544 data as maturation of post-transmission [PIN^{+}_{T27P}]s to heritable prion variants with characteristic
545 stabilities that is mostly completed within ~60 cell divisions but may continue longer and go
546 through intermediate variants for some isolates.
547

548 **Rnq1$_{T27P}$ can join the amyloid [*PIN*$^{+}$] aggregates formed by Rnq1$_{WT}$**

549 The strength of transmission barriers is determined by two key factors: the efficiency of
550 transmission of the prion state from the donor prion, [PIN^{+}_{WT}], to the recipient protein, Rnq1$_{T27P}$,
551 and the ability of the recipient protein-based prion, [PIN^{+}_{T27P}], to propagate efficiently. The data
552 presented in the previous section indicate that the inefficient propagation of post-transmission
553 [PIN^{+}_{T27P}]s is definitely a contributing factor to the barrier. After the *RNQ1$_{WT}$* plasmid was shuffled
554 out, [PIN^{+}_{T27P}] was very unstable in all isolates tested and further conformational adaptation was
555 required for [PIN^{+}_{T27P}] stability to increase (see Figs 5C and 5D). We now ask if extreme
556 instability of non-adapted [PIN^{+}_{T27P}] was likely the only reason for presence of only 1.5 - 2%
557 [PIN^{+}_{T27P}] cells in post-shuffle cultures or if other mechanisms were also contributing.
558 Here, we tested if Rnq1$_{T27P}$ could join the pre-existing [PIN^{+}_{WT}] prion aggregates because
559 a block at this step would inhibit the transmission of the prion state regardless of the resulting
560 stability of [PIN^{+}_{T27P}] prions. The Rnq1$_{WT}$-CFP and Rnq1$_{T27P}$-YFP were co-expressed in a
561 [PIN^{+}_{WT}] strain from *CEN* plasmids where constructs were controlled by the *CUP1* promoter. To
562 make sure that no significant *de novo* induction of [PIN^{+}_{T27P}] has occurred before cell analysis,
563 cultures of co-transformants were grown to mid-log in the plasmid-selective no-copper media,

564 and $CuSO_4$ was added to 5μM only 2 hours prior to microscopy (see Materials and Methods). At
565 this low concentration of $CuSO_4$, Rnq1 is expressed at levels approximately equal to those of
566 chromosomally encoded Rnq1 (Fig S3). As shown in Fig 6A, $Rnq1_{WT}$-CFP and $Rnq1_{T27P}$-YFP co-
567 localized in bright fluorescent foci in most cells, indicative of $Rnq1_{T27P}$ being able to join [PIN^{+}_{WT}]
568 aggregates. We confirmed that $Rnq1_{T27P}$-YFP joins [PIN^{+}] aggregates just as efficiently as
569 $Rnq1_{WT}$-CFP (Figs S2A and S2B). Co-localization was retained even after prolonged incubation
570 or a higher-level expression of the constructs (5μM $CuSO_4$ overnight, 20μM$cuSO_4$ for 2 hours or
571 overnight, or 50μM$cuSO_4$ for 4 hours; not shown). The appearance of $Rnq1_{T27P}$-YFP foci was
572 indistinguishable from that of $Rnq1_{WT}$-CFP foci and corresponded to a foci pattern characteristic
573 of the "multi-dot high" [PIN^{+}] variant (Bradley and Liebman, 2003) used for these experiments.
574 Also, there was no evidence suggesting that $Rnq1_{T27P}$-YFP aggregates were just seeded by
575 $Rnq1_{WT}$ but then formed next to pre-existing [PIN^{+}] aggregates not incorporating $Rnq1_{WT}$: the
576 overlap of $Rnq1_{T27P}$-YFP and $Rnq1_{WT}$-CFP foci was usually complete in the focal plane imaged
577 (Figs 6A, S2A, and S2B) and in the focal planes immediately above and below. The foci with co-
578 localized $Rnq1_{WT}$-CFP and $Rnq1_{T27P}$-YFP were not sensitive to 1,6 hexanediol (Hex; Fig 6A),
579 with $Rnq1_{T27P}$ retaininged after the treatment, suggesting that the fluorescently tagged proteins
580 were joining the typical amyloid [PIN^{+}_{WT}] aggregates (see also Fig 8A for ThT staining). Thus, the
581 transmission barrier is not due to the inability of $Rnq1_{T27P}$ to join pre-existing [PIN^{+}_{WT}] aggregates
582 formed by $Rnq1_{WT}$ or to convert into amyloid.
583

584 **The co-expression of $Rnq1_{T27P}$ does not lead to loss of [PIN^{+}_{WT}]**

585 We then asked if introduction of the $Rnq1_{T27P}$ expressing plasmid led to a rapid loss of [PIN^{+}_{WT}]
586 prior to the plasmid shuffle. One possibility is that incorporation of $Rnq1_{T27P}$ into the [PIN^{+}_{WT}]
587 aggregates "poisoned" these aggregates and blocked the prion propagation. This hypothesis

588 was used to explain the curing of the [*URE3*] prion upon the overexpression of Ure2-GFP or
589 some Ure2 fragments (Edskes et al., 1999) and curing of [*PSI*$^{+}$] by dominant "[*PSI*$^{+}$] no more"
590 *PNM* mutations within Sup35 PD (Kochneva-Pervukhova et al., 1998; Derkatch et al., 1999;
591 DiSalvo et al., 2011; Pei et al., 2017).

592 However, we have found that transforming the [*PIN*$^{+}_{WT}$] strain used in the genetic screen
593 ([*PIN*$^{+}$] [*psi*$^{-}$] *rnq1-Δ* carrying the *CEN URA3 RNQ1*$_{WT}$ [*PIN*$^{+}$] maintainer and the *CEN HIS3 GAL-*
594 *SUP35NM-YFP* [*PSI*$^{+}$] inducer; see Fig 1B) with the *CEN LEU2 RNQ1*$_{T27P}$ plasmid did not lead to
595 loss of the [*PIN*$^{+}$] prion. All 240 transformants tested in this "no shuffle" experiment remained Pin^{+}
596 even after four more passages on media selective for all the plasmids. Furthermore, no reduction
597 of [*PSI*$^{+}$] induction was observed in such cells compared to the control transformants with *CEN*
598 *LEU2 RNQ1*$_{WT}$ or *CEN LEU2* EV in the nonsense suppression test (Fig 6B) and when *de novo*
599 induction of [*PSI*$^{+}$] was measured as a fraction of cells with Sup35NM-YFP aggregates during
600 overexpression of the Sup35NM-YFP construct (regardless of the plasmid introduced, ~50%
601 cells had line-, ring-, and dot-shaped aggregates after 48 hours of growth on SGal-UraLeuHis
602 media; data not shown).

603 Also, there was no indication of incompatibility of Rnq1$_{WT}$ and Rnq1$_{T27P}$: there was no
604 growth inhibition for the *RNQ1*$_{T27P}$ carrying cells compared to the *RNQ1*$_{WT}$ and EV transformants
605 (Fig 6B). The stability of the [*PIN*$^{+}_{WT}$] maintainer plasmid, *CEN URA3 RNQ1*$_{WT}$, was the same in
606 the *CEN LEU2 RNQ1*$_{T27P}$, *CEN LEU2 RNQ1*$_{WT}$, and *CEN LEU2* EV transformants (AVE ± SD are
607 38.4 ± 11.3%, 41.9 ± 10.3%, and 41.6 ± 5.8%, respectively). Also, there was no difference in the
608 stability of the *CEN LEU2 RNQ1*$_{T27P}$, *CEN LEU2 RNQ1*$_{WT}$, and *CEN LEU2* EV (AVE ± SD are
609 39.9 ± 7.8%, 34.8 ± 10.2%, and 38.0 ± 7.7%, respectively; see Materials and Methods for the
610 description of the test).

611 We also analyzed if similar or different arrays of [*PSI*$^{+}$] variants were induced by
612 Sup35NM-YFP overexpression in cells co-expressing Rnq1$_{WT}$ and Rnq1$_{T27P}$ compared to cells

613 expressing two copies of $Rnq1_{WT}$. For either the cells co-expressing $Rnq1_{WT}$ and $Rnq1_{T27P}$ or
614 cells expressing two copies of $Rnq1_{WT}$ most [*PSI*$^+$] variants were moderate (76.1 and 89.7%,
615 respectively), and strong [*PSI*$^+$] variants were rare (~3%). However, the percentage of weak
616 [*PSI*$^+$] variants was significantly higher in cells co-expressing $Rnq1_{T27P}$ and $Rnq1_{WT}$ (21.0 *vs*
617 6.5%; $p < 0.01$; Table 4).
618
619 **Table 4. Co-expression of $Rnq1_{T27P}$ and $Rnq1_{WT}$ leads to a slight shift towards the**
620 **induction of weak [*PSI*$^+$] variants compared to expression of two copies of $Rnq1_{WT}$.**

Plasmid introduced	[*PSI*$^+$] variants: number isolated (% ± SD)				621
	Weak	Medium	Strong	Total	622
RNQ1$_{WT}$	9 (6.5 ± 5.5)	125 (89.7 ± 8.9)	5 (3.8 ± 6.6)	139 (100)	623
RNQ1$_{T27P}$	15 (21.1 ± 5.1)	54 (76.1 ± 4.9)	2 (2.8 ± 3.2)	71 (100)	624
EV	2 (3.1 ± 3.6)	64 (96.9 ± 3.6)	0 (0 ± 0)	66 (100)	625

626

627 Table 4 Legend. Following the induction of [*PSI*$^+$] by high level expression of Sup35NM-
628 YFP on SGal-UraLeuHis media selective for all plasmids, yeast were replica plated on
629 glucose SD-Ade media not selective for any plasmid and incubated at 20^{0}C for 25 days.
630 Then Ade$^+$ cells were scraped from the SD-Ade plates and colony purified on YPD.
631 Random individual colonies were patched on YPD before color developed. [*PSI*$^+$]s isolated
632 from at least four independent transformants carrying the indicated plasmids were
633 analyzed by the color test on YPD, growth on adenineless media and curability by GuHCl.
634 Results of all three tests were consistent for ~99% [*PSI*$^+$] variants.
635
636 Thus, the barrier for the transmission of the [*PIN*$^+_{WT}$] prion state to $Rnq1_{T27P}$ is not due to
637 $Rnq1_{T27P}$ being incompatible with $Rnq1_{WT}$ co-expression or "poisoning" of the [*PIN*$^+_{WT}$] prion

638 aggregates, but upon joining [PIN^{+}_{WT}] aggregates $Rnq1_{T27P}$ changes the ability of the Rnq1-
639 based prion to promote the induction of particular [PSI^{+}] variants.
640

641 **The transmission barrier created by the T27P mutation in the NPD is eliminated by**
642 **deletion of the first two QN-rich regions in Rnq1 PD**

643 Data presented in the previous sections indicate that the major reason for the transmission
644 barrier is the inability of $Rnq1_{T27P}$ to attain an efficiently propagating prion conformation when
645 seeded by the [PIN^{+}_{WT}] variant used in our studies. We now ask if other conformational variants
646 of Rnq1-based prions would be more acceptable donors of the prion state for $Rnq1_{T27P}$. In our
647 earlier studies we uncovered transmission barriers with subsequent conformational adaptation
648 for the transfer of prion conformations between the [PIN^{+}_{WT}] variant used in the current study and
649 Rnq1 fragments lacking one or more QN-rich regions in the PD (Kadnar et al., 2010; see Fig 1A).
650 The stable prion variants that were formed by these Rnq1 fragments after crossing the
651 transmission barrier from full-length Rnq1 ($Rnq1_{FL}$) and consequent conformational adaptation
652 were collectively named [*mini-PIN*$^{+}$]s and were confirmed to have prion conformations different
653 from those of [PIN^{+}_{FL}]. Thus, we tested if the transmission barrier to $Rnq1_{T27P}$ was reduced when
654 these stable [*mini-PIN*$^{+}$]s not carrying the T27P mutation were used as donors of the prion
655 conformation instead of full length [PIN^{+}_{WT}]. From now on, the **nomenclature** will include both
656 the presence of full-length Rnq1 or of a Rnq1 fragment, as well as the WT or T27P allele (e.g.
657 [$PIN^{+}_{FL\text{-}WT}$] or [$PIN^{+}_{FL\text{-}T27P}$]). For the Rnq1 fragments, the nomenclature reflects the deleted part of
658 the PD, which includes the QN-rich region(s) numbered as in Fig 1A and an adjacent helical
659 stretch(es) indicated in Fig 1A by letters (e.g. [$PIN^{+}_{\Delta B1C2\text{-}WT}$] or [$PIN^{+}_{\Delta B1C2\text{-}T27P}$]).

660 The plasmid shuffle experiment described in Fig 1B was repeated using stable [*mini-*
661 PIN^{+}_{WT}] stains instead of [$PIN^{+}_{FL\text{-}WT}$]. According to the nonsense suppression-based [PSI^{+}]

662 induction test, transmission of the prion state to Rnq1$_{FL\text{-}T27P}$ from [*PIN*$^{+}_{\Delta B1C2\text{-}WT}$] and [*PIN*$^{+}_{\Delta B1\text{-}WT}$]
663 but not from [*PIN*$^{+}_{\Delta 2D\text{-}WT}$] or [*PIN*$^{+}_{\Delta 3E\text{-}WT}$] was considerably more efficient compared to
664 transmission from [*PIN*$^{+}_{FL\text{-}WT}$] (Fig 7A). In the case of transmission from [*PIN*$^{+}_{\Delta B1C2\text{-}WT}$], a colony
665 purification experiment done as described in Fig 5A was used to confirm that growth on
666 adenineless media in Fig 7A was indeed due to a higher fraction of [*PIN*$^{+}_{FL\text{-}T27P}$] cells in the "post-
667 shuffle" cultures (Fig 7B; the difference is statistically significant, $p<0.01$). This supports the
668 hypothesis that the T27P mutation in the NPD changes the range of prion conformations
669 permissible for PD and that [*PIN*$^{+}_{\Delta B1C2\text{-}WT}$] and [*PIN*$^{+}_{\Delta B1\text{-}WT}$] fall into this range of acceptable
670 conformations while [*PIN*$^{+}_{FL\text{-}WT}$] does not.
671 Considering the indication that deletion of the B1C2 region of the Rnq1 PD reduced the
672 transmission barrier, we asked if this region fully determined the inability of Rnq1$_{FL\text{-}T27P}$ to take on
673 the prion conformation compatible with [*PIN*$^{+}_{FL\text{-}WT}$]. The T27P mutation was introduced into the
674 Rnq1 fragment lacking the B1C2 region (the Rnq1$_{\Delta B1C2\text{-}T27P}$ construct), and transmission of the
675 prion state to this construct was assessed using [*PIN*$^{+}_{\Delta B1C2\text{-}WT}$] as a donor of the prion state. We
676 found that a significantly higher fraction of Pin^{+} cells was present in the "post-transmission"
677 cultures when both the donor and recipient of the prion state lacked the B1C2 region (Fig 7C;
678 $p<0.01$). However, no subsequent change of mitotic stability was observed following such
679 transmissions: after four rounds of consecutive colony purifications done as in Fig 5C, the
680 [*PIN*$^{+}_{\Delta B1C2\text{-}T27P}$] isolates retained the same stability as immediately after the transmission (Fig 7C,
681 no statistically significant difference between R1 and R2 through R4). Furthermore, one more
682 round of analysis of R4 [*PIN*$^{+}_{\Delta B1C2\text{-}T27P}$] isolates with the highest fraction of prion-retaining cells
683 did not indicate that these isolates underwent a heritable conformational shift leading to higher
684 mitotic stability (not shown). One explanation for these data is that the T27P mutation limits the
685 fragmentation of all or most [*PIN*$^{+}_{\Delta B1C2\text{-}T27P}$] prion variants thus preventing them from propagating

686 efficiently enough to achieve high mitotic stability. The alternative explanation is that there is no
687 transmission barrier between [*PIN*$^{+}_{\Delta B1C2\text{-}WT}$] and Rnq1$_{\Delta B1C2\text{-}T27P}$. In this case, transmission of the
688 prion state from [*PIN*$^{+}_{\Delta B1C2\text{-}WT}$] to Rnq1$_{\Delta B1C2\text{-}T27P}$ will result in all cells attaining the same heritable
689 [*PIN*$^{+}_{\Delta B1C2\text{-}WT}$] prion conformation with a particular mitotic stability (that happens to be ~45% after
690 ~19 cell generations), and then this [*PIN*$^{+}_{\Delta B1C2\text{-}T27P}$] variant propagates faithfully without
691 undergoing any further conformational adaptation. Because there is no selection favoring the
692 maintenance of the [*PIN*$^{+}_{\Delta B1C2\text{-}T27P}$] prion in our experimental system, we do not expect to detect
693 rare switches to mitotically stable variants within the relatively small sample sizes tested. Also,
694 the proportion of Pin^{+} cells in Round 1 analysis is expected to reflect the 100% efficient
695 transmission of the prion state between [*PIN*$^{+}_{\Delta B1C2\text{-}WT}$] and Rnq1$_{\Delta B1C2\text{-}T27P}$ and then the loss of
696 [*PIN*$^{+}_{\Delta B1C2\text{-}T27P}$] in cells divisions between the elimination of the *RNQ1*$_{\Delta B1C2\text{-}WT}$ plasmid and the
697 start of the analysis of "post-shuffle" cultures, which is ~18-20 cells divisions, i.e. similar to the
698 ~19 number of divisions between subsequent rounds.

699 To distinguish between these two explanations, transmission of the prion state to
700 Rnq1$_{\Delta B1C2\text{-}T27P}$ was attempted using [*PIN*$^{+}_{FL\text{-}WT}$] as a donor. Data in Fig 7D indicate the existence
701 of a strong transmission barrier, similar to that between [*PIN*$^{+}_{FL\text{-}WT}$] and Rnq1$_{FL\text{-}T27P}$, and
702 subsequent conformational adaptation which allowed for the establishment of [*PIN*$^{+}_{\Delta B1C2\text{-}T27P}$]
703 variants with different levels of mitotic stability, including high mitotic stability that was maintained
704 in subsequent rounds of analysis (see asterisks in Fig 7D). This excludes the explanation that
705 the T27P mutation makes [*PIN*$^{+}_{\Delta B1C2\text{-}T27P}$] variants intrinsically unstable and supports the
706 alternative explanation that the T27P mutation in the NPD creates a transmission barrier through
707 the effect on the conformational flexibility of the B1C2 region of the PD. Comparison of data
708 presented in Figs 7C and 7D supports the idea that when both the donor and the recipient lack
709 this region, the mutant attains the prion conformation without a barrier but the mutation slightly

710 inhibits the stability of the resulting [$PIN^{+}_{\Delta B1C2\text{-}T27P}$] variant. The deletion of the B1C2 region only
711 in the T27P carrying recipient and not in the non-mutant donor is not sufficient to eliminate the
712 transmission barrier. However, in transmissions from [$PIN^{+}_{FL\text{-}WT}$], the subsequent increase of
713 mitotic stability was significantly faster for [$PIN^{+}_{\Delta B1C2\text{-}T27P}$] compared to [$PIN^{+}_{FL\text{-}T27P}$] (Fig 7D),
714 indicative of the effect of the B1C2 region of PD on the conformational adaptation properties of
715 T27P mutants.

716 Because the [PSI^{+}] induction test in Fig 7A indicated that deletion of only the B1 region
717 within the PD could also reduce the transmission barrier, we asked if the first QN-rich region of
718 the PD, QN1, was solely responsible for the effect on both the WT to T27P transmission barrier
719 and conformational adaptation of the T27P carrying prions observed for ΔB1C2 fragments. This
720 is particularly interesting because QN1 is very short, only 12aa (NSNNNNQQGQNQ). Thus, the
721 T27P mutation was introduced into the Rnq1 fragment lacking QN1 but retaining QN2 (the
722 $Rnq1_{\Delta B1\text{-}T27P}$ construct) and the [$PIN^{+}_{\Delta B1\text{-}WT}$] donor was used to transmit the prion state to this
723 construct. Like in the similar experiments with WT and T27P carrying ΔB1C2 Rnq1 fragments,
724 the fraction of [$PIN^{+}_{\Delta B1\text{-}T27P}$] cells in the "post-shuffle" cultures was significantly increased
725 compared to the transmissions between FL constructs ($p<0.01$; compare Fig 7E with 7D), even
726 though the fraction of Pin^{+} cells was slightly lower in [$PIN^{+}_{\Delta B1\text{-}T27P}$] than in [$PIN^{+}_{\Delta B1C2\text{-}T27P}$] samples
727 ($p<0.05$; compare Figs 7C and 7E). However, in the [$PIN^{+}_{\Delta B1\text{-}T27P}$] isolates, subsequent
728 appearance of [$PIN^{+}_{\Delta B1\text{-}T27P}$]s with high mitotic stability, indicative of the ongoing conformational
729 adaptation, led us to conclude that removal of only the B1 region in both the donor and the
730 recipient did not eliminate the transmission barrier created by the T27P mutation. This finding
731 suggested that the QN2 region of the Rnq1 PD was also involved in the interaction of the PD
732 with the T27P mutation in the NPD. Yet, similar experiments attempting to transmit the prion
733 state from the [$PIN^{+}_{\Delta 2D\text{-}T27P}$] donor to the $Rnq1_{\Delta 2D\text{-}T27P}$ recipient did not suggest that deleting the

734 QN2 region reduced the transmission barrier or led to the establishment of the T27P carrying
735 prions not prone to further conformational adaptation (Fig 7F). Thus, the NPD exerts its effect on
736 the QN1 and QN2 regions of the PD acting in concert rather than individually. Finally, consistent
737 with data shown in Fig 7A, we obtained no evidence suggesting that the deletion of the QN3
738 region of the Rnq1 PD (Δ3E) could remove the transmission barrier created by the T27P
739 mutation or affect conformational adaptation of [*PIN*$^{+}_{\Delta 3E\text{-}T27P}$] prion variants after crossing the
740 barrier (Fig 7G).
741

742 **Unlike Rnq1$_{WT}$-YFP, Rnq1$_{T27P}$-YFP readily forms liquid-like droplets when**
743 **expressed in [*pin*$^{-}$] cells**

744 While Rnq1 aggregation in [*PIN*$^{+}$] strains can be visualized by expression of Rnq1$_{WT}$, its PD, or
745 PD fragments fused to C-terminal fluorescent tags from the GFP family (Sondheimer and
746 Lindquist, 2000; Derkatch et al., 2001; Osherovich and Weissman, 2001; Vitrenko et al., 2007b;
747 Kadnar et al., 2010), overexpression of Rnq1$_{WT}$ fused to such tags (e.g. Rnq1$_{WT}$-GFP) in [*pin*$^{-}$]
748 strains does not lead to the formation of visible aggregates and to the *de novo* appearance of
749 [*PIN*$^{+}$] (Derkatch et al., 2001; Kadnar et al., 2010). One possible explanation is that the extreme
750 C-terminus of the Rnq1 PD encompassing the last QN-rich region, QN4 (see Fig 1A), is
751 important during the step of the *de novo* [*PIN*$^{+}$] prion formation, and bulky C-terminal tags
752 interfere with this process (Galliamov et al., 2024). However, once [*PIN*$^{+}$] is formed, other QN-
753 rich regions within the RNQ1 PD get engaged in the maintenance of the prion structure and
754 blocking of QN4 by a tag is not critical for the prion maintenance (Kadnar et al., 2010).
755 Because our data indicate that the T27P mutation changes the conformational flexibility
756 of the Rnq1 PD through particular QN-rich regions, we asked if, in the presence of T27P, the C-
757 terminally tagged constructs retain aggregation properties despite the tag partially blocking the

758 QN4 region. As seen in Fig 8A, in contrast to $Rnq1_{WT}$, when $Rnq1_{T27P}$-YFP is expressed in [*pin*$^-$]
759 cells, it readily forms dot aggregates, one or several dots per cell. Such dot-like aggregates were
760 formed in ~40% of cells even when $Rnq1_{T27P}$-YFP was expressed briefly and at close to
761 physiological levels of expression (5μM $CuSO_4$ for 2 hours; Figs 8B and 8C; also see Fig S3 for
762 protein expression).

763 These dot aggregates are clearly distinct from ribbon-like aggregates of the *de novo*
764 forming [*PIN*$^+_{WT}$]s when GFP-tagged Rnq1 is overexpressed in [*URE3*] cells (Derkatch et al.,
765 2001). Therefore, we tested if $Rnq1_{T27P}$-YFP aggregates forming in [*pin*$^-$] cells are amyloid, and
766 found they are not because the aggregates are not stained by Thioflavin T (Fig 8A). Furthermore,
767 these aggregates are dissolved by a short-term Hexanediol (Hex) treatment, suggesting that they
768 are liquid-like droplets (Figs 8B and 8C). The presence of $Rnq1_{WT}$ is not required for $Rnq1_{T27P}$ to
769 form liquid-like droplets as they also form in *rnq1-Δ* cells (Fig 8D). Finally, $Rnq1_{WT}$-CFP does not
770 join the $Rnq1_{T27P}$-YFP when co-expressed in [*pin*$^-$] cells (Fig 8E). This further supports the idea
771 that the NPD mutation T27P modulates aggregation and conformational properties of QN-rich
772 regions within the PD of Rnq1.
773

774 # Discussion

775 **The T27P mutation in the NPD of Rnq1 creates a barrier for the transmission of the**
776 **[*PIN*$^+$] prion state from $Rnq1_{WT}$**

777 Most known prion-forming proteins have chimeric organization containing: 1) a functional
778 non-prion domain, NPD, that is not essential for prion formation and is required for the protein to
779 perform its main cellular function; 2) a prion domain, PD, which is sufficient for prionization and
780 can form prions in the absence of NPD and even when attached to other proteins. At first glance,
781 Rnq1 shares such chimeric organization except that its NPD is very short, compared to its PD,

782 which constitutes up to 2/3 of the protein and has a very complex organization (see Introduction
783 and Fig 1A). The length of the NPD is ~132 – 153 aa but is not known exactly because *S.*
784 *cerevisiae* Rnq1, as well as its potential homologs from other species have no known function
785 and are poorly conserved (ILD unpublished observations).

786 We aimed at understanding the structure - function of Rnq1 related to its prion-forming
787 abilities. Two approaches were used. Previously, we performed extensive deletion analysis of all
788 potential structural features within the PD (Kadnar et al., 2010). Here, we used random
789 mutagenesis of *RNQ1*. We mutagenized both the PD and NPD because, first, the exact length of
790 the NPD is not known and, second, several lines of evidence indicated that the NPD is involved
791 in [*PIN*$^+$] formation and maintenance (see below). The genetic screen was for the loss of the Pin$^+$
792 phenotype, *i.e.* the ability of [*PIN*$^+$] to facilitate the *de novo* induction of [*PSI*$^+$]. This readout
793 allowed screening for mutations in the context of the complete Rnq1 not fused to reporters that
794 were previously shown to modify its prion forming ability (Sondheimer and Lindquist, 2000;
795 Derkatch et al., 2001; Bardill and True, 2009). Here we describe the Rnq1$_{T27P}$ mutant obtained in
796 this screen. We propose that, through interactions with specific QN-rich regions in the PD, this
797 NPD mutation alters the array of conformations the prion domain can attain and thus creates a
798 transmission barrier with a [*PIN*$^+_{WT}$] prion formed by non-mutant Rnq1. The mutation also alters
799 the aggregation properties of Rnq1 by promoting the formation of liquid-like droplets when
800 Rnq1$_{T27P}$ is fused to a C-terminal YFP tag.

801 The T27P mutation led to the loss of the [*PIN*$^+$] prion in 98 – 98.5% of the cells when
802 Rnq1$_{T27P}$ was substituted for Rnq1$_{WT}$ in a [*PIN*$^+_{WT}$] strain (Table 2). We concluded that this occurs
803 because the mutation creates a barrier for the transmission of the prion state from Rnq1$_{WT}$ to
804 Rnq1$_{T27P}$ after not finding support for the alternative explanation that Rnq1$_{T27P}$ is intrinsically
805 defective in prion formation and propagation. Indeed, Rnq1$_{T27P}$ can form amyloid *in vitro* (Fig 4C).
806 Also, transient overexpression of Rnq1$_{T27P}$ in a *rnq1-Δ* strain leads to a heritable Pin$^+$ phenotype

807 indicative of the *de novo* formation of [PIN^{+}_{T27P}] (Fig 3). Finally, a [PIN^{+}_{T27P}] variant with mitotic
808 stability of >99.9% was obtained upon prolonged mitotic propagation of an unstable [PIN^{+}_{T27P}]
809 retrieved immediately after transmission of the prion state from [PIN^{+}_{WT}] (Fig 5D).
810 The concept of transmission barriers dates to observations that experimental transmission of
811 scrapie between different mammalian species is frequently far less efficient than within the same
812 species (Pattison et al., 1965). These barriers were then attributed to differences in sequences of
813 the PrP protein in different species (Scott et al., 1989). Interspecies transmission barriers were
814 also uncovered for [*PSI*$^{+}$] and [*URE3*] (Santoso et al., 2000; Chen et al., 2007, 2010; Edskes et
815 al., 2009; Afanasieva et al., 2011; Sharma et al., 2016; Wickner et al., 2019). Importantly, the
816 analysis of these barriers focused on the conformational constraints resulting from sequence
817 differences **exclusively within the PDs** of these proteins. In closely related *Saccharomyces*
818 *sensu stricto* species, transmission barriers formed even though PDs are highly homologous and
819 carry only a few individual amino acid changes (Santoso et al., 2000; Chen et al., 2007, 2010).
820 Furthermore, mutagenesis of Sup35 and Rnq1 and analysis of Sup35 from wild isolates revealed
821 that transmission barriers can be created within *S. cerevisiae* by single mutations in the PDs
822 (DePace et al., 1998; Bardill and True, 2009; Bateman and Wickner 2012).
823 However, differences in amino acid sequences in the prion-forming regions are not the only
824 contributing factor to transmission barriers. Studies of mammalian prions eventually concluded
825 that the efficiency of interspecies transmissions is determined by both the PrP sequence and
826 particular PrP^{Sc} conformations in the donor species (Hill et al., 1997; Hill and Collinge 2001;
827 Collinge and Clarke, 2007; Collinge, 2012). Our analysis of the four QN-rich regions within the
828 PD of Rnq1 showed that while any two were generally sufficient for the maintenance of the [*PIN*$^{+}$]
829 prion, deletions of individual QN-rich regions created transmission barriers, and the possibility of
830 transmission across these barriers depended on the presence of at least one common QN-rich

831 region between the donor and recipient constructs. This underscored both the importance of
832 identical amino-acid stretches within the PD for prion transmission and the contribution of
833 conformational differences created by other parts of the PD (Kadnar et al., 2010). Our current
834 study contributes to understanding exclusively conformation-based transmission barriers
835 because the sequence of the entire PD is identical for $Rnq1_{WT}$ and $Rnq1_{T27P}$.

836 We found no evidence that the initial transmission of the prion state from [PIN^{+}_{WT}] to $Rnq1_{T27P}$
837 was blocked. $Rnq1_{T27P}$ joins [PIN^{+}_{WT}] amyloid aggregates as efficiently as $Rnq1_{WT}$ and does not
838 "poison" them (Figs 6A, 6B, 8A, 8B, and S2). But when we scored individual [PIN^{+}_{T27P}] isolates
839 from post-transmission cultures for prion maintenance, the striking observation is that all post-
840 transmission [PIN^{+}_{T27P}] isolates were extremely unstable. Scoring lineages of [PIN^{+}_{T27P}] isolates
841 for prion maintenance following a controlled number of mitotic divisions between rounds of
842 analysis revealed that, while on average mitotic stability of [PIN^{+}_{T27P}] increased compared to the
843 first round of analysis (Fig 5C), mitotic growth also led to the establishment of [PIN^{+}_{T27P}] variants
844 with distinct mitotic stabilities. Along with highly stable [PIN^{+}_{T27P}]s (>99.9% maintenance after 19
845 cell divisions) we obtained lineages with a heritable stability of ~20% (Fig 5D). Importantly, like
846 [PIN^{+}_{WT}] (Derkatch et al., 2000), [PIN^{+}_{T27P}] did not provide a detectable growth advantage relative
847 to [pin^{-}_{T27P}], so there was no selection for cells with more efficiently propagating [PIN^{+}_{T27P}]. Thus,
848 mitotic stability is just a quantitative characteristic that can be used to distinguish different
849 [PIN^{+}_{T27P}] variants established after crossing the transmission barrier.

850 Two models could explain the appearance of heritable [PIN^{+}_{T27P}] variants after multiple
851 mitotic divisions in the presence of [PIN^{+}_{WT}] (Fig 9). Both postulate that the T27P mutation puts
852 conformational constraints on the PD of $Rnq1_{T27P}$, so it cannot form a stable [PIN^{+}] that is
853 conformationally similar to [PIN^{+}_{WT}] even though $Rnq1_{T27P}$ can form stable prions *de novo*. The
854 **first model** proposes that multiple [PIN^{+}_{T27P}] variants are formed in the same cell after
855 transmission, and then daughter cells inherit them randomly, with a higher chance of inheriting

856 variants that produce more seeds (propagons) and are thus more stable in mitotic divisions. This
857 would lead to the rapid disappearance of the least stable variants in the population. However,
858 following individual [PIN^{+}_{T27P}] pedigrees allowed us to detect such unstable variants. In support of
859 this model, the co-existence of different prion variants in the same cell for several generations
860 has been confirmed for [PSI^{+}] (Norton et al., 2024). The **second model** predicts that the
861 transmission barrier leads to formation of a particular [PIN^{+}_{T27P}] variant, but this variant is not
862 conformationally stable and undergoes frequent conformational switches until more energetically
863 favorable states are attained. These stable conformations may have different, even low, mitotic
864 stabilities, but they are not changing frequently anymore. The process of such conformational
865 adaptation may involve multiple steps and some [PIN^{+}_{T27P}] variants may end up in efficiently
866 propagating but "undecided" states that have no preferred path towards conformational
867 stabilization. Our detection of such "undecided" [PIN^{+}_{T27P}] lineages that produce both more and
868 less mitotically stable variants even after 100 cell divisions (Fig 5D and data not shown) supports
869 the conformational adaptation model, but we do not see the models as strictly mutually exclusive.
870 Conformational adaptation in the absence of PD mutations has been proposed e.g. for *de novo*
871 induced [PIN^{+}] and [PSI^{+}], for permanent [PSI^{+}] variant switching in different chaperone
872 environments, and for conversion of *in vitro* made PrP^{Res} into PrP^{Sc} (Derkatch et al., 2001;
873 Sharma and Liebman, 2012; Baskakov, 2014; King, 2022).
874 The T27P mutation specifically interacts with the B1C2 part of the PD since its deletion
875 dramatically increased prion transmission to mutant constructs (Fig 7). Actually, data indicate
876 that there is no transmission barrier between [$PIN^{+}_{\Delta B1C2\text{-}WT}$] and $Rnq1_{\Delta B1C2\text{-}T27P}$. Even though the
877 mitotic stability of [$PIN^{+}_{\Delta B1C2\text{-}T27P}$] was not very high, this level of stability was clearly heritable
878 during subsequent mitotic growth, indicative of the establishment of a [$PIN^{+}_{\Delta B1C2\text{-}T27P}$] variant not
879 undergoing further conformational adaptation (Fig 7C). The alternative explanation that a prion

880 variant used as a [*PIN*$^{+}_{\Delta B1C2\text{-}WT}$] donor is more compatible with prion conformations that could be
881 attained by the T27P mutants is unlikely since deletion of B1C2 also affects the transmission
882 from [*PIN*$^{+}_{FL\text{-}WT}$] to the Rnq1$_{\Delta B1C2\text{-}T27P}$ mutant (Fig 7D). While initially the barrier was strong, mitotic
883 stability of the [*PIN*$^{+}_{\Delta B1C2\text{-}T27P}$] isolates increased much faster compared to [*PIN*$^{+}_{FL\text{-}T27P}$]s obtained
884 from the same donor. Thus, despite carrying the same mutation, Rnq1$_{FL\text{-}T27P}$ and Rnq1$_{\Delta B1C2\text{-}T27P}$
885 form different prion variants. Analysis of transmissions between Rnq1 fragments carrying
886 deletions of only QN1 (ΔB1) or QN2 (Δ2D) regions indicates that simultaneous deletion of both
887 regions is required for the lifting of the transmission barrier created by the T27P mutation, but
888 removing just B1 encompassing a 12 aa QN-rich region is sufficient to reduce the strength of the
889 barrier.

890 Another indication of a difference in amyloid conformations attained by Rnq1$_{WT}$ and Rnq1$_{T27P}$
891 is that amyloid fibers spontaneously formed by these proteins *in vitro* look different in TEM: the
892 bundles of Rnq1$_{WT}$ fibrils are tight and twisted whereas Rnq1$_{T27P}$ fibers are more relaxed and not
893 twisted (Fig 4C).

894 However, the T27P mutation affects more than the array of prion conformations that are
895 possible for the [*PIN*$^{+}_{T27P}$] prion. It changes the conformation of the protein even in the soluble
896 state, indicated by a slight but reproducible increase of mobility of SDS-PAGE gels when purified
897 from yeast or bacteria (Figs 2A and 4A). Indeed, T27P opens an alternative aggregation pathway
898 for the Rnq1 protein. The Rnq1$_{WT,}$ even when overexpressed, is not prone to aggregate when
899 fused to C-terminal GFP family tags unless a heterologous QN-rich amyloid aggregate is present
900 (Derkatch et al., 2001). This may be because a bulky tag blocks QN4, the last QN-rich
901 determinant in the PD, which has recently been shown to initiate [*PIN*$^{+}$] formation (Galliamov et
902 al., 2024, 2025), so heterologous amyloid seeds are needed to overcome this constraint. But
903 Rnq1$_{T27P}$ attached to YFP readily forms liquid-like droplets at physiological levels of expression

904 without the need for heterologous prions (Fig 8). This finding strengthens the evidence that the
905 T27P mutation affects aggregation properties of Rnq1.
906

907 **Is the only function of the Rnq1 "NPD" to regulate the aggregation of Rnq1 PD?**

908 Transmission barriers created by mutations **within the PDs** of yeast prions (see above) as well
909 as the existence of different prion variants can be explained by the parallel-in-register model of
910 protein molecules in amyloid fibrils (Wickner et al., 2008; 2011a). According to this model, prion
911 variants are the result of differences in the length of amyloid cores formed by PDs and relative
912 positioning of amyloid stretches due to turns within regions not involved in β-strand formation.
913 For Rnq1, amyloid formation was detected in the regions roughly corresponding to QN-rich
914 regions, but varies in different prion variants (Galliamov et al., 2024, 2025). So, mutations within
915 or deletions of these regions are expected to create conformational constrains leading to
916 different prion variants. But the T27P mutation is located **outside** the currently defined Rnq1 PD,
917 so its effect on variants of the Rnq1-based prions is not well explained by this model.

918 How could the T27P mutation in the NPD create a transmission barrier? Because NPDs
919 engage in interactions with cellular partners, the absence or inactivation of NPD can block these
920 interactions and thereby increase *de novo* prion formation (Derkatch et al., 1996; Maddelein and
921 Wickner, 1999). Increasing such interactions would, reciprocally, decrease prion formation
922 (Derkatch et al., 1998). However, if the prion-forming protein is indeed chimeric and the NPD and
923 PD domains fold independently, mutations that just change functionality of the NPD are not
924 expected to impose **specific** conformational constrains on the PD and should not lead to
925 transmission barriers. An alternative hypothesis is that in Rnq1 the N-terminal domain, presumed
926 NPD, regulates the conformation and aggregation properties of the PD.

927 Indeed, this hypothesis helps explain multiple previous findings indicating that the NPD of

928 Rnq1 is involved in essentially all prion-related phenotypes associated with [*PIN*$^+$]. First, while
929 constructs where Rnq1 PD is separated from Rnq1 NPD and attached to Sup35MC can form
930 prions, these prions have distinct properties from [*PIN*$^+$] formed by Rnq1$_{FL}$ (Sondheimer and
931 Lindquist, 2000; Bardill and True, 2009). Second, *in vitro* Rnq1$_{FL}$ forms amyloid considerably
932 slower than Rnq1 fragments lacking the NPD (Vitrenko et al., 2007b; Kadnar et al., 2010), which
933 is consistent with inhibition of aggregation by the NPD even in the absence of its cellular
934 interactors. Third, point mutations and deletions in Rnq1 NPD affect the propagation of [*PIN*$^+$]
935 (Vitrenko et al., 2007a, Shibata et al., 2009; Kurahashi et al., 2011a). Curiously, among 13
936 missense mutations uncovered by a screen for loss of [*PIN*$^+$], 12 were in the NPD and two
937 mutations, V23A and A29T, were located very close to our T27P mutation, within the same
938 predicted helical stretch (Shibata et al., 2009; Kurahashi et al., 2011a). The authors interpreted
939 their results as moderate destabilization of [*PIN*$^+$] by the mutations and the possibility of
940 transmission barrier was not tested. However, our results suggest that data in these earlier
941 papers are also consistent with the creation of transmission barriers between [*PIN*$^+_{WT}$] and at
942 least some of the mutants. The Shibata et al. study also supports the likelihood that our genetic
943 screen was close to saturating and that mutations creating strong transmission barriers, like
944 T27P, are extremely rare while most other changes have much milder effect (between 30 and
945 70% of cells carried [*PIN*$^+_{MUTANT}$] prions in their experiments corresponding to Round 1 analysis
946 here). Fourth, a site for interaction with the Sis1 chaperone essential for [*PIN*$^+$]
947 propagation is located in the NPD (aa 91-97) and mutations in this site lead to [*PIN*$^+$]
948 destabilization (Douglas et al., 2008; Shibata et al., 2009). Overexpression of Rnq1$_{FL}$, but not
949 NPD or PD alone, is toxic in [*PIN*$^+$] but not [*pin*$^-$] cells due to oxidative stress, and this toxicity is
950 rescued by overexpression of the Sis1 chaperone (Douglas et al., 2008; Bharthi et al., 2016).
951 To explain this, it was hypothesized that Sis1 directs Rnq1 into non-toxic [*PIN*$^+$] amyloid

952 aggregates, preventing it from forming off-pathway SDS-soluble aggregates that cause oxidative
953 stress (Douglas et al., 2008). Finally, the NPD of Rnq1 also affects interactions of [*PIN*$^+$] with
954 other prions. Overexpression of a fragment with a specific deletion in NPD, Rnq1$_{\Delta 1\text{-}100}$, leads to
955 loss of [*PSI*$^+$], [*URE3*] and huntingtin polyQ aggregates in [*PIN*$^+$] but not in [*pin*$^-$] cells (Kurahashi
956 et al., 2008). Later, similar [*PIN*$^+$]-dependent curing of [*PSI*$^+$] was reported for multiple missense
957 alleles in the Rnq1 NPD, including L26S, S28P and A29T located close to T27P (Kurahashi et
958 al., 2009, 2011a, 2011b). One possible explanation based on our study is that these mutant
959 proteins switch to variant(s) of [*PIN*$^+$] that are incompatible with [*PSI*$^+$], like those reported earlier
960 (Bradley and Liebman, 2003; Mathur et al., 2009; Villali et al., 2020).

961 Curiously, several studies mention that changes in the NPD of Rnq1 led it to form non-
962 amyloid aggregates when tagged with YFP, but these aggregates are different from Rnq1$_{T27P}$
963 liquid-like droplets detected in our study. The SDS-soluble aggregates formed by Rnq1 with a
964 mutated Sis1 binding site are highly toxic even in [*pin*$^-$] cells (Douglas et al., 2008), while
965 Rnq1$_{T27P}$-YFP droplets do not inhibit growth. Also ThT-negative aggregates formed by Rnq1$_{\Delta 1\text{-}}$
966 $_{100}$-YFP (Kurahashi et al., 2008) actively recruit Rnq1$_{FL\text{-}WT}$-CFP which does not join liquid-like
967 droplets formed by T27P. Thus, the Rnq1 NPD can probably control formation of not one, but
968 multiple types of non-amyloid aggregates.

969 While the NPD of Rnq1 is associated with multiple aggregation-related phenotypes, there
970 is no evidence for its activity not related to Rnq1 aggregation. The *RNQ1* gene is not essential,
971 and its deletion or overexpression does not lead to any significant growth defects in [*pin*$^-$] cells
972 (www.yeastgenome.org and our data).

973 The key rationale for [*PSI*$^+$], [*URE3*], and [*PIN*$^+$] being diseases rather than functional
974 prions is based on their lower-than-expected frequency in wild yeast populations (Wickner et al.,
975 2011b; Kelly and Wickner, 2013). But [*PIN*$^+$] is detected in wild and commercial yeast isolates

976 much more frequently than [*PSI*$^+$] and [*URE3*], >10% *vs* <1% (Resende et al., 2003; Nakayashiki
977 et al., 2005; Halfman et al.,2012; Westergard and True, 2014a; Kelly et al., 2014). So, the
978 evidence for its detrimental effect is based on careful assessment of the frequency of outcross
979 matings expected to spread prions and on polymorphism of the PD-encoding part of *RNQ1* locus
980 expected to create transmission barriers (Kelly et al., 2012; Kelly and Wickner, 2013). These
981 calculations assume stable inheritance of [*PIN*$^+$]. However, our study reveals [*PIN*$^+$] variants with
982 heritably low mitotic stability. In addition to conformational switches induced by a transmission
983 barrier, unstable [*PIN*$^+$]s also form *de novo* and during stress or otherwise changing
984 environmental conditions (Derkatch et al., 2000; Newnam et al., 2011; Westergard and True
985 2014b), and their instability may be heritable. Also, meiotic stability of [*PIN*$^+$] is not 100%
986 (Bradley et al., 2002), and at least some of >40 different [*PIN*$^+$] variants (Huang et al., 2013;
987 Westergard and True, 2014a) may be even more meiotically unstable, like [*URE3*] and some
988 [*PSI*$^+$]s (Liebman and All-Robyn 1984; Wickner, 1994; Bradley et al., 2002). Finally, redundancy
989 of the Rnq1 PD makes it resistant to transmission barriers created by mutations: both our genetic
990 screen here and screens mentioned above uncovered NPD rather than PD mutations affecting
991 [*PIN*$^+$]. Thus, [*PIN*$^+$] may not have a strong enough detrimental effect to be considered a disease.
992 In thinking about possible functions for the Rnq1 protein it is instructive to recognize that
993 PDs of both Ure2 and Sup35 do contribute to cellular functions of these proteins (Hoshino et al.,
994 1999; Hosoda et al., 2003; Shewmaker et al., 2007; Edskes et al., 2018), but they are not
995 required for their well-known major jobs. For Sup35, the PD is not required for an essential role
996 in translation termination, but it is critical for at least two non-essential “moonlighting” jobs. One
997 involves interactions with the Pab1 protein (Hosoda et al., 2003), a major component of stress
998 granules known to be enriched in aggregation-prone proteins contributing to their assembly
999 (Fomicheva and Ross, 2021). The other “moonlighting job for Sup35 uncovered in our work (Li et
1000 al., 2014) involves formation of a two-protein amyloid composed of Sup35 PD and the QN-rich

1001 domain of Pub1. The [*PUB1 / SUP35*] complex associates with microtubules and promotes
1002 integrity of the cytoskeleton. Thus, while [*PSI*$^+$] may indeed be an egoistic byproduct of Sup35
1003 aggregation properties, Sup35 function requiring the PD depends on the ability to form prion-like
1004 aggregates. We hypothesize that the same is true for Rnq1. Its cellular function may involve
1005 aggregation through the PD, and the NPD's role is in regulating such aggregation. One such
1006 possible function is positive and negative interactions with other aggregating proteins in order to
1007 induce or eliminate heterologous protein aggregates. Whether this role is carried out by [*PIN*$^+$] or
1008 through other single- or multiprotein aggregates encompassing Rnq1 has yet to be established.
1009

1010 # Materials and Methods

1011 Most of the genetic and biochemical methods used for analysis of the [*PIN*$^+$] prion in yeast,
1012 especially those used in our laboratory, are described in a review by Liebman et al. (2006).
1013

1014 **Strains and Plasmids**

1015 ***Bacterial Strains.*** Unless specifically mentioned, strain DH5α was used (F$^-$ φ80*lacZΔM15*
1016 *Δ*(*lacZYA-argF*)*U169 recA1 endA1 hsdR17*(r_K^-, m_K^+) *phoA supE44* λ$^-$*thi*-1 *gyrA96 relA1*). Strain
1017 KC8 was used to select for the yeast *HIS3* and *LEU2* markers when transformed with DNA
1018 isolated from cells harboring more than one plasmid (*pyrF::Tn5, hsdR, leuB600, trpC9830,*
1019 *lacX74, strA, galUK, hisB436*). Strain BL21-AI was used for recombinant protein purification (F$^-$
1020 *omp*T *hsd*S_B (r_B^-, m_B^-) *gal dcm ara*B*::T7RNAP-tetA*).
1021

1022 ***Yeast Strains***. The original [*PIN*$^+$][*psi*$^-$] isolate of the yeast 74-D694 yeast strain (1Y1, aka
1023 L1749; aka "high multi-dot" [*PIN*$^+$]; Derkatch et al., 1997; Bradley et al., 2002) and its derivatives
1024 were used in all experiments. The genotype of 74-D694 is *MAT***a** *ade1-14* (UGA) *leu2-3,112*

1025 *his3-Δ200 trp1-289* (UAG) *ura3-52* (Chernoff et al., 1995). The 74-D694-based [*PIN*$^+$][*psi*$^-$] *rnq1-Δ*
1026 strain, YID108, and independently obtained isolates of this strain, YID146.2 and 146.3, were
1027 constructed as described in Kadnar et al. (2010). In these strains the entire *RNQ1* ORF and
1028 ~100 bp *RNQ1* terminator sequence is seamlessly disrupted, and [*PIN*$^+$] is maintained by the
1029 *CEN URA3* plasmid carrying the *RNQ1*$_{WT}$ ORF driven by the native *RNQ1* promoter and followed
1030 by the native *RNQ1* terminator sequence (RNQ1$_{WT;}$ pID127). We have previously confirmed
1031 (Kadnar et al., 2010) that in these strains Rnq1 is expressed at a level similar to that of
1032 endogenous Rnq1 and [*PIN*$^+$] is stably maintained (>99.5% stability). Unless specifically
1033 mentioned, the YID108, YID146.2, and YID146.3 strains also carry the *CEN HIS3 GAL-*
1034 *SUP35NM-YFP* plasmid (pID106; Kadnar et al., 2010) allowing the presence of [*PIN*$^+$] to be
1035 scored through the *de novo* [*PSI*$^+$] induction. When indicated, plasmids pID349 (ΔB1C2), pID341
1036 (ΔB1), pID342 (Δ2D), and pID344 (Δ3E) carrying *RNQ1*$_{WT}$ fragments were substituted for the full-
1037 length *RNQ1*$_{WT}$ as [*PIN*$^+$] maintainers in the YID146.3 strain (see Plasmids). We have previously
1038 demonstrated that these fragments are expressed at their expected sizes and can stably
1039 maintain the [*mini-PIN*$^+$] prions and promote [*PSI*$^+$] induction (Kadnar et al., 2010). Stable [*mini-*
1040 *PIN*$^+$] isolates with these maintainers, YID412, YID405, YID407, and YID409, respectively, are
1041 from the Kadnar et al. (2010) study.

1042 A [*pin*$^-$][*psi*$^-$] *rnq1-Δ* strain (YID193) used for analysis of the *de novo* [*PIN*$^+$] induction by
1043 overexpression of Rnq1$_{T27P}$ and analysis of the *de novo* aggregation of Rnq1$_{T27P}$-YFP in the
1044 *rnq1-Δ* background was obtained by selectively eliminating the *URA3* [*PIN*$^+$] maintainer from
1045 YID146.3 on FOA media while maintaining the *GAL-SUP3NM-YFP* [*PSI*$^+$] inducing plasmid. The
1046 [*pin*$^-$][*psi*$^-$] isolate of 74-D694 (1G4; Derkatch et al., 1997) obtained by curing the [*PIN*$^+$] prion on
1047 media containing 5mM GuHCl was used in experiments testing the *de novo* aggregation of
1048 Rnq1$_{T27P}$-YFP and Rnq1$_{WT}$-YFP in the presence of chromosomally encoded Rnq1$_{WT}$.

1049

1050 ***Plasmids***. All yeast plasmids used in this study include the same modules: promoters are *Eco*RI
1051 – *Bam*HI fragments, ORFs are *Bam*HI – *Sac*II fragments, and terminators / fluorescent tags are
1052 *Sac*II – *Sac*I fragments inserted into the poly-linkers of the pRS series plasmids (Sikorski and
1053 Hieter, 1989). Site-directed mutagenesis was done using the QuickChange kit (Stratagene)
1054 according to manufacturer's instructions and primers #360 and #361 (see Table S2).

1055 The pRS416-based *CEN URA3* (pID127) and the pRS415-based *LEU2 CEN* (pID129)
1056 plasmids carrying the $RNQ1_{WT}$ ORF driven by the native *RNQ1* promoter and followed by the
1057 native *RNQ1* terminator sequence ($RNQ1_{WT}$) are described in Kadnar et al. (2010). To make
1058 these plasmids, the *RNQ1* ORF was PCR amplified from 74-D694 chromosomal DNA. An earlier
1059 study (Kadnar et al., 2010) confirmed that from these constructs $Rnq1_{WT}$ is expressed at a level
1060 similar to that of the chromosomally encoded Rnq1 which allows for stable maintenance of [PIN^+]
1061 and does not lead to the induction of the *de novo* appearance of [PIN^+] in [pin^-] cells.

1062 The $RNQ1_{T27P}$ carrying plasmid and other plasmids in the library used for the genetic
1063 screen are pRS415-based, i.e. *LEU2 CEN*, and are identical to pID129 except for the
1064 mutagenized *RNQ1* ORFs. The $RNQ1_{T27P}$ carrying pID335 plasmid was obtained by site-directed
1065 mutagenesis of the pID219 plasmid.

1066 Plasmids carrying the T27P mutation within *RNQ1* fragments lacking the sequences
1067 encoding the indicated QN regions and adjacent hydrophobic helices within Rnq1 PD were
1068 constructed by site-directed mutagenesis introducing T27P into the constructs previously
1069 described in Kadnar et al. (2010): pID331 encoding $Rnq1_{\Delta B1C2\text{-}T27P}$ is based on the $Rnq1_{\Delta B1C2\text{-}WT}$
1070 (pID370; ΔB1C2) plasmid lacking QN1, QN2 and helices B and C; pID332 encoding $Rnq1_{\Delta B1\text{-}T27P}$
1071 – on the $Rnq1_{\Delta B1\text{-}WT}$ (pID369; ΔB1) plasmid lacking QN1 and helix B); pID333 encoding $Rnq1_{\Delta 2D\text{-}T27P}$
1072 – on the $Rnq1_{\Delta 2D\text{-}WT}$ (pID358; Δ2D) plasmid lacking QN2 and helix D; and pID334 encoding

1073 Rnq1$_{\Delta 3E\text{-}T27P}$ – on the Rnq1$_{\Delta 3E\text{-}WT}$ (pID387; Δ3E) plasmid lacking QN3 and helix E (Fig 1A). The
1074 pID370, pID369, pID358, and pID387 plasmids were used as controls for experiments with the
1075 corresponding abovementioned *LEU2* constructs carrying *RNQ1*$_{T27P}$. Except for deletions in the
1076 *RNQ1* PD these plasmids are identical to pID335 (RNQ$_{FL\text{-}T27P}$) and pID129 (RNQ$_{FL\text{-}WT}$),
1077 respectively: pRS415-based, *LEU2 CEN,* original *RNQ1* promoter and terminator. Plasmids
1078 pID349 (Rnq1$_{\Delta B1C2\text{-}WT}$), pID341 (Rnq1$_{\Delta B1\text{-}WT}$), pID342 (Rnq1$_{\Delta 2D\text{-}WT}$), and pID344 (Rnq1$_{\Delta 3E\text{-}WT}$) are
1079 identical to pID370, pID369, pID358, and pID387, respectively, except that, like pID127, they
1080 carry the *URA3* marker. These plasmids were used as [*PIN*$^{+}$] maintainers for experiments testing
1081 transmission barriers to Rnq1$_{FL\text{-}T27P}$ or Rnq1 fragments carrying Rnq1$_{T27P}$.
1082 To overexpress Rnq1$_{WT}$ and Rnq1$_{T27P}$, respectively, the pID336 and pID337 plasmids
1083 were constructed. Both plasmids are pRS416-based, *URA3*, *CEN* and the full-length ORFs are
1084 controlled by the *CUP1* promoter and followed by the original *RNQ1* terminator.
1085 In the pRS416-based *CEN LEU2 CUP-RNQ*$_{WT}$*-CFP* plasmid (pID121; Kadnar et al.,
1086 2010), a fusion of complete *RNQ1*$_{WT}$ ORF to *CFP*, is driven by the inducible *CUP1* promoter. The
1087 pRS415-based *URA3*-marked pID403 and pID404 plasmids are similar except they carry,
1088 respectively, *CUP-RNQ*$_{WT}$*-YFP* and *CUP-RNQ*$_{T27P}$*-YFP*.
1089 The pRS413-based *CEN HIS3 GAL-SUP35NM-YFP* plasmid (pID106, Kadnar et al.,
1090 2010) carries *SUP35NM-YFP* encoding the PD of the [*PSI*$^{+}$]-forming Sup35 protein fused to the
1091 YFP reporter and placed under control of the inducible *GAL1* promoter.
1092 Bacterial expression plasmids for Rnq1$_{WT}$ and Rnq1$_{T27P}$ are pJC45-based and express N-
1093 terminally 10xHIS tagged proteins. The ΔB1C2D3$_{WT}$ plasmid (pID257; aka QN4 only) and full-
1094 length RNQ1$_{WT}$ (pID249/250) constructs are described in Kadnar et al. (2010) and Vitrenko et al.
1095 (2007b), respectively. The ΔB1C2D3$_{WT}$ construct expresses the Rnq1NPD through the QG
1096 repeat region (aa1-172) fused to the helical region E and QN4 in the PD (aa 320-405); the fusion

1097 is seamless, *i.e* no additional amino acids are introduced in between. The ΔB1C2D3$_{T27P}$ and
1098 RNQ1$_{T27P}$ differ only by the T27P mutation that was introduced by site-directed mutagenesis into
1099 ΔB1C2D3$_{WT}$ and RNQ1$_{WT}$, respectively.
1100

1101 **Yeast Media and Cultivation**

1102 Standard yeast media and cultivation procedures were used (Sherman et al., 1987; Rose et al.,
1103 1990; Amberg et al., 2005). Unless specifically mentioned yeast transformants were grown at
1104 30^{0}C on solid synthetic glucose media selective for plasmid maintenance (e.g. SD-UraLeuHis). In
1105 addition to synthetic glucose SD-Ade media, synthetic ethanol SEt-Ade media supplemented
1106 with 2% ethanol as the only carbon source was used to score for [*PSI*$^+$] (see below).
1107 Untransformed strains and cultures for protein isolation were grown on complete glucose media,
1108 YPD. The *GAL* promoter was induced on solid synthetic media selective for plasmid
1109 maintenance and supplemented with 2% galactose as a single carbon source (e.g. SGal-
1110 LeuHis). The *CUP* promoter was induced by supplementing SD media selective for plasmid
1111 maintenance with the indicated concentration of $CuSO_4$ (5, 20 or 50µM; see Results and Figure
1112 Legends for details of specific experiments). To selectively eliminate plasmids with the *URA3*
1113 marker, yeast were passaged twice on solid SD supplemented with 5-fluoroorotic acid (5-FOA;
1114 Boeke et al., 1984) selective for other plasmids. Solid YPD supplemented with 5mM guanidine
1115 hydrochloride (GuHCl; Tuite et al., 1981) was used to cure the [*PSI*$^+$] and [*PIN*$^+$] prions.
1116 YPGlycerol media supplemented with 2% glycerol as a single carbon source was used to detect
1117 Pet$^-$ colonies that may be confused with [*PSI*$^+$] by color.
1118

1119 ***RNQ1* Mutagenesis and Genetic Screen**

1120 To mutagenize *RNQ1*, the complete 1.2 kb *RNQ1* ORF was PCR amplified from pID129 using
1121 *Taq* polymerase (New England Biolabs), primers # 7 and # 8 (see Table S2), and manufacturer's
1122 recommended reaction conditions, which was expected to yield ~1 mutation per 1,000 bps after
1123 32 cycles. To eliminate mutagenic bias from any one PCR reaction, seven independent PCR
1124 reactions were pooled. PCR products were digested with *Bam*HI and *Sac*II and re-introduced
1125 into the *Bam*HI- and *Sac*II- digested pID129 vector between the *RNQ1* promoter and *RNQ1*
1126 terminator sequences with a stop codon right after the *Sac*II site. Ligation reactions were
1127 transformed into *E. coli*. Approximately 30,600 transformant colonies were washed off with ~1
1128 ml LB from three transformant selection plates (banks pID142 – pID144) and ~200μl of
1129 suspensions were added to 50ml LB+Amp (30 mg/l) and grown for five hours at 37^0C prior to
1130 plasmid DNA isolation. Plasmid DNA was introduced into the YID108 yeast cells. Sequencing the
1131 *RNQ1* ORF from two randomly selected *E. coli* transformants with primers #119 and #8
1132 confirmed the presence of 1 mutation per the Rnq1 PD. At this estimated rate of mutagenesis,
1133 screening ~12,000 plasmids was expected to result in >95% chance of scoring all three possible
1134 nucleotide changes at each base.

1135 The genetic screen is described in Results and is illustrated in Fig 1B. Approximately 40
1136 patches of yeast transformants were analyzed per plate. Each plate had negative (EV) and
1137 positive (pID129) control transformants. Passages on all indicated media were by replica plating.
1138 Two passages on SD-LeuHis not selective for the *URA3 RNQ1*$_{WT}$ plasmid preceded replica
1139 plating to FOA to accumulate cells that lost this plasmid. Two passages on 5-FOA were sufficient
1140 for the selective elimination of all cells carrying the *URA3*-marked *RNQ1*$_{WT}$ plasmid (confirmed
1141 by replica plating to SD media lacking uracil). Induction of [*PSI*$^+$] was scored, after one and two
1142 passages on SGal-LeuHis, on SD-Ade at 30^0C and 20^0C and on SEt-Ade at 30^0C after up to 25
1143 days of incubation, which is sufficient for the detection of even the weakest [*PSI*$^+$] variants.

1144 No [*PSI*$^{+}$] induction was detected in ~500 transformants with mutated plasmids.
1145 Immediately excluded were the candidates that: (i) were Pet^{-} (detected as lack of growth on
1146 YPGlycerol to which all patches were also replica plated); (ii) carried *RNQ1*$_{MUTANT}$ plasmids
1147 lacking the full-length 1.2 kb *RNQ1* ORF insert (detected by PCR using primers #7 and #8 and
1148 total yeast DNA from after-shuffle cultures). Also, to exclude plasmids that carried frameshift
1149 mutations (usually -1) within the forward primer used to amplify the *RNQ1* ORF or stop codons in
1150 the very beginning of the ORF, a blue-white ligation-based assay was developed. The first ~100
1151 bps of the *RNQ1* ORF were PCR amplified using forward primers #127 or #124 and reverse
1152 primer #129 and cloned into the pUC18 plasmid as *Bcl*I – *Hin*dIII, *Bam*HI – *Hin*dIII, or *Bgl*II –
1153 *Hin*dIII fragments to create the in-frame, -1, and +1 fusions with the *lacZ* gene. The ligation
1154 mixes were transformed into the DH5α *E. coli* strain to test for the complementation of the
1155 φ80*lac*ZΔM15 allele. White or light blue color of most bacterial transformants on the LB+Amp
1156 media supplemented with 40μg/ml XGal was indicative of the disruption of LacZ synthesis in this
1157 particular frame. The test was validated by sequencing ~30 plasmids with presumptive early
1158 frameshift and nonsense mutations and >100 plasmids with no mutations in the beginning of the
1159 *RNQ1* ORF predicted by this assay.
1160 For the remaining candidates, the *RNQ1*$_{MUTANT}$ plasmids were isolated for further
1161 analysis. To selectively isolate only the *LEU2*-marked *RNQ1*$_{MUTANT}$ plasmids and not the *HIS3*-
1162 marked *GAL-SUP35NM-YFP* plasmids, the *E. coli* KC8 strain (see *Strains* above) was
1163 transformed with total yeast DNA extracts, and Leu^{+} transformants were selected on M9-based
1164 media lacking leucine. Digestion of plasmids with restriction endonucleases was used to exclude
1165 *RNQ1*$_{MUTANT}$ plasmids with re-arrangements outside of the *RNQ1* ORF. Then, for each
1166 candidate, DNA from at least two independent *E. coli* transformants was re-transformed into the
1167 original yeast strain and re-tested according to the same scheme as in the original screen (see

1168 Fig 1B); in total, at least 12 yeast transformants were tested for each candidate. The re-
1169 transformation test provided proof that a mutation in the *RNQ1*$_{MUTANT}$ plasmid was the cause of
1170 the Pin$^-$ phenotype in the after-shuffle cultures. Alternatively, the Pin$^-$ phenotype could be either
1171 due to spontaneous loss of the [*PIN*$^+$] prion (0.2 – 0.5% in control experiments where the
1172 *RNQ1*$_{WT}$ plasmid was shuffled-in) or due to chromosomal mutations e.g. either eliminating [*PIN*$^+$]
1173 or inhibiting [*PSI*$^+$] induction. Primers #7, #8, #17, #18, #19, and #30 were used to sequence the
1174 *RNQ1* ORF and adjacent promoter and terminator regions (see Table S2).
1175

1176 **Scoring for the presence of the [*PIN*$^+$] prion and Pin phenotype**

1177 Induction of the *de novo* appearance of the [*PSI*$^+$] prion upon overexpression of the PD of the
1178 Sup35 protein, Sup35NM, was used to score for the presence of [*PIN*$^+$] (see Liebman et al.,
1179 2006). The assay is based on our finding that [*PIN*$^+$] is required for the efficient induction of [*PSI*$^+$]
1180 (Derkatch et al., 1997). In [*PIN*$^+$] cells expressing Sup35NM-YFP at an ~5-fold increased level
1181 compared to the expression of endogenous Sup35 for ~10 cell generations, [*PSI*$^+$] forms in ~10%
1182 cells, whereas appearance of [*PSI*$^+$] in [*pin*$^-$] cultures is extremely rare, $<10^{-4}$. Transformants
1183 carrying the *CEN HIS3 GAL-SUP35NM-YFP* [*PSI*$^+$] inducing construct and other indicated
1184 plasmids were grown on SD media selective for all the plasmids and then replica plated onto the
1185 inducing SGal media, also selective for all the plasmids. Growth on SGal was for 2 days (5-7
1186 generations), a second passage on SGal was done to increase the number of generations and
1187 thus the chance of [*PSI*$^+$] induction. As a negative control, the same cultures were passaged on
1188 non-inducing SD media and then analyzed in parallel with induced cultures. Three methods were
1189 used to score for the appearance of [*PSI*$^+$].
1190 **(1)** For qualitative/semi-quantitative analysis, yeast were replica plated from SGal (or
1191 control SD) media onto SD media lacking adenine and not selective for plasmids. An Ade$^+$

1192 phenotype after SGal and not after SD is indicative of [*PSI*$^+$] induction. Growth of [*PSI*$^+$] cells on
1193 adenineless media is due to suppression of a premature UGA stop codon in the *ADE1* gene
1194 present in our strains (*ade1-14*). The nonsense suppression is due to the sequestration of the
1195 chromosomally encoded full-length Sup35 protein, a translation termination factor, into the [*PSI*$^+$]
1196 prion aggregates initiated by Sup35NM-YFP overexpression. For all such experiments, both SD-
1197 Ade and SEt-Ade media were used. Cultures on SD-Ade were incubated at 30^{0}C and 20^{0}C;
1198 cultures on SEt-Ade were incubated at 30^{0}C. Growth was recorded multiple times between 3 and
1199 25 days of incubation. This approach allows detection of [*PSI*$^+$] variants of different strengths
1200 (some very weak [*PSI*$^+$] variants grow only on SEt-Ade or at lower temperatures, and only after a
1201 very long incubation).

1202 **(2)** For quantitative analysis, yeast were colony purified on YPD from galactose (or
1203 control glucose) media. On YPD, [*PSI*$^+$] cells form white or pink colonies whereas [*psi*$^-$] cells are
1204 red due to the accumulation of a red pigment from the adenine precursor accumulating in the
1205 *ade1-14* cells. The appearance of white and pink Ade$^+$ colonies (among red Ade$^-$ colonies)
1206 following Sup35NM-YFP overexpression is indicative of [*PSI*$^+$] induction.

1207 However, nonsense suppression and white color in (1) and (2) can also be caused by
1208 genomic mutations in *SUP35* and other genes. Such genomic mutations are rare compared to
1209 the induced [*PSI*$^+$] *de novo* formation in [*PIN*$^+$] cultures. Yet, and especially in cultures where only
1210 a few Ade$^+$ or white / pink colonies were detected, such colonies were confirmed to be [*PSI*$^+$]. For
1211 the GuHCl test, white / pink colonies were patched onto YPD, then passaged three times on
1212 YPD+5mM GuHCl and then returned to YPD. Because GuHCl cures [*PSI*$^+$] (Tuite et al., 1981),
1213 [*PSI*$^+$] patches turn red on GuHCl media and remain red when returned to YPD. Chromosomal
1214 mutants may turn red on GuHCl (Bradley et al., 2003) but return to their white or pink color once
1215 back on YPD. Alternatively, for colonies that retained the *HIS3 GAL-SUP35NM-YFP* plasmid, the

1216 presence of [*PSI*$^+$] was confirmed by fluorescence microscopy: after an overnight growth on
1217 SGal-His media, dot-shaped foci are detected in most cells in [*PSI*$^+$] cultures.
1218 **(3)** To directly visualize newly forming [*PSI*$^+$]s, yeast cells from SGal media were
1219 analyzed by fluorescent microscopy utilizing the YFP tag attached to Sup35NM in the [*PSI*$^+$]
1220 inducing construct. Newly forming [*PSI*$^+$]s can be seen as ring-, line- or dot-shaped foci; cells
1221 with already established [*PSI*$^+$] have dot foci; in [*psi*$^-$] cells fluorescence is evenly distributed
1222 (Patino et al., 1996; Zhou et al., 2001).
1223

1224 **Assessing the [*PSI*$^+$] prion variants**

1225 To assess the arrays of the [*PSI*$^+$] prion variants induced in cells expressing $Rnq1_{T27P}$ *vs* $Rnq1_{WT}$,
1226 the Ade$^+$ cells from patches replica plated from SGal to SD-Ade [*PSI*$^+$] selective media and
1227 grown for 25 days at 20^{0}C were thoroughly scraped and colony purified on YPD and individual
1228 colonies were randomly picked up from YPD for further analysis before color had developed. At
1229 least 12 transformants were analyzed for either $Rnq1_{T27P}$ or $Rnq1_{WT}$. The same approach was
1230 used to obtain [*PSI*$^+$]s appearing in [*pin*$^-$] cultures carrying EV. Alternatively, yeast were colony
1231 purified on YPD from the second pass on SGal-LeuHis media, where [*PSI*$^+$]s were induced.
1232 Three assays were used to assess [*PSI*$^+$] strength. **(1)** Color on YPD (the lighter the color, the
1233 stronger the [*PSI*$^+$] variant). **(2)** Growth on adenineless media: SD-Ade at 30^{0}C and at 20^{0}C, and
1234 SEt-Ade at 30^{0}C (the more robust the Ade$^+$ phenotype, the stronger the [*PSI*$^+$]). **(3)** Efficiency of
1235 curing by GuHCl: after three passages on YPD+GuHCl yeast were replica plated onto the same
1236 set of adenineless media as in (**2**). While weak [*PSI*$^+$]s were usually cured completely, occasional
1237 Ade$^+$ colonies were detected for stronger [*PSI*$^+$]s.
1238

1239 **Analysis of the *de novo* induction of [*PIN*$^+_{T27P}$]**

1240 Both variants of this experiment are succinctly explained in Results related to Figs 3A and B. See
1241 Supplementary Materials and Methods for plasmid numbers and details on controls.
1242

1243 **Plasmid stability analysis**

1244 To compare stability of the Rnq1 expressing plasmids in yeast transformants carrying the *CEN*
1245 *URA3 RNQ1*$_{WT}$ and *CEN LEU2 RNQ1*$_{T27P}$ plasmids *vs* transformants carrying two *RNQ1*$_{WT}$
1246 plasmids (*CEN URA3* and *CEN LEU2*) or a *RNQ1*$_{WT}$ (*CEN URA3*) plasmid and the EV (*CEN*
1247 *LEU2*), fresh transformants were patched onto SD-UraLeu media selective for both plasmids,
1248 then passaged twice on media selective for only one of the plasmids (SD-Ura or SD-Leu), then
1249 colony purified on the same media and replica plated to both that media and to the reciprocal
1250 media. Plasmid stability was determined as the fraction of colonies grown on the reciprocal
1251 media where only colonies formed by cells retaining the plasmid despite of the lack of selection
1252 were expected to grow.
1253

1254 **Western Blot Analysis of Rnq1$_{T27P}$ expression in yeast**

1255 Yeast cell lysates were prepared essentially as described in Liebman et al. (2006) and Kadnar et
1256 al. (2010). See Supplementary Materials and Methods for a detailed protocol. Either 30 or 60μg
1257 of total protein (concentration determined with BCA™ Protein Assay Kit, Pierce) were separated
1258 on SDS-PAGE gels. Rnq1 was detected by Western blot with polyclonal antibodies raised in
1259 rabbits against the first 185 aa of Rnq1 (type 1A, a kind gift from E. Craig, University of
1260 Wisconsin-Madison). Sup35 was detected with a monoclonal antibody against the Sup35C
1261 raised in mouse (BE4). HRP-conjugated anti-rabbit and anti-mouse secondary antibodies and
1262 the Super Signal Western PICO ECL kit (Pierce) were used for detection.
1263

1264 **Recombinant protein purification from *E. coli***

1265 Recombinant protein purification was essentially as described in Kadnar et al. (2010). See
1266 Supplementary Materials and Methods for a detailed protocol. Protein concentration was
1267 determined by the BCA™ Protein Assay Kit (Pierce). Purity of recombinant proteins was
1268 estimated by SDS-PAGE as >95% (see Fig 4A).

1269

1270 **Analysis of *in vitro* fiber formation**

1271 Analysis of *in vitro* fiber formation by $Rnq1_{WT}$ and $Rnq1_{T27P}$ was performed essentially as in
1272 Kadnar et al. (2010). Specifically, 200 μl reactions were assembled in the fiber formation buffer
1273 (1M urea, final concentration; 100mM NaH_2PO_4, pH 7.4; 300mM NaCl) in the presence of 5 μM
1274 thioflavin T (ThT). Fiber formation was monitored by ThT fluorescence (LeVine, 1999) in a
1275 Molecular Devices SpectraMax M-5 plate reader at RT (λ_{ex}=450 nm; λ_{em}=483 nm). Readings
1276 were taken every 15 min, samples were shaken for 5 sec prior to each reading.

1277

1278 **Transmission Electron Microscopy (TEM)**

1279 TEM was performed at the Image Core Facility at the NYU School of Medicine. Following
1280 incubation to allow for amyloid fiber formation, protein / fiber suspensions were diluted 2.5-fold in
1281 water. Then 4 μl of diluted suspensions were applied to carbon-coated 400 mesh Cu/Rh grids
1282 (Ted Pella Inc.). Grids were washed 3 times with water to get rid of urea present in the fiber
1283 formation buffer. Then grids were negatively stained at 25^0C with 1% uranyl acetate (applied
1284 twice briefly and then for 5 min). Images were captured using Philips CM12 TEM supplied with a
1285 Gatan 1k61k digital camera and processed using the Gatan Digital Micrograph software.

1286

1287 **Fluorescence Microscopy, ThT staining, and 1,6 Hexanediol treatment**

1288 Cells were observed using a Nikon Eclipse E600 microscope with a 60x / 1.4 NA oil immersion
1289 objective. YFP and CFP filters were used to observe YFP- and CFP-tagged constructs,
1290 respectively. Fluorescent and brightfield images of the same field were captured with a Zeiss
1291 AxioCam MRm digital camera and processed with AxioVision AxioVs40 V 4.8.2.0 software. In all
1292 experiments, representative groups of cells were scored, including cells of different sizes, with
1293 and without buds and with different levels of construct expression. For Rnq1 aggregation
1294 analysis, cells from at least three transformants were counted, at least 250 cells from each. For
1295 analysis of Sup35NM-YFP aggregation shown in Table 1 and Fig 2C, at least 11 vision fields
1296 were scored for each construct, ~500 cells total per construct, while qualitative assessment of
1297 aggregation was done on a much larger scale. ImageJ software was used for cell counting.
1298 Photoshop was used for merging and adjusting images (only brightness and contrast were
1299 adjusted, no other processing). For all images shown, differences in cell size, budding and
1300 fluorescence intensity are within population variability range.
1301 Staining with thioflavin T (ThT) was done essentially as described in Douglas et al.
1302 (2008). See Supplementary Materials and Methods for a detailed protocol. The CFP filter was
1303 used for ThT fluorescence analysis.
1304 To dissolve liquid-like droplets with 1,6 Hexanediol (Hex), yeast transformants were
1305 grown overnight in liquid SD media selective for all plasmids. Then OD_{595} was adjusted to 1.0,
1306 $CuSO_4$ was added to 5μM, and cultures were grown for two more hrs. Cells were harvested,
1307 resuspended in 100 – 500μl of the same SD media with 10% Hex (Fisher) and 0.2μg/μl digitonin
1308 (Sigma; 200 mg/ml stock in water) and incubated on a shaker for 10 min at 30^0C. Then cells
1309 were centrifuged, resuspended in the same SD, and imaged using the filter matching the Rnq1
1310 fluorescent tag.
1311

1312 **Statistics**

1313 Standard methods of statistical analysis were used. Averages and Standard Deviations
1314 (STDEV.S) were calculated in Excell (16.105.2 and earlier versions). Unless specifically
1315 mentioned, SD is included. Standard Error of the Mean (SEM) was calculated by dividing
1316 STDEV.S by square root of the number of datapoints. Excell and GraphPad Prism
1317 (10.6.1(892))were used for graphs. Statistics Kingdom (statisticskingdom.com) was used for T-
1318 tests (two sample Welch's T-test; unknown / unequal SD). Unless specifically mentioned, the
1319 cutoff for the significance of variation was $p<0.01$.

1320

1321 **Acknowledgements**

1322 We thank Elizabeth Craig for providing the anti-Rnq1 antibody. We are grateful to Gulnara
1323 Articov for help with *in-vitro* experiments and to Alice Liang and Eric Roth at the NYU School of
1324 Medicine Image Core Facility for performing TEM. We also thank Sei-Kyoung Park for helpful
1325 discussions of the data.

1326 **Funding statement**

1327 This work was supported by grants from NIH - R01 GM070934-06 (ILD) and MIRA
1328 1R35GM136229-05 (SWL). National Science Foundation - 0518482 (ILD), and US Army – ARO
1329 W911NF-23-1-0122 (ILD). The funders had no role in study design, data collection and
1330 analysis, decision to publish, or preparation of the manuscript.

1331

1332 **Conflicts of Interest Statement:** The authors declare no conflicts of interest.

1333 **Data availability**

1334 The authors confirm that all data underlying the findings are fully available without
1335 restriction. All relevant data are within the paper and its Supporting Information files.

1336 **Author Contributions**

1337 Conceived and designed the experiments: ILD. Performed the experiments: SP, DMM, MLK, MA,
1338 APF, ILD. Analyzed the data: SP, MLK, SWL, ILD. Contributed reagents/materials/analysis tools:
1339 ILD, SWL. Wrote the manuscript: ILD, SWL.

1340

1341 **References**

1342 Afanasieva EG, Kushnirov VV, Tuite MF, Ter-Avanesyan MD. Molecular basis for transmission barrier and
1343 interference between closely related prion proteins in yeast. J Biol Chem. 2011 May 6;286(18):15773-80.
1344 doi: 10.1074/jbc.M110.183889. Epub 2011 Mar 15. PMID: 21454674; PMCID: PMC3091186.

1345 Amberg, D.C., Burke, D., Strathern, J.N., and Cold Spring Harbor Laboratory. (2005). Methods in yeast
1346 genetics: a Cold Spring Harbor Laboratory course manual, 2005 edn (Cold Spring Harbor, N.Y., Cold
1347 Spring Harbor Laboratory Press).

1348 Ayers JI, Paras NA, Prusiner SB. Expanding spectrum of prion diseases. Emerg Top Life Sci. 2020 Sep
1349 8;4(2):155-167. Doi: 10.1042/ETLS20200037. PMID: 32803268.

1350 Barbitoff YA, Matveenko AG, Zhouravleva GA. Differential Interactions of Molecular Chaperones and
1351 Yeast Prions. J Fungi (Basel). 2022 Jan 27;8(2):122. Doi: 10.3390/jof8020122. PMID: 35205876; PMCID:
1352 PMC8877571.

1353 Bardill JP, True HL. Heterologous prion interactions are altered by mutations in the prion protein Rnq1p. J
1354 Mol Biol. 2009 May 8;388(3):583-96. doi: 10.1016/j.jmb.2009.03.036. Epub 2009 Mar 24. PMID:
1355 19324054; PMCID: PMC2706087.

1356 Baskakov IV. The many shades of prion strain adaptation. Prion. 2014 Mar-Apr;8(2):169–72. doi:
1357 10.4161/pri.27836. Epub 2014 Feb 11. PMID: 24518385; PMCID: PMC4189885.

1358 Bateman DA, Wickner RB. [PSI+] Prion transmission barriers protect Saccharomyces cerevisiae from
1359 infection: intraspecies 'species barriers'. Genetics. 2012 Feb;190(2):569-79. doi:
1360 10.1534/genetics.111.136655. Epub 2011 Nov 17. PMID: 22095075; PMCID: PMC3276615.

1361 Bateman DA, Wickner RB. The [PSI+] prion exists as a dynamic cloud of variants. PLoS Genet.
1362 2013;9(1):e1003257. doi: 10.1371/journal.pgen.1003257. Epub 2013 Jan 31. Erratum in: PLoS Genet.
1363 2017 Feb 3;13(2):e1006591. doi: 10.1371/journal.pgen.1006591. PMID: 23382698; PMCID: PMC3561065.

1364 Béringue V, Vilotte JL, Laude H. Prion agent diversity and species barrier. Vet Res. 2008 Jul-Aug;39(4):47.
1365 Doi: 10.1051/vetres:2008024. Epub 2008 Jun 3. PMID: 18519020.

1366 Bessen RA, Marsh RF. Identification of two biologically distinct strains of transmissible mink
1367 encephalopathy in hamsters. J Gen Virol. 1992 Feb;73 (Pt 2):329-34. Doi: 10.1099/0022-1317-73-2-329.
1368 PMID: 1531675.

1369 Bessen RA, Kocisko DA, Raymond GJ, Nandan S, Lansbury PT, Caughey B. Non-genetic propagation of

1370 strain-specific properties of scrapie prion protein. Nature. 1995 Jun 22;375(6533):698-700. Doi:
1371 10.1038/375698a0. PMID: 7791905.

1372 Bharathi V, Girdhar A, Prasad A, Verma M, Taneja V, Patel BK. Use of ade1 and ade2 mutations for
1373 development of a versatile red/white colour assay of amyloid-induced oxidative stress in saccharomyces
1374 cerevisiae. Yeast. 2016 Dec;33(12):607-620. Doi: 10.1002/yea.3209. Epub 2016 Oct 13. PMID: 27654890.

1375 Boeke JD, LaCroute F, Fink GR. A positive selection for mutants lacking orotidine-5'-phosphate
1376 decarboxylase activity in yeast: 5-fluoro-orotic acid resistance. Mol Gen Genet. 1984;197(2):345-6. Doi:
1377 10.1007/BF00330984. PMID: 6394957.

1378 Borkhsenius AS, Sasnauskas K, Gedvilaĭte A, Inge-Vechtomov SG. Khimernye priony drozhzheĭ s
1379 nestabil'nym nasledovaniem [Chimeric yeast prions with unstable inheritance]. Genetika. 2002
1380 Mar;38(3):300-5. Russian. PMID: 11963556.

1381 Bradley ME, Edskes HK, Hong JY, Wickner RB, Liebman SW. Interactions among prions and prion
1382 "strains" in yeast. Proc Natl Acad Sci U S A. 2002 Dec 10;99 Suppl 4(Suppl 4):16392-9. Doi:
1383 10.1073/pnas.152330699. Epub 2002 Jul 30. PMID: 12149514; PMCID: PMC139899.

1384

1385 Bradley ME, Liebman SW. Destabilizing interactions among [PSI(+)] and [PIN(+)] yeast prion variants.
1386 Genetics. 2003 Dec;165(4):1675-85. Doi: 10.1093/genetics/165.4.1675. Erratum in: Genetics. 2011
1387 Aug;188(4):1023. PMID: 14704158; PMCID: PMC1462903.

1388 Bradley ME, Bagriantsev S, Vishveshwara N, Liebman SW. Guanidine reduces stop codon read-through
1389 caused by missense mutations in SUP35 or SUP45. Yeast. 2003 May;20(7):625-32. Doi: 10.1002/yea.985.
1390 PMID: 12734800.

1391 Chang HY, Lin JY, Lee HC, Wang HL, King CY. Strain-specific sequences required for yeast [PSI+] prion
1392 propagation. Proc Natl Acad Sci U S A. 2008 Sep 9;105(36):13345-50. doi: 10.1073/pnas.0802215105.
1393 Epub 2008 Aug 29. PMID: 18757753; PMCID: PMC2533192.

1394 Chen B, Newnam GP, Chernoff YO. Prion species barrier between the closely related yeast proteins is
1395 detected despite coaggregation. Proc Natl Acad Sci U S A. 2007 Feb 20;104(8):2791-6. doi:
1396 10.1073/pnas.0611158104. Epub 2007 Feb 12. PMID: 17296932; PMCID: PMC1815260.

1397 Chen B, Bruce KL, Newnam GP, Gyoneva S, Romanyuk AV, Chernoff YO. Genetic and epigenetic control
1398 of the efficiency and fidelity of cross-species prion transmission. Mol Microbiol. 2010 Jun;76(6):1483-99.
1399 doi: 10.1111/j.1365-2958.2010.07177.x. Epub 2010 Apr 23. PMID: 20444092; PMCID: PMC3025758.

1400 Chernoff YO, Lindquist SL, Ono B, Inge-Vechtomov SG, Liebman SW. Role of the chaperone protein
1401 Hsp104 in propagation of the yeast prion-like factor [psi+]. Science. 1995 May 12;268(5212):880-4. doi:
1402 10.1126/science.7754373. PMID: 7754373.

1403 Chuang E, Hori AM, Hesketh CD, Shorter J. Amyloid assembly and disassembly. J Cell Sci. 2018 Apr
1404 13;131(8):jcs189928. doi: 10.1242/jcs.189928. PMID: 29654159; PMCID: PMC5963839.

1405 Collinge J, Clarke AR. A general model of prion strains and their pathogenicity. Science. 2007 Nov
1406 9;318(5852):930-6. doi: 10.1126/science.1138718. PMID: 17991853.

1407 Collinge J. Cell biology. The risk of prion zoonoses. Science. 2012 Jan 27;335(6067):411-3. doi:
1408 10.1126/science.1218167. PMID: 22282797.

1409 DePace AH, Santoso A, Hillner P, Weissman JS. A critical role for amino-terminal glutamine/asparagine
1410 repeats in the formation and propagation of a yeast prion. Cell. 1998 Jun 26;93(7):1241-52. doi:
1411 10.1016/s0092-8674(00)81467-1. PMID: 9657156.

1412 Derkatch IL, Chernoff YO, Kushnirov VV, Inge-Vechtomov SG, Liebman SW. Genesis and variability of
1413 [PSI] prion factors in Saccharomyces cerevisiae. Genetics. 1996 Dec;144(4):1375-86. doi:
1414 10.1093/genetics/144.4.1375. PMID: 8978027; PMCID: PMC1207691.

1415 Derkatch IL, Bradley ME, Zhou P, Chernoff YO, Liebman SW. Genetic and environmental factors affecting
1416 the de novo appearance of the [PSI+] prion in Saccharomyces cerevisiae. Genetics. 1997 Oct;147(2):507-
1417 19. doi: 10.1093/genetics/147.2.507. PMID: 9335589; PMCID: PMC1208174.

1418 Derkatch IL, Bradley ME, Liebman SW. Overexpression of the SUP45 gene encoding a Sup35p-binding
1419 protein inhibits the induction of the de novo appearance of the [PSI+] prion. Proc Natl Acad Sci U S A.
1420 1998 Mar 3;95(5):2400-5. doi: 10.1073/pnas.95.5.2400. PMID: 9482897; PMCID: PMC19355.

1421 Derkatch IL, Bradley ME, Zhou P, Liebman SW. The PNM2 mutation in the prion protein domain of SUP35
1422 has distinct effects on different variants of the [PSI+] prion in yeast. Curr Genet. 1999 Mar;35(2):59-67. doi:
1423 10.1007/s002940050433. PMID: 10079323.

1424 Derkatch IL, Bradley ME, Masse SV, Zadorsky SP, Polozkov GV, Inge-Vechtomov SG, Liebman SW.
1425 Dependence and independence of [PSI+] and [PIN+]: a two-prion system in yeast? EMBO J. 2000 May
1426 2;19(9):1942-52. doi: 10.1093/emboj/19.9.1942. PMID: 10790361; PMCID: PMC305693.

1427 Derkatch IL, Bradley ME, Hong JY, Liebman SW. Prions affect the appearance of other prions: the story of
1428 [PIN(+)]. Cell. 2001 Jul 27;106(2):171-82. doi: 10.1016/s0092-8674(01)00427-5. PMID: 11511345.

1429 Derkatch IL, Liebman SW. Prion-prion interactions. Prion. 2007 Jul-Sep;1(3):161-9. doi:
1430 10.4161/pri.1.3.4837. Epub 2007 Jul 6. PMID: 19164893; PMCID: PMC2634589.

1431 DiSalvo S, Derdowski A, Pezza JA, Serio TR. Dominant prion mutants induce curing through pathways
1432 that promote chaperone-mediated disaggregation. Nat Struct Mol Biol. 2011 Apr;18(4):486-92. doi:
1433 10.1038/nsmb.2031. Epub 2011 Mar 20. PMID: 21423195; PMCID: PMC3082495.

1434 Dobson CM. The Amyloid Phenomenon and Its Links with Human Disease. Cold Spring Harb Perspect
1435 Biol. 2017 Jun 1;9(6):a023648. doi: 10.1101/cshperspect.a023648. PMID: 28062560; PMCID:
1436 PMC5453392.

1437 Douglas PM, Treusch S, Ren HY, Halfmann R, Duennwald ML, Lindquist S, Cyr DM. Chaperone-
1438 dependent amyloid assembly protects cells from prion toxicity. Proc Natl Acad Sci U S A. 2008 May
1439 20;105(20):7206-11. doi: 10.1073/pnas.0802593105. Epub 2008 May 14. PMID: 18480252; PMCID:
1440 PMC2438228.

1441 Du Z, Park KW, Yu H, Fan Q, Li L. Newly identified prion linked to the chromatin-remodeling factor Swi1 in
1442 Saccharomyces cerevisiae. Nat Genet. 2008 Apr;40(4):460-5. doi: 10.1038/ng.112. Epub 2008 Mar 23.
1443 PMID: 18362884; PMCID: PMC2633598.

1444 Du Z, Goncharoff DK, Cheng X, Li L. Analysis of [SWI^{+}] formation and propagation events. Mol Microbiol.

1445 2017 Apr;104(1):105-124. doi: 10.1111/mmi.13616. Epub 2017 Jan 26. PMID: 28035761; PMCID:
1446 PMC5364053.

1447 Edskes HK, Gray VT, Wickner RB. The [URE3] prion is an aggregated form of Ure2p that can be cured by
1448 overexpression of Ure2p fragments. Proc Natl Acad Sci U S A. 1999 Feb 16;96(4):1498-503. doi:
1449 10.1073/pnas.96.4.1498. PMID: 9990052; PMCID: PMC15494.

1450 Edskes HK, McCann LM, Hebert AM, Wickner RB. Prion variants and species barriers among
1451 Saccharomyces Ure2 proteins. Genetics. 2009 Mar;181(3):1159-67. doi: 10.1534/genetics.108.099929.
1452 Epub 2009 Jan 5. PMID: 19124570; PMCID: PMC2651050.

1453 Edskes HK, Mukhamedova M, Edskes BK, Wickner RB. *Hermes* Transposon Mutagenesis Shows [URE3]
1454 Prion Pathology Prevented by a Ubiquitin-Targeting Protein: Evidence for Carbon/Nitrogen Assimilation
1455 Cross Talk and a Second Function for Ure2p in *Saccharomyces cerevisiae*. Genetics. 2018
1456 Jul;209(3):789-800. doi: 10.1534/genetics.118.300981. Epub 2018 May 16. PMID: 29769283; PMCID:
1457 PMC6028256.

1458 Fomicheva A, Ross ED. From Prions to Stress Granules: Defining the Compositional Features of Prion-
1459 Like Domains That Promote Different Types of Assemblies. Int J Mol Sci. 2021 Jan 27;22(3):1251. doi:
1460 10.3390/ijms22031251. PMID: 33513942; PMCID: PMC7865556.

1461 Fuentealba RA, Udan M, Bell S, Wegorzewska I, Shao J, Diamond MI, Weihl CC, Baloh RH. Interaction
1462 with polyglutamine aggregates reveals a Q/N-rich domain in TDP-43. J Biol Chem. 2010 Aug
1463 20;285(34):26304-14. doi: 10.1074/jbc.M110.125039. Epub 2010 Jun 16. PMID: 20554523; PMCID:
1464 PMC2924052.

1465 Galliamov AA, Malukhina AD, Kushnirov VV. Mapping of Prion Structures in the Yeast Rnq1. Int J Mol Sci.
1466 2024 Mar 17;25(6):3397. doi: 10.3390/ijms25063397. PMID: 38542372; PMCID: PMC10970677.

1467 Galliamov AA, Urakov VN, Dergalev AA, Kushnirov VV. On the Significance of the Terminal Location of
1468 Prion-Forming Regions of Yeast Proteins. Int J Mol Sci. 2025 Feb 14;26(4):1637. doi:
1469 10.3390/ijms26041637. PMID: 40004101; PMCID: PMC11855515.

1470 Halfmann R, Jarosz DF, Jones SK, Chang A, Lancaster AK, Lindquist S. Prions are a common mechanism
1471 for phenotypic inheritance in wild yeasts. Nature. 2012 Feb 15;482(7385):363-8. doi:
1472 10.1038/nature10875. PMID: 22337056; PMCID: PMC3319070.

1473 Hill AF, Desbruslais M, Joiner S, Sidle KC, Gowland I, Collinge J, Doey LJ, Lantos P. The same prion
1474 strain causes vCJD and BSE. Nature. 1997 Oct 2;389(6650):448-50, 526. doi: 10.1038/38925. PMID:
1475 9333232.

1476 Hill AF, Collinge J. Strain variations and species barriers. Contrib Microbiol. 2001;7:48-57. doi:
1477 10.1159/000060375. PMID: 11923935.

1478 Hoshino S, Imai M, Kobayashi T, Uchida N, Katada T. The eukaryotic polypeptide chain releasing factor
1479 (eRF3/GSPT) carrying the translation termination signal to the 3 -poly(A) tail of mRNA. J Biol Chem
1480 1999;274:16677–80.

1481 Hosoda N, Kobayashii T, Uchida N, Funakoshi Y, Kikuchi Y, Hoshino S, et al. Translation termination
1482 factor eRF3 mediates mRNA decay through the regulation of deadenylation. J Biol Chem
1483 2003;278:38287–91.

1484 Houston F, Andréoletti O. Animal prion diseases: the risks to human health. Brain Pathol. 2019

1485 Mar;29(2):248-262. doi: 10.1111/bpa.12696. Epub 2019 Jan 22. PMID: 30588682; PMCID: PMC8028554.

1486 Huang VJ, Stein KC, True HL. Spontaneous variants of the [RNQ+] prion in yeast demonstrate the
1487 extensive conformational diversity possible with prion proteins. PLoS One. 2013 Oct 25;8(10):e79582. doi:
1488 10.1371/journal.pone.0079582. PMID: 24205387; PMCID: PMC3808357.

1489 Igel-Egalon A, Béringue V, Rezaei H, Sibille P. Prion Strains and Transmission Barrier Phenomena.
1490 Pathogens. 2018 Jan 1;7(1):5. doi: 10.3390/pathogens7010005. PMID: 29301257; PMCID: PMC5874731.

1491 Joshi T, Ahuja N. The Prion Basis of Progressive Neurodegenerative Disorders. Interdiscip Perspect Infect
1492 Dis. 2023 Feb 14;2023:6687264. doi: 10.1155/2023/6687264. PMID: 36825209; PMCID: PMC9943612.

1493 Kadnar ML, Articov G, Derkatch IL. Distinct type of transmission barrier revealed by study of multiple prion
1494 determinants of Rnq1. PLoS Genet. 2010 Jan 22;6(1):e1000824. doi: 10.1371/journal.pgen.1000824.
1495 PMID: 20107602; PMCID: PMC2809767.

1496 Ke PC, Zhou R, Serpell LC, Riek R, Knowles TPJ, Lashuel HA, Gazit E, Hamley IW, Davis TP, Fändrich
1497 M, Otzen DE, Chapman MR, Dobson CM, Eisenberg DS, Mezzenga R. Half a century of amyloids: past,
1498 present and future. Chem Soc Rev. 2020 Aug 7;49(15):5473-5509. doi: 10.1039/c9cs00199a. Epub 2020
1499 Jul 7. PMID: 32632432; PMCID: PMC7445747.

1500 Kelly AC, Shewmaker FP, Kryndushkin D, Wickner RB. Sex, prions, and plasmids in yeast. Proc Natl Acad
1501 Sci U S A. 2012 Oct 2;109(40):E2683-90. doi: 10.1073/pnas.1213449109. Epub 2012 Sep 4. PMID:
1502 22949655; PMCID: PMC3479589.

1503 Kelly AC, Wickner RB. Saccharomyces cerevisiae: a sexy yeast with a prion problem. Prion. 2013 May-
1504 Jun;7(3):215-20. doi: 10.4161/pri.24845. PMID: 23764836; PMCID: PMC3783106.

1505 Kelly AC, Busby B, Wickner RB. Effect of domestication on the spread of the [PIN+] prion in
1506 Saccharomyces cerevisiae. Genetics. 2014 Jul;197(3):1007-24. doi: 10.1534/genetics.114.165670. Epub
1507 2014 May 8. PMID: 24812307; PMCID: PMC4096356.

1508 King CY. The Mutability of Yeast Prions. Viruses. 2022 Oct 25;14(11):2337. doi: 10.3390/v14112337.
1509 PMID: 36366434; PMCID: PMC9696419.

1510 Kochneva-Pervukhova NV, Paushkin SV, Kushnirov VV, Cox BS, Tuite MF, Ter-Avanesyan MD.
1511 Mechanism of inhibition of Psi+ prion determinant propagation by a mutation of the N-terminus of the yeast
1512 Sup35 protein. EMBO J. 1998 Oct 1;17(19):5805-10. doi: 10.1093/emboj/17.19.5805. PMID: 9755180;
1513 PMCID: PMC1170908.

1514 Kurahashi H, Ishiwata M, Shibata S, Nakamura Y. A regulatory role of the Rnq1 nonprion domain for prion
1515 propagation and polyglutamine aggregates. Mol Cell Biol. 2008 May;28(10):3313-23. doi:
1516 10.1128/MCB.01900-07. Epub 2008 Mar 10. PMID: 18332119; PMCID: PMC2423166.

1517 Kurahashi H, Shibata S, Ishiwata M, Nakamura Y. Selfish prion of Rnq1 mutant in yeast. Genes Cells.
1518 2009 May;14(5):659-68. doi: 10.1111/j.1365-2443.2009.01297.x. Epub 2009 Apr 15. PMID: 19371377.

1519 Kurahashi H, Pack CG, Shibata S, Oishi K, Sako Y, Nakamura Y. [PSI(+)] aggregate enlargement in rnq1
1520 nonprion domain mutants, leading to a loss of prion in yeast. Genes Cells. 2011(a) May;16(5):576-89. doi:
1521 10.1111/j.1365-2443.2011.01511.x. Epub 2011 Apr 1. PMID: 21453425.

1522 Kurahashi H, Oishi K, Nakamura Y. A bipolar personality of yeast prion proteins. Prion. 2011(b) Oct-
1523 Dec;5(4):305-10. doi: 10.4161/pri.18307. Epub 2011 Oct 1. PMID: 22156730; PMCID: PMC4012401.

1524 LeVine H 3rd. Quantification of beta-sheet amyloid fibril structures with thioflavin T. Methods Enzymol.
1525 1999;309:274-84. doi: 10.1016/s0076-6879(99)09020-5. PMID: 10507030.

1526 Li X, Rayman JB, Kandel ER, Derkatch IL. Functional role of Tia1/Pub1 and Sup35 prion domains:
1527 directing protein synthesis machinery to the tubulin cytoskeleton. Mol Cell. 2014 Jul 17;55(2):305-18. doi:
1528 10.1016/j.molcel.2014.05.027. Epub 2014 Jun 26. PMID: 24981173; PMCID: PMC4425694.

1529 Lieberman AP, Shakkottai VG, Albin RL. Polyglutamine Repeats in Neurodegenerative Diseases. Annu

1530 Rev Pathol. 2019 Jan 24;14:1-27. doi: 10.1146/annurev-pathmechdis-012418-012857. Epub 2018 Aug 8.
1531 PMID: 30089230; PMCID: PMC6387631.

1532 Liebman SW, All-Robyn JA. A non-Mendelian factor, [eta(+)], causes lethality of yeast omnipotent-
1533 suppressor strains. Curr Genet. 1984 Oct;8(8):567-73. doi: 10.1007/BF00395701. PMID: 24177995.

1534 Liebman SW, Bagriantsev SN, Derkatch IL. Biochemical and genetic methods for characterization of
1535 [PIN+] prions in yeast. Methods. 2006 May;39(1):23-34. doi: 10.1016/j.ymeth.2006.04.010. PMID:
1536 16793281.

1537 Liebman SW, Chernoff YO. Prions in yeast. Genetics. 2012 Aug;191(4):1041-72. doi:
1538 10.1534/genetics.111.137760. PMID: 22879407; PMCID: PMC3415993.

1539 Lopez N, Aron R, Craig EA. Specificity of class II Hsp40 Sis1 in maintenance of yeast prion [RNQ+]. Mol
1540 Biol Cell. 2003 Mar;14(3):1172-81. doi: 10.1091/mbc.e02-09-0593. PMID: 12631732; PMCID:
1541 PMC151588.

1542 Maddelein ML, Wickner RB. Two prion-inducing regions of Ure2p are nonoverlapping. Mol Cell Biol. 1999
1543 Jun;19(6):4516-24. doi: 10.1128/MCB.19.6.4516. PMID: 10330190; PMCID: PMC104409.

1544 Mathur V, Hong JY, Liebman SW. Ssa1 overexpression and [PIN(+)] variants cure [PSI(+)] by dilution of
1545 aggregates. J Mol Biol. 2009 Jul 10;390(2):155-67. doi: 10.1016/j.jmb.2009.04.063. Epub 2009 May 5.
1546 PMID: 19422835; PMCID: PMC2738641.

1547 McGlinchey RP, Kryndushkin D, Wickner RB. Suicidal [PSI+] is a lethal yeast prion. Proc Natl Acad Sci U
1548 S A. 2011 Mar 29;108(13):5337-41. doi: 10.1073/pnas.1102762108. Epub 2011 Mar 14. PMID: 21402947;
1549 PMCID: PMC3069153.

1550 Meriin AB, Zhang X, He X, Newnam GP, Chernoff YO, Sherman MY. Huntington toxicity in yeast model
1551 depends on polyglutamine aggregation mediated by a prion-like protein Rnq1. J Cell Biol. 2002 Jun
1552 10;157(6):997-1004. doi: 10.1083/jcb.200112104. Epub 2002 Jun 10. Erratum in: J Cell Biol 2002 Aug
1553 5;158(3):591. PMID: 12058016; PMCID: PMC2174031.

1554 Moriyama H, Edskes HK, Wickner RB. [URE3] prion propagation in Saccharomyces cerevisiae:
1555 requirement for chaperone Hsp104 and curing by overexpressed chaperone Ydj1p. Mol Cell Biol. 2000
1556 Dec;20(23):8916-22. doi: 10.1128/MCB.20.23.8916-8922.2000. PMID: 11073991; PMCID: PMC86546.

1557 Nakayashiki T, Kurtzman CP, Edskes HK, Wickner RB. Yeast prions [URE3] and [PSI+] are diseases.
1558 Proc Natl Acad Sci U S A. 2005 Jul 26;102(30):10575-80. doi: 10.1073/pnas.0504882102. Epub 2005 Jul
1559 15. PMID: 16024723; PMCID: PMC1180808.

1560 Newnam GP, Birchmore JL, Chernoff YO. Destabilization and recovery of a yeast prion after mild heat
1561 shock. J Mol Biol. 2011 May 6;408(3):432-48. doi: 10.1016/j.jmb.2011.02.034. Epub 2011 Mar 15. PMID:
1562 21392508; PMCID: PMC3095851.

1563 Nizhnikov AA, Ryzhova TA, Volkov KV, Zadorsky SP, Sopova JV, Inge-Vechtomov SG, Galkin AP.
1564 Interaction of Prions Causes Heritable Traits in Saccharomyces cerevisiae. PLoS Genet. 2016 Dec
1565 27;12(12):e1006504. doi: 10.1371/journal.pgen.1006504. PMID: 28027291; PMCID: PMC5189945.

1566 Norton J, Seah N, Santiago F, Sindi SS, Serio TR. Multiple aspects of amyloid dynamics *in vivo* integrate
1567 to establish prion variant dominance in yeast. Front Mol Neurosci. 2024 Jul 30;17:1439442. doi:
1568 10.3389/fnmol.2024.1439442. PMID: 39139213; PMCID: PMC11319303.

1569 Osherovich LZ, Weissman JS. Multiple Gln/Asn-rich prion domains confer susceptibility to induction of the
1570 yeast [PSI(+)] prion. Cell. 2001 Jul 27;106(2):183-94. doi: 10.1016/s0092-8674(01)00440-8. PMID:
1571 11511346.

1572 Park SK, Hong JY, Arslan F, Kanneganti V, Patel B, Tietsort A, Tank EMH, Li X, Barmada SJ, Liebman
1573 SW. Overexpression of the essential Sis1 chaperone reduces TDP-43 effects on toxicity and proteolysis.
1574 PLoS Genet. 2017 May 22;13(5):e1006805. doi: 10.1371/journal.pgen.1006805. PMID: 28531192;
1575 PMCID: PMC5460882.

1576 Patino MM, Liu JJ, Glover JR, Lindquist S. Support for the prion hypothesis for inheritance of a phenotypic
1577 trait in yeast. Science. 1996 Aug 2;273(5275):622-6. doi: 10.1126/science.273.5275.622. PMID: 8662547.

1578 Pattison, I. H. (1965) Experiments with scrapie with special reference to the nature of the agent and the
1579 pathology of the disease: Slow, latent and temperate virus infections. NINDB Monograph 2, 249–257.

1580 Pei F, DiSalvo S, Sindi SS, Serio TR. A dominant-negative mutant inhibits multiple prion variants through a
1581 common mechanism. PLoS Genet. 2017 Oct 30;13(10):e1007085. doi: 10.1371/journal.pgen.1007085.
1582 PMID: 29084237; PMCID: PMC5679637.

1583 Resende CG, Outeiro TF, Sands L, Lindquist S, Tuite MF. Prion protein gene polymorphisms in
1584 Saccharomyces cerevisiae. Mol Microbiol. 2003 Aug;49(4):1005-17. doi: 10.1046/j.1365-
1585 2958.2003.03608.x. PMID: 12890024.

1586 Rose M, Winston F, Hieter P. (1990) Methods in yeast genetics — A laboratory course manual by pp 198.
1587 Cold Spring Harbor Laboratory Press, Cold Spring Harbor, New York. ISBN 0-87969-354-1.

1588 Salnikova AB, Kryndushkin DS, Smirnov VN, Kushnirov VV, Ter-Avanesyan MD. Nonsense suppression in
1589 yeast cells overproducing Sup35 (eRF3) is caused by its non-heritable amyloids. J Biol Chem. 2005 Mar
1590 11;280(10):8808-12. doi: 10.1074/jbc.M410150200. Epub 2004 Dec 23. PMID: 15618222.

1591 Santoso A, Chien P, Osherovich LZ, Weissman JS. Molecular basis of a yeast prion species barrier. Cell.
1592 2000 Jan 21;100(2):277-88. doi: 10.1016/s0092-8674(00)81565-2. PMID: 10660050.

1593 Satpute-Krishnan P, Langseth SX, Serio TR. Hsp104-dependent remodeling of prion complexes mediates
1594 protein-only inheritance. PLoS Biol. 2007 Feb;5(2):e24. doi: 10.1371/journal.pbio.0050024. PMID:
1595 17253904; PMCID: PMC1779812.

1596 Schlumpberger M, Prusiner SB, Herskowitz I. Induction of distinct [URE3] yeast prion strains. Mol Cell Biol.
1597 2001 Oct;21(20):7035-46. doi: 10.1128/MCB.21.20.7035-7046.2001. PMID: 11564886; PMCID:
1598 PMC99879.

1599 Scott M, Foster D, Mirenda C, Serban D, Coufal F, Wälchli M, Torchia M, Groth D, Carlson G, DeArmond
1600 SJ, Westaway D, Prusiner SB. Transgenic mice expressing hamster prion protein produce species-specific
1601 scrapie infectivity and amyloid plaques. Cell. 1989 Dec 1;59(5):847-57. doi: 10.1016/0092-8674(89)90608-
1602 9. PMID: 2574076.

1603 Sharma J, Liebman SW. [PSI(+)] prion variant establishment in yeast. Mol Microbiol. 2012 Nov;86(4):866-
1604 81. doi: 10.1111/mmi.12024. Epub 2012 Sep 24. PMID: 22998111; PMCID: PMC3543502.

1605 Sharma J, Liebman SW. Variant-specific prion interactions: Complicating factors. Cell Logist. 2013 Jan
1606 1;3(1):e25698. doi: 10.4161/cl.25698. Epub 2013 Sep 12. PMID: 24475372; PMCID: PMC3891757.

1607 Sherman, F., Fink, G., Hicks, J. (1987) *Methods in Yeast Genetics: A Laboratory Course Manual.* Cold
1608 Spring Harbor Laboratory Press. ISBN 9780879691974.

1609 Sharma A, Bruce KL, Chen B, Gyoneva S, Behrens SH, Bommarius AS, Chernoff YO. Contributions of the
1610 Prion Protein Sequence, Strain, and Environment to the Species Barrier. J Biol Chem. 2016 Jan
1611 15;291(3):1277-88. doi: 10.1074/jbc.M115.684100. Epub 2015 Nov 12. PMID: 26565023; PMCID:
1612 PMC4714215.

1613 Shewmaker F, Mull L, Nakayashiki T, Masison DC, Wickner RB. Ure2p function is enhanced by its prion
1614 domain in Saccharomyces cerevisiae. Genetics 2007;176:1557–65.

1615 Shibata S, Kurahashi H, Nakamura Y. Localization of prion-destabilizing mutations in the N-terminal non-
1616 prion domain of Rnq1 in Saccharomyces cerevisiae. Prion. 2009 Oct-Dec;3(4):250-8. doi:
1617 10.4161/pri.3.4.10388. Epub 2009 Oct 20. PMID: 20009538; PMCID: PMC2807699.

1618 Sikorski RS, Hieter P. A system of shuttle vectors and yeast host strains designed for efficient
1619 manipulation of DNA in Saccharomyces cerevisiae. Genetics. 1989 May;122(1):19-27. doi: 10.
1620 1093/genetics/122.1.19. PMID: 2659436; PMCID: PMC1203683.

1621 Sondheimer N, Lindquist S. Rnq1: an epigenetic modifier of protein function in yeast. Mol Cell. 2000
1622 Jan;5(1):163-72. doi: 10.1016/s1097-2765(00)80412-8. PMID: 10678178.

1623 Sondheimer N, Lopez N, Craig EA, Lindquist S. The role of Sis1 in the maintenance of the [RNQ+] prion.
1624 EMBO J. 2001 May 15;20(10):2435-42. doi: 10.1093/emboj/20.10.2435. PMID: 11350932; PMCID:
1625 PMC125465.

1626 Taneja V, Maddelein ML, Talarek N, Saupe SJ, Liebman SW. A non-Q/N-rich prion domain of a foreign
1627 prion, [Het-s], can propagate as a prion in yeast. Mol Cell. 2007 Jul 6;27(1):67-77. doi:
1628 10.1016/j.molcel.2007.05.027. PMID: 17612491; PMCID: PMC1995001.

1629 Tuite MF, Mundy CR, Cox BS. Agents that cause a high frequency of genetic change from [psi+] to [psi-] in
1630 Saccharomyces cerevisiae. Genetics. 1981 Aug;98(4):691-711. doi: 10.1093/genetics/98.4.691. PMID:
1631 7037537; PMCID: PMC1214469.

1632 Villali J, Dark J, Brechtel TM, Pei F, Sindi SS, Serio TR. Nucleation seed size determines amyloid
1633 clearance and establishes a barrier to prion appearance in yeast. Nat Struct Mol Biol. 2020 Jun;27(6):540-
1634 549. doi: 10.1038/s41594-020-0416-6. Epub 2020 May 4. PMID: 32367069; PMCID: PMC7293557.

1635 Vitrenko YA, Pavon ME, Stone SI, Liebman SW. Propagation of the [PIN+] prion by fragments of Rnq1
1636 fused to GFP. Curr Genet. 2007(a) May;51(5):309-19. doi: 10.1007/s00294-007-0127-0. Epub 2007 Apr 6.
1637 PMID: 17415568; PMCID: PMC2597802.

1638 Vitrenko YA, Gracheva EO, Richmond JE, Liebman SW. Visualization of aggregation of the Rnq1 prion
1639 domain and cross-seeding interactions with Sup35NM. J Biol Chem. 2007(b) Jan 19;282(3):1779-87. doi:
1640 10.1074/jbc.M609269200. Epub 2006 Nov 22. PMID: 17121829.

1641 Wegrzyn RD, Bapat K, Newnam GP, Zink AD, Chernoff YO. Mechanism of prion loss after Hsp104
1642 inactivation in yeast. Mol Cell Biol. 2001 Jul;21(14):4656-69. doi: 10.1128/MCB.21.14.4656-4669.2001.
1643 PMID: 11416143; PMCID: PMC87136.

1644 Weissmann C. Mutation and selection of prions. PLoS Pathog. 2012;8(3):e1002582. doi:
1645 10.1371/journal.ppat.1002582. Epub 2012 Mar 29. PMID: 22479179; PMCID: PMC3315487.

1646 Westergard L, True HL. Wild yeast harbour a variety of distinct amyloid structures with strong prion-
1647 inducing capabilities. Mol Microbiol. 2014a Apr;92(1):183-93. doi: 10.1111/mmi.12543. Epub 2014 Mar 7.
1648 PMID: 24673812; PMCID: PMC4708258.

1649 Westergard L, True HL. Extracellular environment modulates the formation and propagation of particular
1650 amyloid structures. Mol Microbiol. 2014b May;92(4):698-715. doi: 10.1111/mmi.12579. Epub 2014 Apr 9.
1651 PMID: 24628771; PMCID: PMC4739623.

1652 Wickner RB. [URE3] as an altered URE2 protein: evidence for a prion analog in Saccharomyces
1653 cerevisiae. Science. 1994 Apr 22;264(5158):566-9. doi: 10.1126/science.7909170. PMID: 7909170.

1654 Wickner RB, Dyda F, Tycko R. Amyloid of Rnq1p, the basis of the [PIN+] prion, has a parallel in-register
1655 beta-sheet structure. Proc Natl Acad Sci U S A. 2008 Feb 19;105(7):2403-8. doi:
1656 10.1073/pnas.0712032105. Epub 2008 Feb 11. PMID: 18268327; PMCID: PMC2268149.

1657 Wickner RB, Edskes HK, Kryndushkin D, McGlinchey R, Bateman D, Kelly A. Prion diseases of yeast:
1658 amyloid structure and biology. Semin Cell Dev Biol. 2011(a) Jul;22(5):469-75. doi:
1659 10.1016/j.semcdb.2011.02.021. Epub 2011 Feb 21. PMID: 21345375; PMCID: PMC3117979.

1660 Wickner RB, Edskes HK, Bateman D, Kelly AC, Gorkovskiy A. The yeast prions [PSI+] and [URE3] are
1661 molecular degenerative diseases. Prion. 2011(b) Oct-Dec;5(4):258-62. doi: 10.4161/pri.17748. Epub 2011
1662 Oct 1. PMID: 22052353; PMCID: PMC4012404.

1663 Wickner RB, Son M, Edskes HK. Prion Variants of Yeast are Numerous, Mutable, and Segregate on
1664 Growth, Affecting Prion Pathogenesis, Transmission Barriers, and Sensitivity to Anti-Prion Systems.
1665 Viruses. 2019 Mar 9;11(3):238. doi: 10.3390/v11030238. PMID: 30857327; PMCID: PMC6466074.

1666 Zhou P, Derkatch IL, Liebman SW. The relationship between visible intracellular aggregates that appear
1667 after overexpression of Sup35 and the yeast prion-like elements [PSI(+)] and [PIN(+)]. Mol Microbiol. 2001
1668 Jan;39(1):37-46. doi: 10.1046/j.1365-2958.2001.02224.x. PMID: 11123686.

1669 Zhouravleva GA, Bondarev SA, Trubitsina NP. How Big Is the Yeast Prion Universe? Int J Mol Sci. 2023
1670 Jul 19;24(14):11651. doi: 10.3390/ijms241411651. PMID: 37511408; PMCID: PMC10380529.

1671

1672 ## Figures

1673 **Fig 1. Genetic screen for mutations in Rnq1 that, when substituted for Rnq1$_{WT}$ in a [*PIN*$^{+}$]**
1674 **strain (Pin^{+} phenotype), lead to a Pin^{-} phenotype.** (**A**) Structural organization of the Rnq1
1675 protein. Shown are NPD (aa 1-132, yellow) with the position of the T27P mutation, and PD (aa
1676 133-405) with a stretch of ten QG repeats (aa 153-172, blue), four distinct QN-regions (brown;
1677 QN1 through QN4), and five hydrophobic repeats with the LA$^{S}/_{A}$ $^{L}/_{M}$ A core (light grey; A through
1678 E). The QN1 region is aa 185-198, QN2 - aa 218-263, QN3 - aa 279-319, QN4 - aa 337-405;
1679 patterned blocs indicate QN-rich repeats within QN2, QN3 and QN4). (**B)** Scheme of the genetic
1680 screen (see text).
1681

1682 **Fig 2. The T27P mutation in Rnq1 NPD leads to a dramatic reduction of the Pin^{+} phenotype**
1683 **when Rnq1$_{T27P}$ is substituted for Rnq1$_{WT}$ in a [*PIN*$^{+}$] strain.** (**A**) Western blot analysis of the
1684 expression of Rnq1$_{T27P}$ and Rnq1$_{T27P}$ in *the rnq1-Δ* strain. The *rnq1-Δ* YID193 strain was
1685 transformed with the indicated *CEN LEU2* plasmids. For *RNQ1$_{WT}$* the pID129 plasmid was used.
1686 For*RNQ1$_{T27P}$*, shown is expression from the original plasmid from the mutagenized library and
1687 from two independent isolates of the pID335 plasmid where the T27P mutation was introduced
1688 by site-directed mutagenesis. Expression of Sup35 is used as a loading control. Both panels are
1689 from the same Western blot: anti-Rnq1 and anti-Sup35 antibodies were added simultaneously.
1690 Mobilities of Rnq1 and Sup35 are as expected based on protein molecular weights. Expression
1691 of Rnq1$_{T27P}$ is ~2-fold lower compared to Rnq1$_{WT}$. (**B)** Rnq1$_{T27P}$ leads to a dramatic reduction of
1692 the Pin^{+} phenotype when substituted for Rnq1$_{WT}$ in a [*PIN*$^{+}$] strain. Shown is the image of the
1693 YID146.3 cells with *RNQ1$_{T27P}$* (or indicated control plasmids) substituted for *RNQ1$_{WT}$* incubated
1694 on SD-Ade media for 14 days at 30^{0}C after previously being grown either on the [*PSI*$^{+}$] inducing
1695 SGal-LeuHis media, or on the control SD-LeuHis (two passages). Each row includes patches of

1696 5 independent transformants. See Fig S1 for images of the same cultures on SD-LeuHis and and
1697 SGal-LeuHis from which cells were transferred onto SD-Ade. (**C**) Upon high-level expression of
1698 Sup35NM-YFP in the cultures where *RNQ1*$_{T27P}$ is substituted for *RNQ1*$_{WT}$, the *de novo* forming
1699 Sup35 aggregates are rare, but similar in appearance to aggregates forming in the control
1700 *RNQ1*$_{WT}$ cultures. Shown are fluorescent and bright-field images of cells carrying *GAL-*
1701 *SUP35NM-YFP* and the indicated *RNQ1* construct grown on SGal-LH for ~48hrs at 30^{0}C after
1702 the plasmid shuffle described in Fig 1B. See Table 1 for quantification. A typical group of cells is
1703 shown for the *RNQ1*$_{WT}$ culture. For *RNQ1*$_{T27P}$, all cells have the evenly distributed fluorescence
1704 in a typical group of cells representative of the 97.5% of the culture. Additionally shown for
1705 *RNQ1*$_{T27P}$ are rare cells with dot-, line-, and ring- aggregates, as well as aggregate-containing
1706 mother-daughter pairs (a line and a dot, or a ring shared by a mother and a daughter).
1707
1708 **Fig 3. The T27P mutation does not interfere with the ability of the Rnq1 protein to acquire**
1709 **a heritable Pin$^+$ state upon overexpression, indicative of the *de novo* formation of the**
1710 **[*PIN*$^+_{T27P}$] prion.** For the description of Experiment 1 (**A**) and Experiment 2 (**B**) see Results and
1711 Materials and Methods. The (++), (+), and ($\pm$) indicate the relative level of [*PSI*$^+$] induction based
1712 on growth on adenineless media compared to lack of [*PSI*$^+$] induction (-), with (++) being the
1713 most robust. In (B) some negative control experiments are grouped together.
1714 * Occasional Ade$^+$ colonies were detected after induction of the *GAL* promoter-driven Sup35NM-
1715 YFP in cultures where *CUP1*-driven *RNQ1*$_{T27P\ (or\ WT)}$ constructs were not overexpressed. This is
1716 indicative of a low-level of induction of Rnq1-based prions, probably due to residual expression
1717 of *CUP1-RNQ1* constructs in all or some cells on regular SD media which contains 0.16μM
1718 $CuSO_4$. The number of such Ade$^+$ colonies gradually increased after multiple passages prior to

1719 the induction of Sup35NM-YFP but never reached the level of Pin$^+$ phenotypes observed in
1720 cultures that went through transient Rnq1$_{T27P\ (or\ WT)}$ overexpression on 50μM $CuSO_4$.
1721
1722 **Fig 4. Full-length Rnq1$_{T27P}$ and ΔB1C2D3$_{T27P}$ can form amyloid fibers *in vitro*. (A)** Western
1723 blot analysis of bacterially expressed and purified ΔB1C2D3$_{T27P}$ (T27P; two independent
1724 constructs) and ΔB1C2D3$_{WT}$ (WT). The expected size for both constructs is 27kDa. Note slightly
1725 slower mobility for ΔB1C2D3$_{T27P}$. Anti-His tag antibody was used for detection. **(B)** Kinetics of *in*
1726 *vitro* aggregation of ΔB1C2D3$_{T27P}$ and ΔB1C2D3$_{WT}$ monitored by ThT fluorescence. Samples and
1727 concentrations are indicated on the graph. **(C)** TEM micrographs of negatively stained fibers of
1728 Rnq1$_{T27P}$ and Rnq1$_{WT}$. Scale bars are for 100nm. Note lateral association of fibrils in the fibers for
1729 Rnq1$_{T27P}$ and twisted appearance of Rnq1$_{WT}$ fibers.
1730
1731 **Fig 5. The T27P mutation creates a barrier for the transmission of the prion state from**
1732 **[*PIN*$^+_{WT}$] to Rnq1$_{T27P}$.** (**A**) Scheme of experiments testing the frequency of [*PIN*$^+$] loss after
1733 substituting Rnq1$_{T27P}$ for Rnq1$_{WT}$ and mitotic stability of [*PIN*$^+_{T27P}$] isolates. See text. Red circle
1734 indicates a step at which yeast were colony purified for the analysis of the fraction of [*PIN*$^+_{T27P}$]
1735 cells in the cultures right after substituting *RNQ1*$_{T27P}$ for *RNQ1*$_{WT}$ (data shown in Table 2 and
1736 illustrated in (B); also corresponds to Round 1 in (C) and (D), and, for other donor and recipient
1737 construct combinations, to data in Fig 7B and Round 1 in Figs 7C through 7G). Green circle
1738 indicates the step at which [*PIN*$^+_{T27P}$] isolates were colony purified for the analysis of their mitotic
1739 stability (corresponds to data in Table 3 and Round 2 in (C) and (D), and, for other donor and
1740 recipient combinations, to Round 2 in Figs 7C through 7G). (**B**) After-shuffle cultures expressing
1741 Rnq1$_{T27P}$ contain Pin$^+$ and Pin$^-$ cells. Sample SD-Ade plates after [*PSI*$^+$] induction on SGal-
1742 LeuHis with patches expressing the indicated Rnq1 allele or carrying the empty vector. Shown is

1743 growth on SD-Ade after 13 days of incubation at 20^{0}C. All patches were Ade$^-$ after incubation on
1744 the control SD-LeuHis media (not shown). **(C)** Increase of mitotic stability of [*PIN*$^+_{T27P}$] indicative
1745 of gradual conformational adaptation of the prion. See text and (A) for the description of the
1746 experiment. Data for Round 1 come from colony purification of 12 Rnq1$_{T27P}$ post-shuffle cultures
1747 transferred from FOA to SD-LeuHis. Data for Round 2 come from colony purification of the Pin$^+$
1748 Rnq1$_{T27P}$ isolates obtained in Round 1; 13 out of 15 obtained isolates were analyzed (the
1749 remaining 2 were lost due to contamination). For Round 3, seven Pin$^+$ cultures used in Round 2
1750 analysis were randomly chosen, and for each three randomly chosen Pin$^+$ isolates were colony
1751 purified and scored for Pin$^+$ (a total of 21 data points). In Round 4, the analysis was continued for
1752 all twelve cultures originating from four out of seven Round 2 cultures (three randomly chosen
1753 Pin$^+$ isolates for each culture, a total of 36 data points) and for partial lineages of two more
1754 Round 2 isolates (a total of 6 more data points). Data for positive (Rnq1$_{WT}$ shuffled to Rnq1$_{WT}$)
1755 and negative (Rnq1$_{WT}$ to EV) controls is not included for simplicity, but these experiments were
1756 carried through Round 2 on a similar scale and through further rounds on a limited scale.
1757 [*PIN*$^+_{WT}$] maintained ~100% stability in all isolates tested, with no switching to less stable
1758 variants, and yeast with shuffled-in EV did not accumulate Pin$^+$ cells. (**D**) Maturation of post-
1759 transmission [*PIN*$^+_{T27P}$] to heritable prion variants with characteristic stabilities. See Results for
1760 the description of this experiment and explanation of pedigrees. The R4, R5 and R6 labels
1761 correspond to the round of the analysis of mitotic stability of post-shuffle [*PIN*$^+_{T27P}$]. Asterisks
1762 mark directly related parts of the pedigree of the meta-stable [*PIN*$^+_{T27P}$] prion variant that is prone
1763 to yield more stable (red) and less stable (green) [*PIN*$^+_{T27P}$] variants . Differences between
1764 pedigrees 1, 2, and 3 are statistically significant for all rounds of analysis ($p<0.01$). There are no
1765 significant differences within pedigrees 1 and 2 between shown rounds of analysis. For pedigree
1766 3, there is no significant difference between R4 and R5, but for R6 there is a significant
1767 difference ($p<0.01$) due to gradual stabilization of [*PIN*$^+_{T27P}$] in some isolates (green asterisks).

1768

1769 **Fig 6. The transmission barrier between [*PIN*$^{+}_{WT}$] and Rnq1$_{T27P}$ is not caused by the**

1770 **inability of Rnq1$_{T27P}$ to co-aggregate with Rnq1$_{WT}$ or by loss of the [*PIN*$^{+}$] prion during co-**

1771 **expression of Rnq1$_{WT}$ and Rnq1$_{T27P}$.** (**A**) Rnq1$_{T27P}$ can join the [*PIN*$^{+}_{WT}$] prion aggregates. The

1772 [*PIN*$^{+}$] 74-D694 strain was co-transformed with the *CEN LEU2 CUP1-RNQ1$_{WT}$-CFP* and *CEN*

1773 *URA3 CUP-RNQ1$_{T27P}$-YFP* plasmids. Cultures of co-transformants were grown overnight (~to

1774 mid-log) in no-copper SD-LeuHis media, diluted to OD_{595}=1.0 into SD-LeuHis+5μM $CuSO_4$ and

1775 grown for 2 more hours prior to observing the cells with or without Hex treatment. A

1776 representative group of cells is shown. See Fig S2A for an image of a larger field and analysis of

1777 Rnq1$_{WT}$ and Rnq1$_{T27P}$ co-localization individual cells. (**B**) Rnq1$_{T27P}$ does not affect the Pin^{+}

1778 phenotype when co-expressed with Rnq1$_{WT}$ in a [*PIN*$^{+}$] stain. Shown are the images of the

1779 transformants of the YID146.3 cells carrying the *GAL-SUP35NM-YFP* [*PSI*$^{+}$] inducing construct

1780 along with the indicated plasmid combinations. “Galactose” and “Glucose” indicate SGal-

1781 UraLeuHis and SD-UraLeuHis media, respectively. Images on these media were taken after 48

1782 hours of growth at 30^{0}C. From these media yeast were replica plated to SD-Ade. Images were

1783 taken after 14 days at 30^{0}C. Note that these are patches from the plates shown on Fig 2B and

1784 Fig S1 but before plasmid shuffle.

1785

1786 **Fig 7. The transmission barrier created by the T27P mutation in the NPD is imposed**

1787 **through the first two QN-rich regions in Rnq1 PD. (A)** Deletion of B1 and B1C2 but not 2D

1788 and 3E regions in the PD of Rnq1$_{WT}$ reduces the transmission barrier from [*mini-PIN*$^{+}_{WT}$]s

1789 towards Rnq1$_{FL-T27P}$. The [*PSI*$^{+}$] induction test was done in cultures where the Rnq1$_{FL-WT}$, Rnq1$_{FL-}$

1790 $_{T27P}$ recipient constructs (or EV) were substituted for the indicated deletion constructs in the [*mini-*

1791 *PIN*$^{+}_{WT}$] or [*PIN*$^{+}_{FL-WT}$] prion donor strains. Shown are images of growth on SD-Ade plates replica

1792 plated from either the [*PSI*$^{+}$] inducing SGal-LeuHis or the control glucose media and grown for 10

1793 days at 30^{0}C. **(B – G)** Analysis of the role of QN-rich regions in the NPD of Rnq1 on the
1794 transmission barriers and subsequent conformational adaptation of Rnq1-based prions in the
1795 presence of the T27P mutation in the NPD. Experiments were performed as described in Fig 5.
1796 Donor and recipient constructs for prion transmission are indicated; nomenclature marks the
1797 deleted regions within the PD (ΔB1C2, ΔB1, Δ2D, or Δ3E; see Fig 1A) compared to the full-length
1798 Rnq1 protein (FL) and the presence or absence of the T27P mutation in the construct (T27P or
1799 WT, respectively). Shown is the fraction of prion-carrying cells in the cultures after plasmid
1800 shuffle (B and R1 in C – G) and mitotic stability of the resulting prions during further propagation
1801 of randomly chosen isolates (R2 through R4; ~19 cell generations between each round of
1802 analysis). In (D) asteriscs indicate related progeny for cultures in R3 and R4 highlighting the
1803 establishment of [$PIN^{+}_{\Delta B1C2}$] variants with high (red and blue) and low (green) mitotic stability.
1804 **Experiments in (B – G) were conducted in parallel, so all data can be compared between**
1805 **the graphs.** Some control experiments (e.g. analysis of transmissions between non-mutant
1806 constructs and lack of transmissions in substitutions for EV) are omitted on graphs for simplicity:
1807 the results were as expected and in full agreement with Kadnar et al. (2010). All conclusions in
1808 Results are based on statistically significant differences or lack of thereof (0.05 or 0.01
1809 probability cutoff).
1810
1811 **Fig 8. The T27P mutation in the NPD of Rnq1 promotes the formation of liquid-like**
1812 **droplets by Rnq1$_{FL\text{-}T27P}$-YFP expressed in [*pin*$^{-}$] cells even at levels close to the expression**
1813 **of endogenous Rnq1. (A)** Unlike Rnq1$_{FL\text{-}WT}$-YFP, Rnq1$_{FL\text{-}T27P}$-YFP forms aggregates in [*pin*$^{-}$]
1814 cells and these aggregates are not amyloid. Cultures of isogenic [*PIN*$^{+}$] and [*pin*$^{-}$] strains
1815 transformed with plasmids carrying the indicated constructs under the control of *CUP1* promoter
1816 were grown overninght in SD plasmid selective media to OD_{595} ~ 0.8. Then expression of the

1817 constructs was induced by addition of $CuSO_4$ to 50μM and growth was continued for 4 more
1818 hours prior to ThT staining and imaging. **(B - C)** Aggregates formed by $Rnq1_{FL\text{-}T27P}$-YFP in [*pin*$^-$]
1819 cells are liquid-like droplets. Yeast transformants were grown overnight in liquid SD media
1820 selective for plasmids. Then OD_{595} was adjusted to 1.0, $CuSO_4$ was added to 5μM, and cultures
1821 were grown for two more hrs before Hex treatment. (C) is quantification of data in experiment
1822 illustrated in (B). Asterisks indicate statistically significant differences ($p<0.01$). **(D)** $Rnq1_{FL\text{-}T27P}$-
1823 YFP forms liquid-like droplets in *rnq1-Δ* cells. Experiment was performed as described for (B -
1824 C). **(E)** $Rnq1_{FL\text{-}WT}$-CFP does not join liquid-like droplets formed by $Rnq1_{FL\text{-}T27P}$-YFP in [*pin*$^-$] cells.
1825 The [*pin*$^-$] strain was co-transformed with the *CEN LEU2 CUP1-RNQ1*$_{WT}$*-CFP* and *CEN URA3*
1826 *CUP-RNQ1*$_{T27P}$*-YFP* plasmids. Experiment was performed exactly as in Fig 6A where $Rnq1_{FL\text{-}T27P}$-YFP is shown co-aggregate with $Rnq1_{FL\text{-}WT}$-CFP in [*PIN*$^+_{WT}$] cells.
1827
1828
1829 **Fig 9. Models explaining the establishment of heritable [*PIN*$^+_{T27P}$] variants after across-the-**
1830 **barrier transmissions from [*PIN*$^+_{WT}$].** See text.
1831

1832 Supporting information

1833 **Fig S1. The T27P mutation in Rnq1 does not lead to inhibition of growth in the presence of**
1834 **the highly expressed Sup35NM-YFP construct.** *RNQ1*$_{WT}$ was substituted with *RNQ1*$_{T27P}$ or
1835 control plasmids (indicated) in a [*PIN*$^+$] [*psi*$^-$] *rnq1-Δ* strain as described in Fig. 1B. Shown are the
1836 images of patches of five transformants for each plasmid substitution after they were replica
1837 plated from the *RNQ1*$_{WT}$ (*URA3*) counter-selecting FOA media to Sup35NM-YFP inducing SGal-
1838 LeuHis media or non-inducing SD-LeuHis. Before imaging, cells were incubated at 30^0C for
1839 ~48hrs. These are images of plates used for replica plating to adenineless media shown in
1840 Figure 2B.

1841

1842 **Fig S2. Rnq1$_{T27P}$ joins [*PIN*$^{+}$*$_{WT}$*] prion aggregates as efficiently as Rnq1$_{WT}$.** The [*PIN*$^{+}$] 74-
1843 D694 strain was co-transformed, respectively, with the *CEN LEU2 CUP1-RNQ1$_{WT}$-CFP* and *CEN*
1844 *URA3 CUP-RNQ1$_{T27P}$-YFP* plasmids (**A**), or with *CEN LEU2 CUP1-RNQ1$_{WT}$-CFP* and *CEN*
1845 *URA3 CUP-RNQ1$_{WT}$-YFP* (**B**). Cultures of co-transformants were grown overnight (~to mid-log)
1846 in no-copper SD-LeuHis media, diluted to OD_{595}=1.0 into SD-LeuHis+5μM $CuSO_4$ and grown for
1847 2 more hours prior to observing the cells. In both images (A) and (B) CFP- and YFP-marked
1848 constructs co-localized in bright fluorescent foci in most cells (squares 1 and 2 for both (A) and
1849 (B); enlarged images are shown in panels below). However, there were cells with bright foci, for
1850 which only YFP or only CFP fluorescence is easily detectable on merged images. To test if there
1851 are cells in images from experiment (A) where only Rnq1$_{WT}$ but not Rnq1$_{T27P}$ joins [*PIN*$^{+}$*$_{WT}$*]
1852 aggregates, at total of ~150 cells from three different transformants with only CFP detectable on
1853 merge images were analyzed more carefully. For all of them, either no evenly distributed YFP
1854 fluorescence was detected, indicative of the loss or rearrangement of the *CUP-RNQ1$_{T27P}$-YFP*
1855 plasmid (see e.g. square 4 on Fig. S2A), or weak but definitely co-localizing YFP foci were
1856 detected on YFP images, indicative of reduced amounts of Rnq1$_{T27P}$-YFP in the cell (e.g. square
1857 5 on Fig. S2A). We also asked if there were Rnq1$_{T27P}$-YFP aggregates not incorporating Rnq1$_{WT}$.
1858 However, after analyzing ~150 cells with only YFP detectable on the merge, we concluded that
1859 the lack of the CFP signal within these foci was also either due to the *CUP-RNQ1$_{WT}$-CFP*
1860 plasmid loss (e.g. square 3 on Fig. S2A) or reduced abundance of Rnq1$_{WT}$-CFP (e.g. square 6
1861 on Fig. S6A). Analogous analysis in experiment (B) led to the same conclusion: squares 3 and 4
1862 represent cells with reduced fluorescence for one of the constructs, and squares 5 and 6 – cells
1863 where one of the constructs is lost or rearranged.

1864

1865 **Fig S3. Growth on media supplemented with 5μM $CuSO_4$ results in the level of $Rnq1_{T27P}$-**
1866 **YFP expression similar to that of chromosomally encoded $Rnq1_{WT}$.** A transformant of a [*pin*$^-$]
1867 strain with the *CEN URA3 CUP-RNQ1*$_{T27P}$*-YFP* plasmid was grown overnight (~to mid-log) in the
1868 no-copper plasmid-selective SD-Ura media, then diluted to OD_{595}=1.0 into SD-Ura+5μM $CuSO_4$
1869 and grown for 2 more hours prior to protein extraction (see Materials and Methods and
1870 Supplementary Materials and Methods). Approximately 30μg of total protein were separated on
1871 an SDS-PAGE gel. Rnq1 was detected by Western blot with polyclonal antibodies raised in
1872 rabbits against the first 185 aa of Rnq1 (type 1A Ab).
1873
1874 **Table S1. Similar arrays of [*PSI*$^+$] variants are induced in cultures expressing $Rnq1_{T27P}$,**
1875 **$Rnq1_{WT}$, or not expressing Rnq1 after shuffling out the *CEN URA3 RNQ1*$_{WT}$ [*PIN*$^+_{WT}$]**
1876 **maintainer plasmid.** See Results and Materials and Methods for the description of the
1877 experiment. [*PSI*$^+$]s isolated from at least eight independent transformants carrying the indicated
1878 plasmids were analyzed by the color test on YPD, growth on adenineless media and curability by
1879 GuHCl. Results of all three assays were consistent for ~99% [*PSI*$^+$] variants.
1880
1881 **Table S2. PCR primers used in this study.** Sites for restriction endonucleases used for cloning
1882 are underlined; the ATG start codon is in bold.
1883
1884 **File S1. Supplementary Materials and Methods.**

Figure 1

A

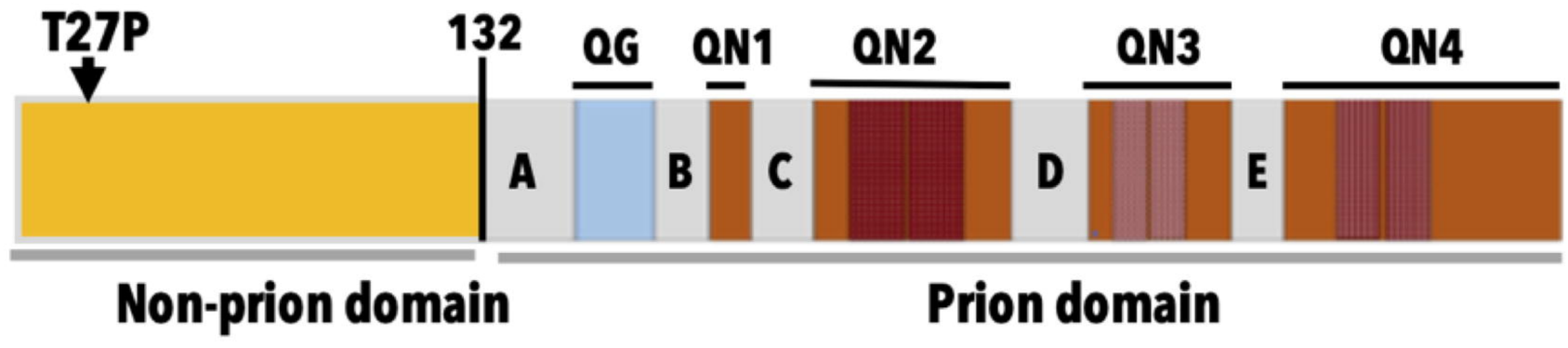
T27P
132
QG
QN1
QN2
QN3
QN4
A
B
C
D
E
Non-prion domain
Prion domain

B

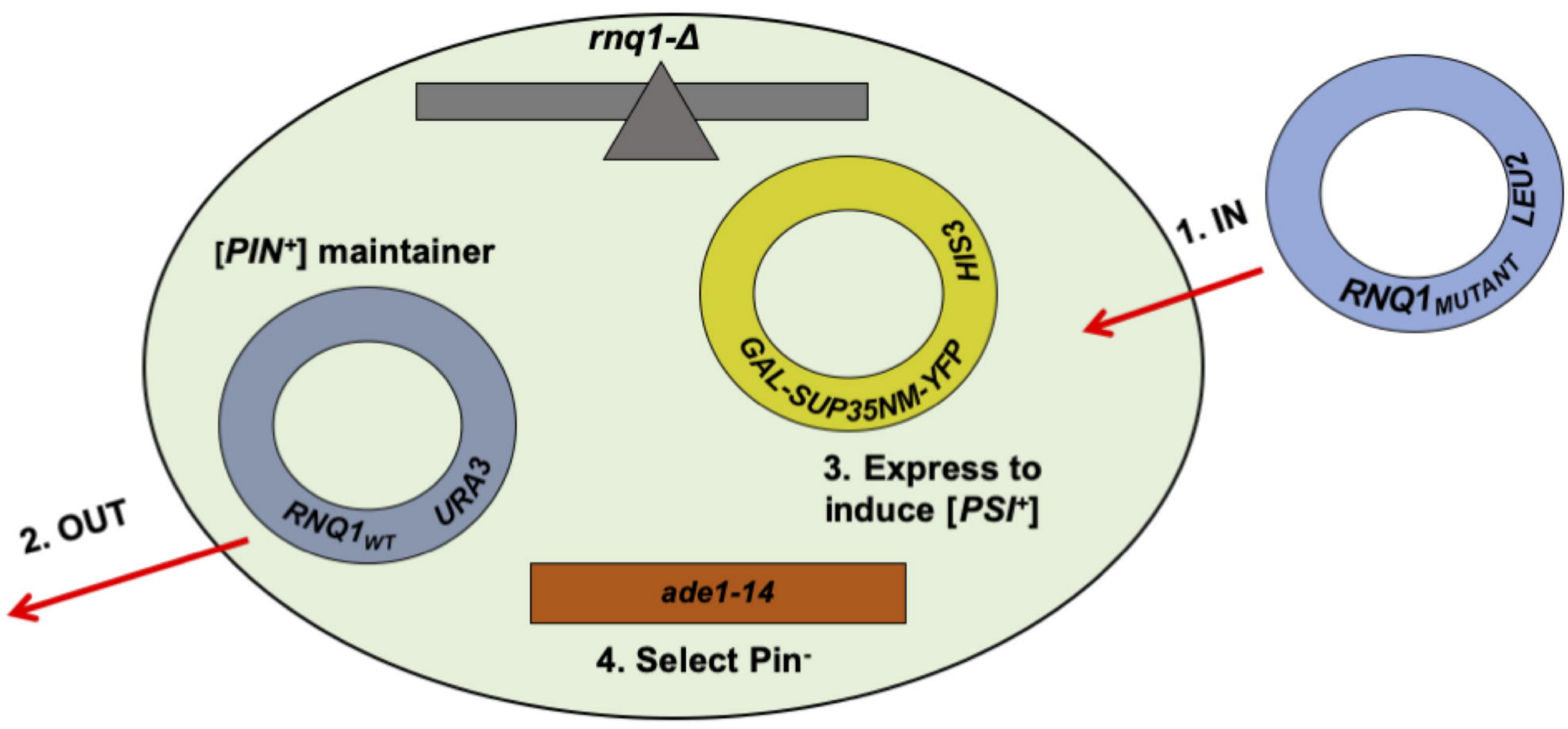
rnq1-Δ
[PIN+] maintainer
RNQ1WT
URA3
HIS3
GAL-SUP35NM-YFP
1. IN
RNQ1MUTANT
LEU2
2. OUT
3. Express to induce [PSI+]
ade1-14
4. Select Pin-

Figure 2

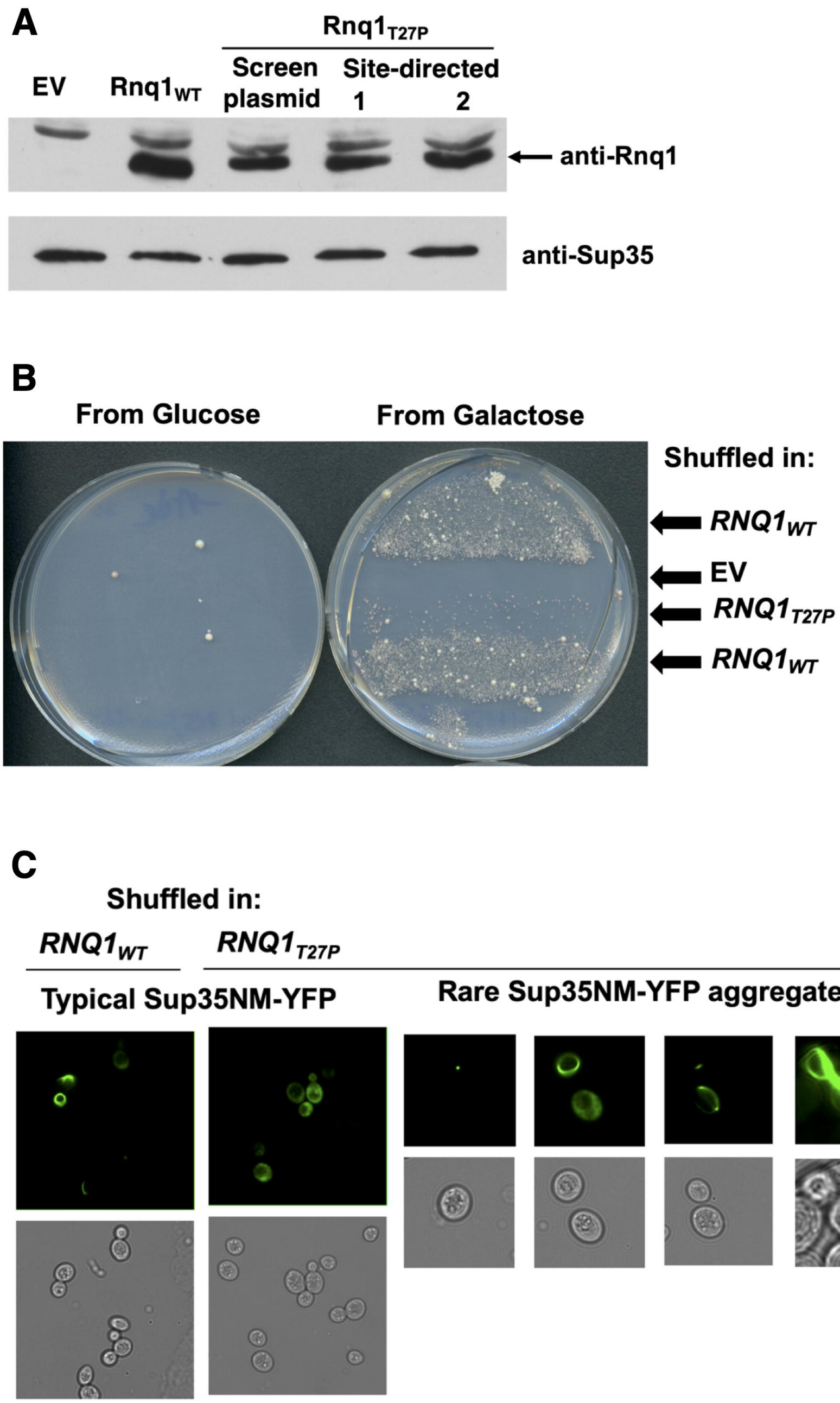
A
Rnq1T27P
EV
Rnq1WT
Screen plasmid
Site-directed 1
Site-directed 2
anti-Rnq1
anti-Sup35
B
From Glucose
From Galactose
Shuffled in:
RNQ1WT
EV
RNQ1T27P
RNQ1WT
C
Shuffled in:
RNQ1WT
RNQ1T27P
Typical Sup35NM-YFP
Rare Sup35NM-YFP aggregates

Figure 3

A

Rnq1 ↑ ($CuSO_4$)	Sup35NM-YFP ↑ (Gal)
YES	YES
NO	YES
YES	NO
NO	NO

Replica plate to -Ade

[*PSI*$^+$] induction for indicated constructs

$Rnq1_{T27P}$	$Rnq1_{WT}$	EV
+	+	-
- *	- *	-
-	-	-
-	-	-

B

Rnq1 ↑ ($CuSO_4$)

Passages on Glu w/o extra $CuSO_4$

Sup35NM-YFP ↑ (Gal)

YES	0	YES
YES	1	YES
YES	2	YES
YES	3	YES
YES	4	YES
YES	0, 1, 2, 3 or 4	NO
NO	0, 1, 2, 3 or 4	NO
NO	0, 1, 2, 3 or 4	YES

Replica plate to -Ade

[*PSI*$^+$] induction for indicated constructs

$Rnq1_{T27P}$	$Rnq1_{WT}$	EV
++	+	-
++	+	-
+	±	-
±	±	-
±	±	-
-	-	-
-	-	-
- *	- *	-

Figure 4

A

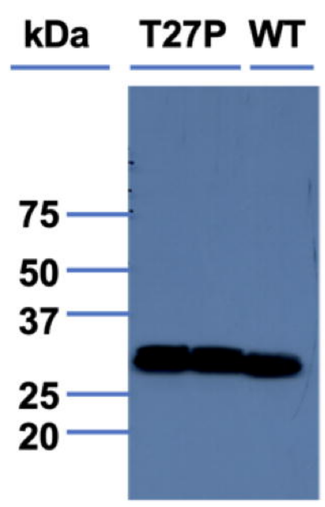
kDa
T27P
WT
75
50
37
25
20

B

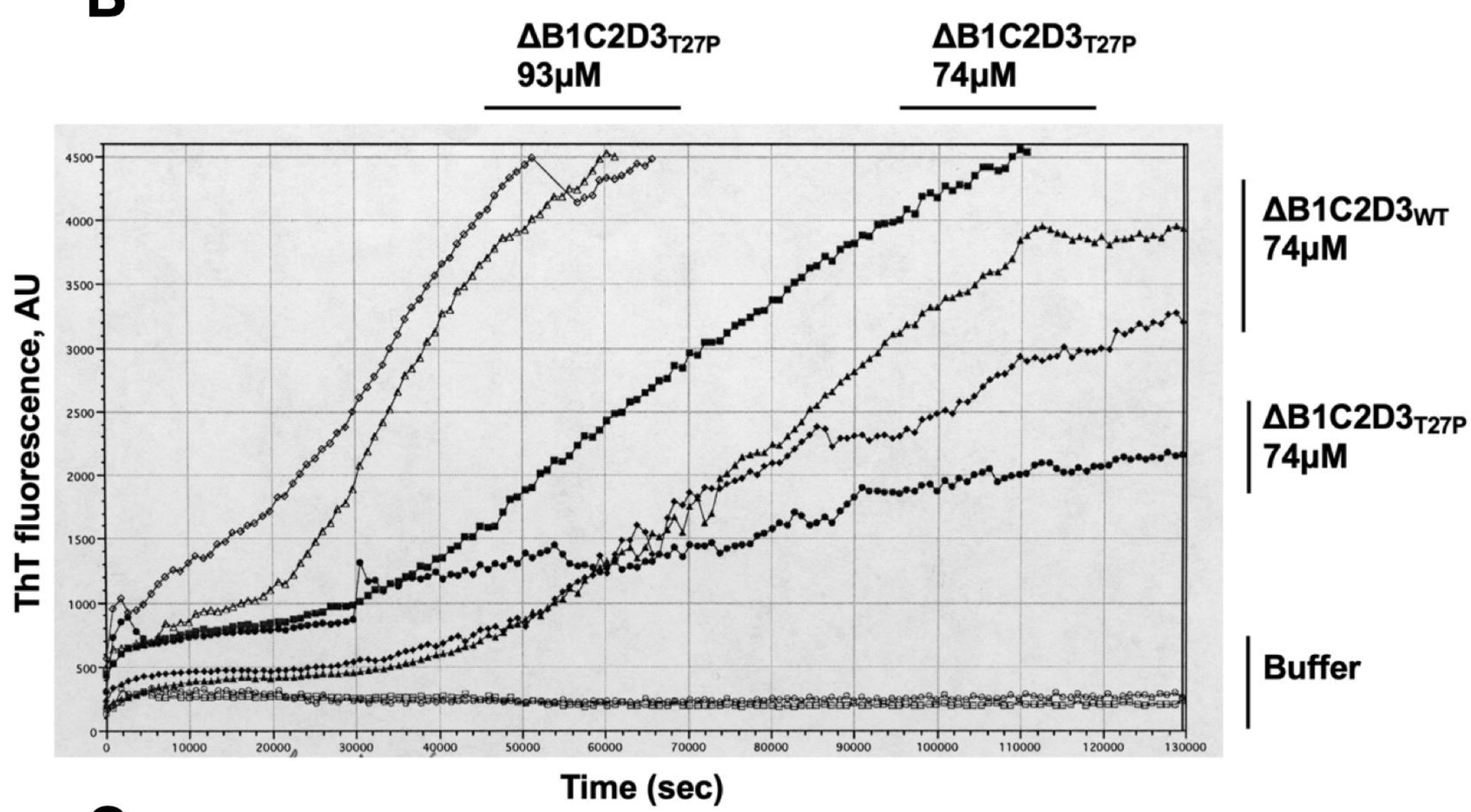
ΔB1C2D3T27P 93μM
ΔB1C2D3T27P 74μM
ΔB1C2D3WT 74μM
ΔB1C2D3T27P 74μM
Buffer
ThT fluorescence, AU
Time (sec)

C

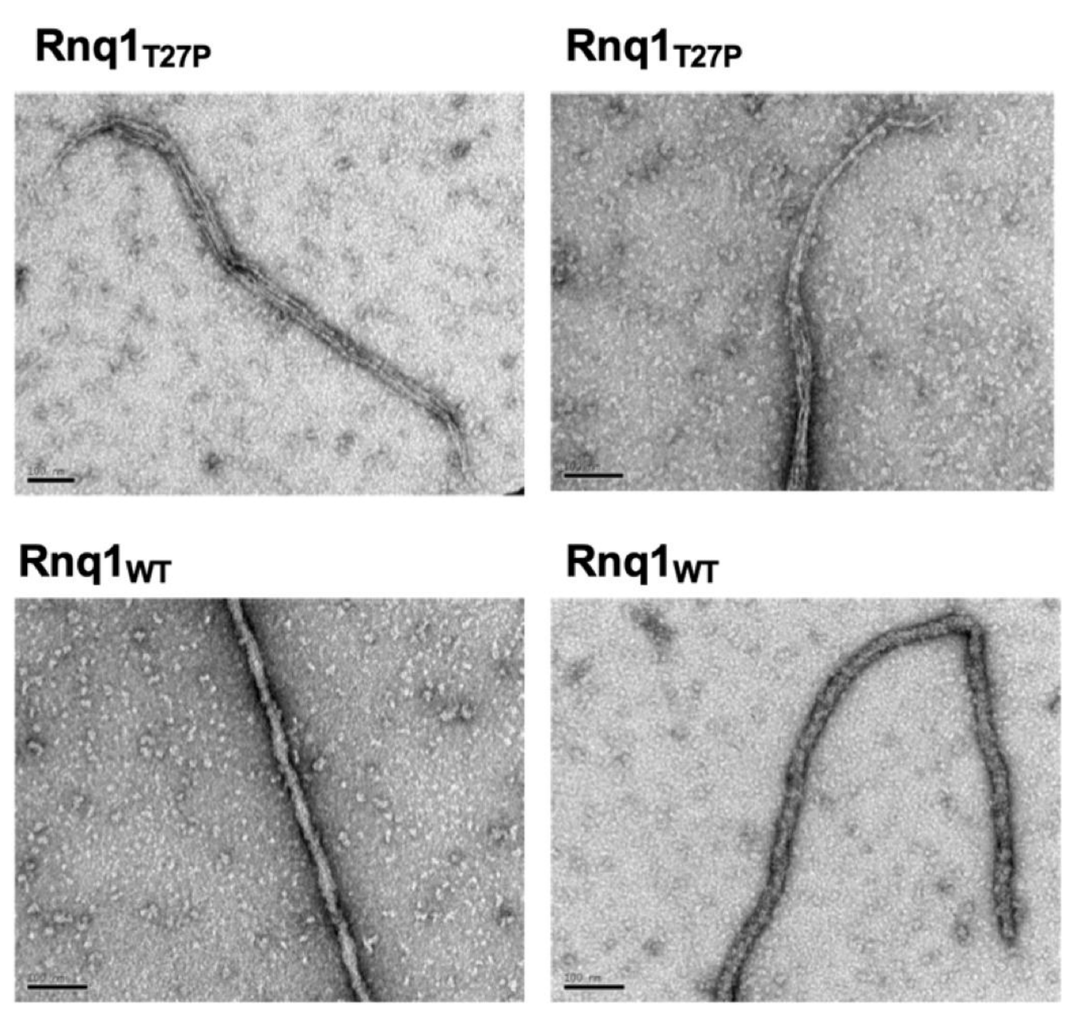
Rnq1T27P
Rnq1T27P
Rnq1WT
Rnq1WT

Figure 5

A

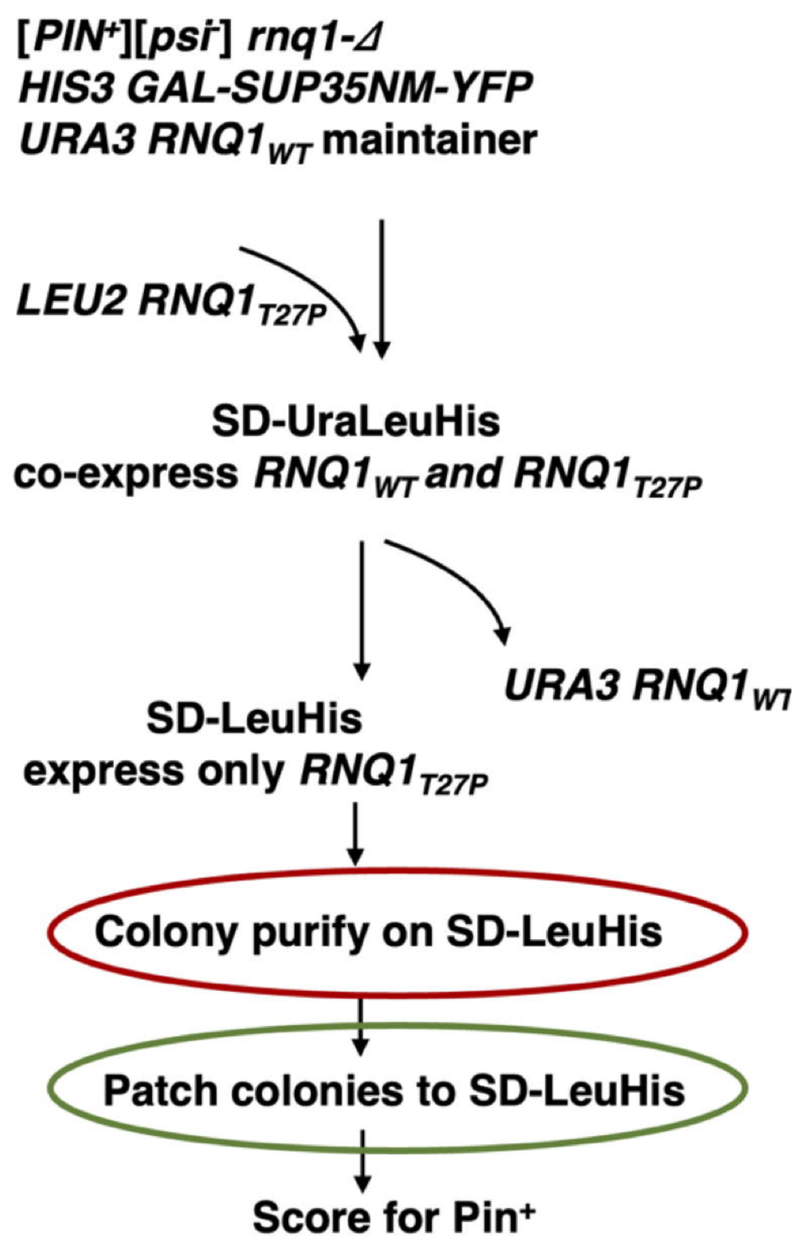

B

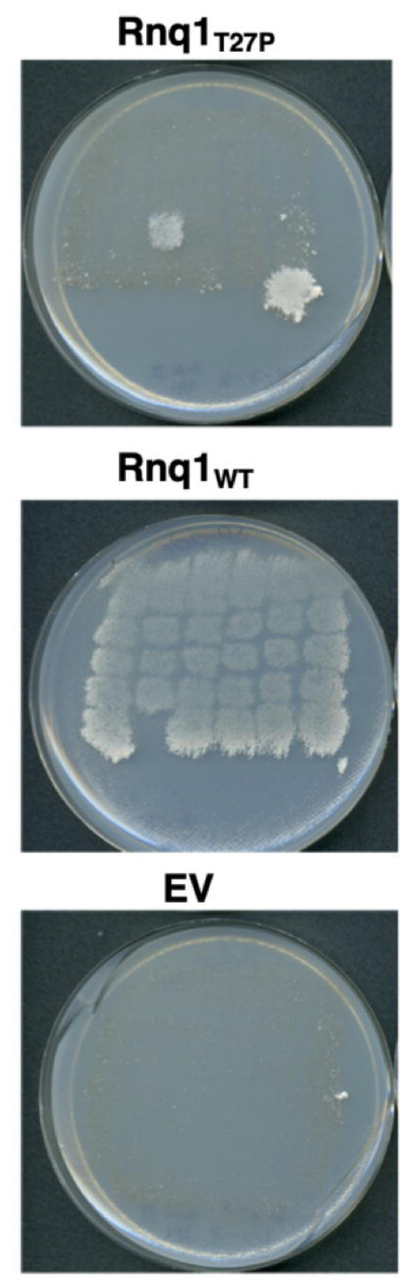

C

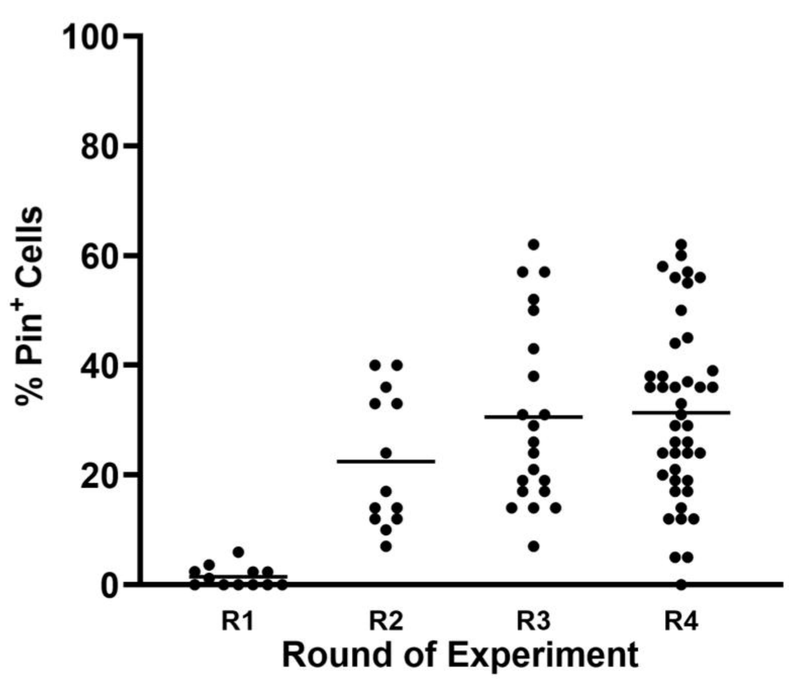

D

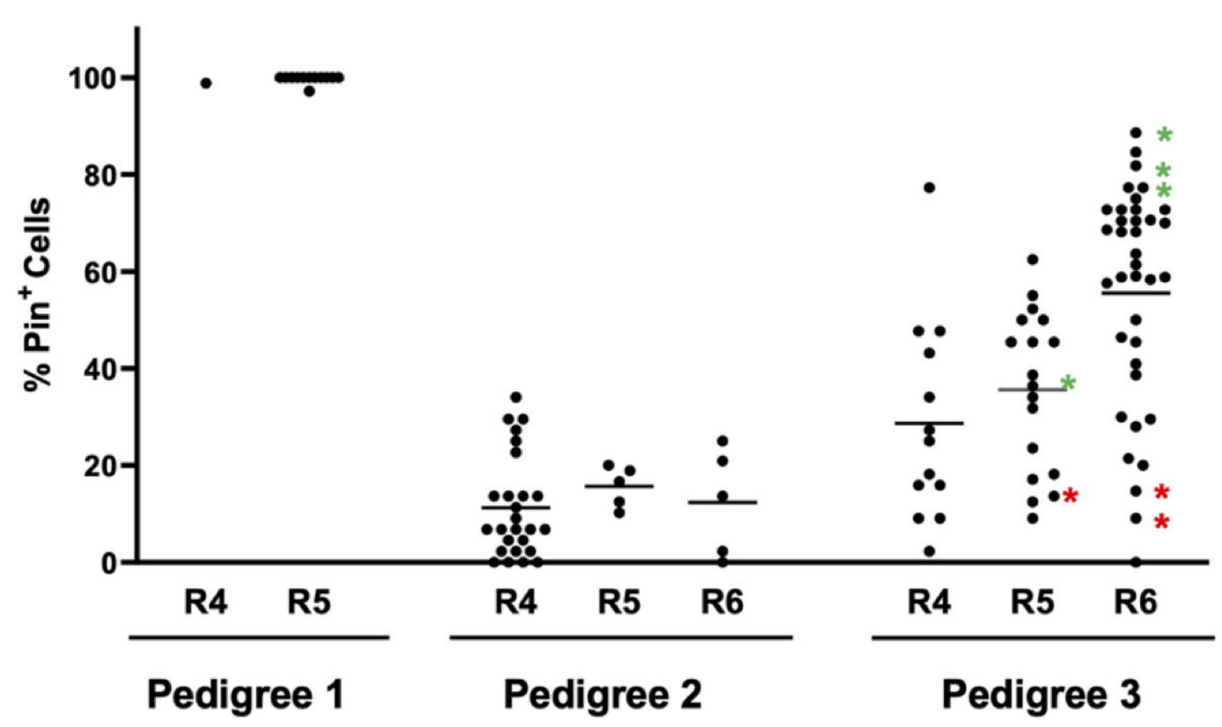

Figure 6

A

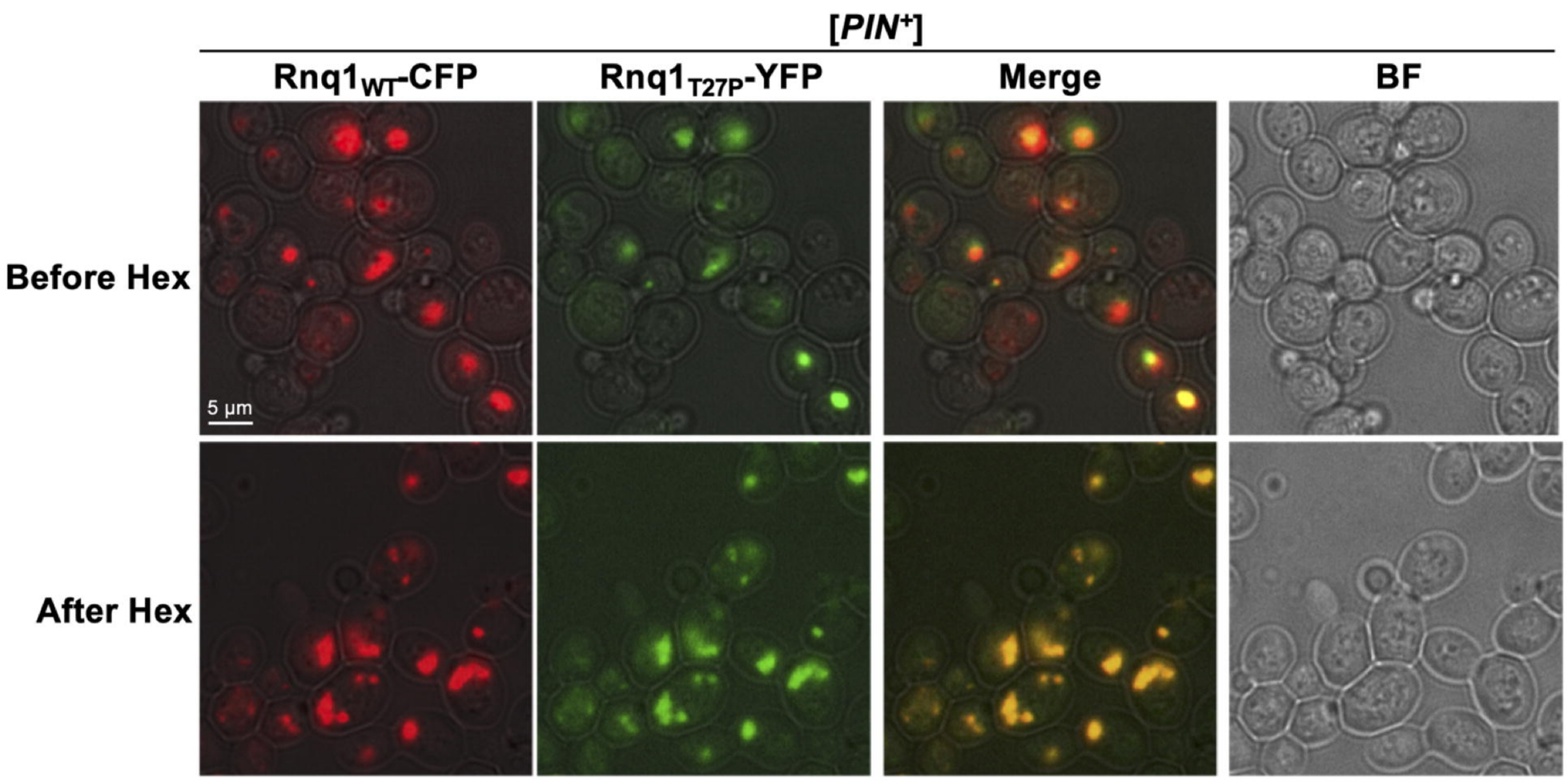
[PIN+]
Rnq1WT-CFP
Rnq1T27P-YFP
Merge
BF
Before Hex
After Hex
5 µm

B

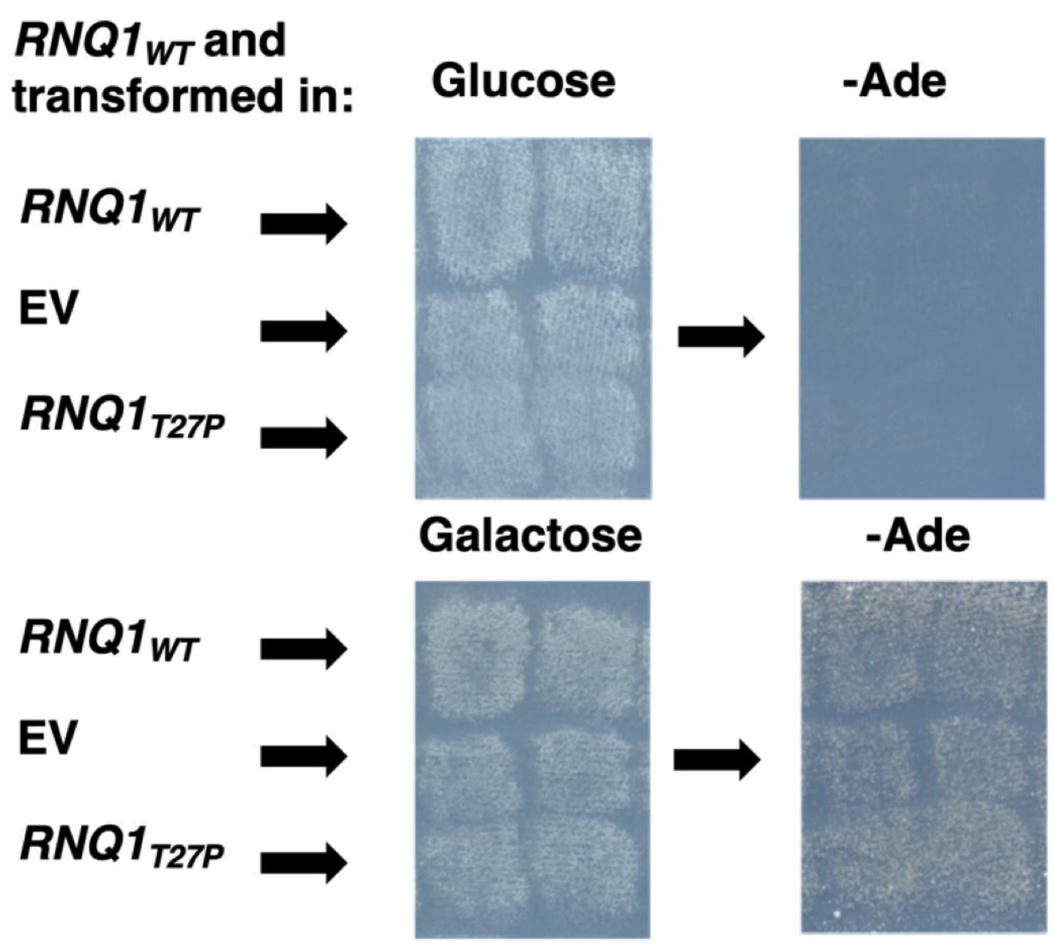
RNQ1WT and transformed in:
Glucose
-Ade
RNQ1WT
EV
RNQ1T27P
Galactose
-Ade
RNQ1WT
EV
RNQ1T27P

Figure 7

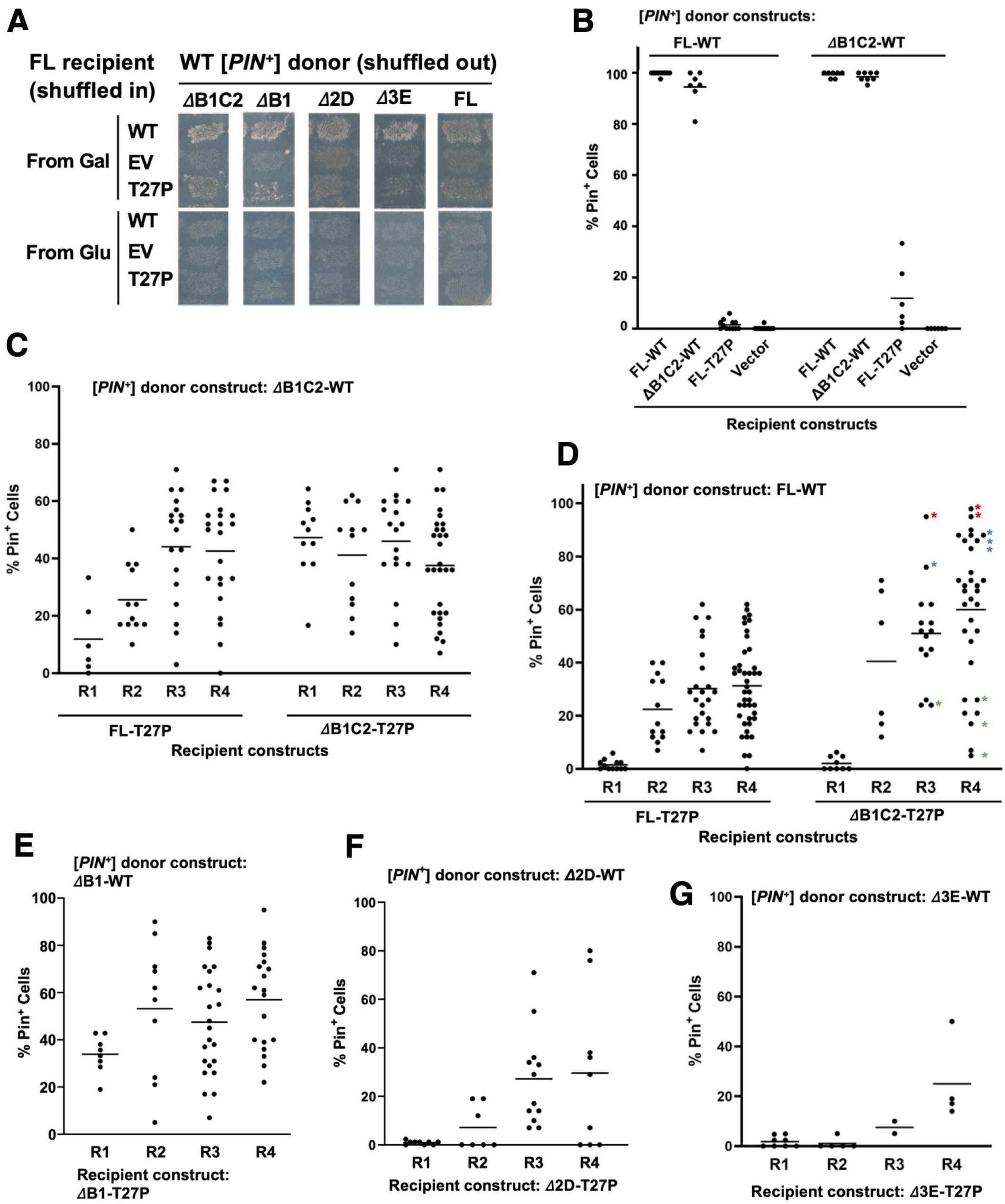
A
FL recipient (shuffled in)
WT [PIN+] donor (shuffled out)
ΔB1C2
ΔB1
Δ2D
Δ3E
FL
From Gal
WT
EV
T27P
From Glu
WT
EV
T27P
B
[PIN+] donor constructs:
FL-WT
ΔB1C2-WT
% Pin+ Cells
FL-WT
ΔB1C2-WT
FL-T27P
Vector
Recipient constructs
C
[PIN+] donor construct: ΔB1C2-WT
% Pin+ Cells
R1
R2
R3
R4
FL-T27P
ΔB1C2-T27P
Recipient constructs
D
[PIN+] donor construct: FL-WT
% Pin+ Cells
FL-T27P
ΔB1C2-T27P
Recipient constructs
E
[PIN+] donor construct: ΔB1-WT
% Pin+ Cells
Recipient construct: ΔB1-T27P
F
[PIN+] donor construct: Δ2D-WT
% Pin+ Cells
Recipient construct: Δ2D-T27P
G
[PIN+] donor construct: Δ3E-WT
% Pin+ Cells
Recipient construct: Δ3E-T27P

Figure 8

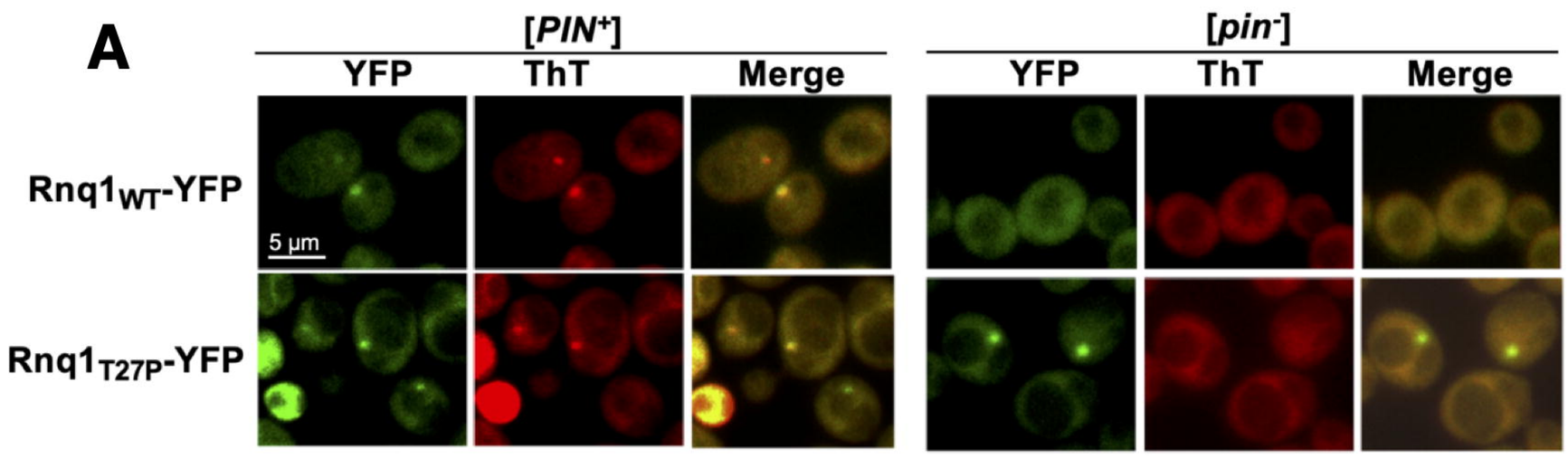
A
[PIN+]
[pin-]
YFP
ThT
Merge
YFP
ThT
Merge
Rnq1WT-YFP
Rnq1T27P-YFP
5 µm

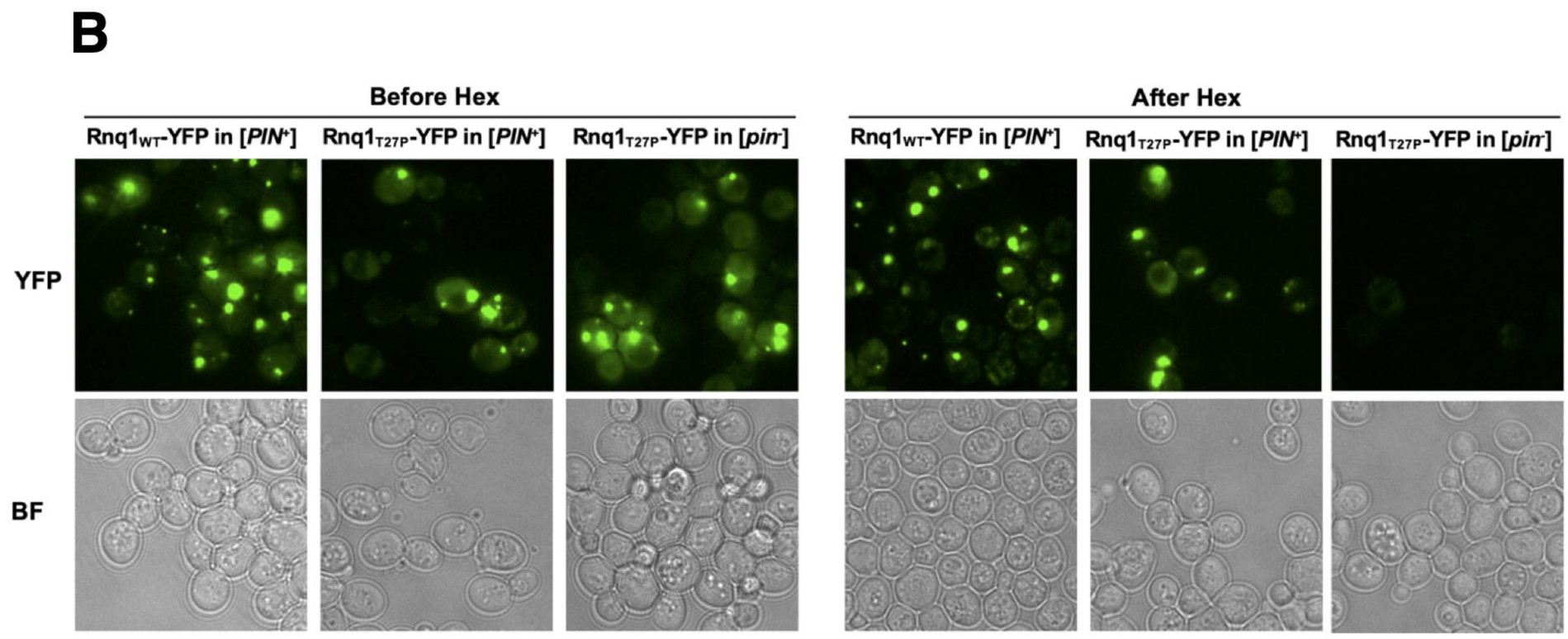
B
Before Hex
After Hex
Rnq1WT-YFP in [PIN+]
Rnq1T27P-YFP in [PIN+]
Rnq1T27P-YFP in [pin-]
Rnq1WT-YFP in [PIN+]
Rnq1T27P-YFP in [PIN+]
Rnq1T27P-YFP in [pin-]
YFP
BF

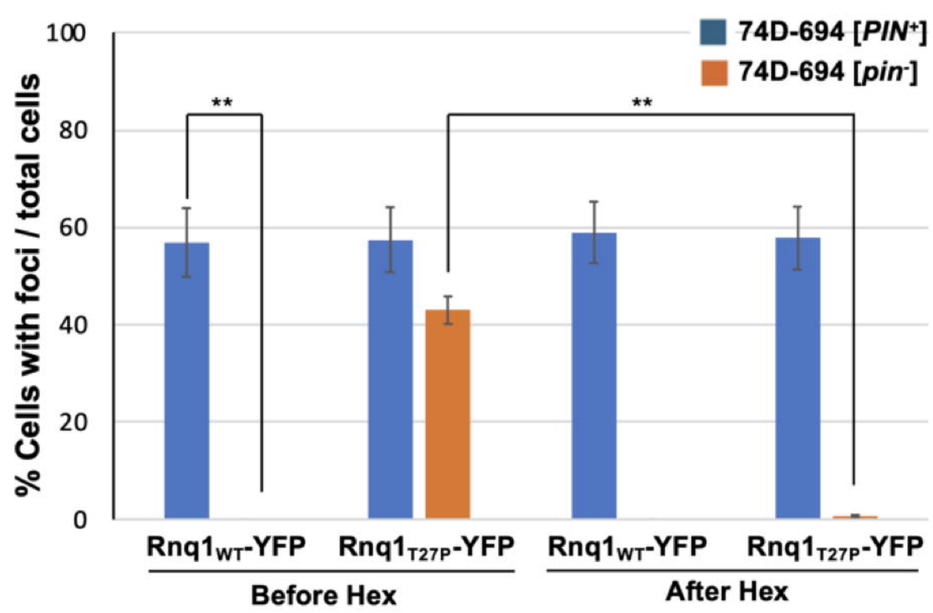
C
74D-694 [PIN+]
74D-694 [pin-]
% Cells with foci / total cells
100
80
60
40
20
0
**
**
Rnq1WT-YFP
Rnq1T27P-YFP
Rnq1WT-YFP
Rnq1T27P-YFP
Before Hex
After Hex

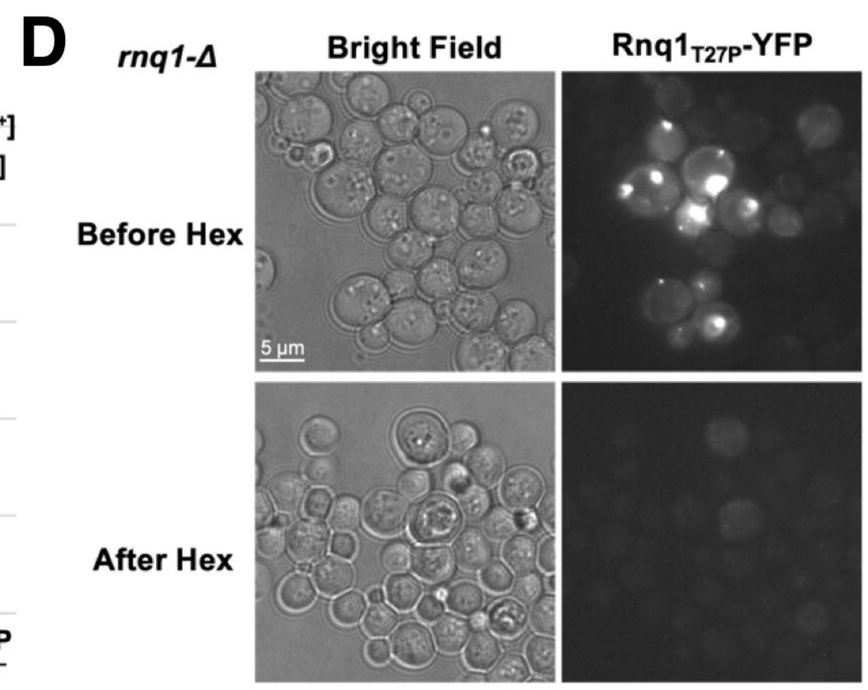
D
rnq1-Δ
Bright Field
Rnq1T27P-YFP
Before Hex
After Hex
5 µm

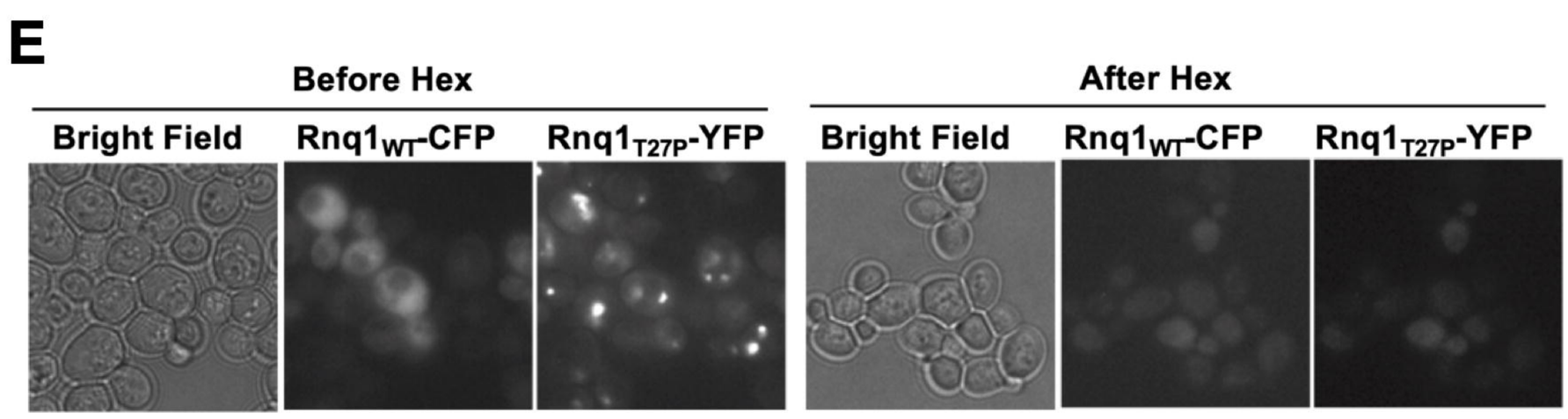
E
Before Hex
After Hex
Bright Field
Rnq1WT-CFP
Rnq1T27P-YFP
Bright Field
Rnq1WT-CFP
Rnq1T27P-YFP

Figure 9

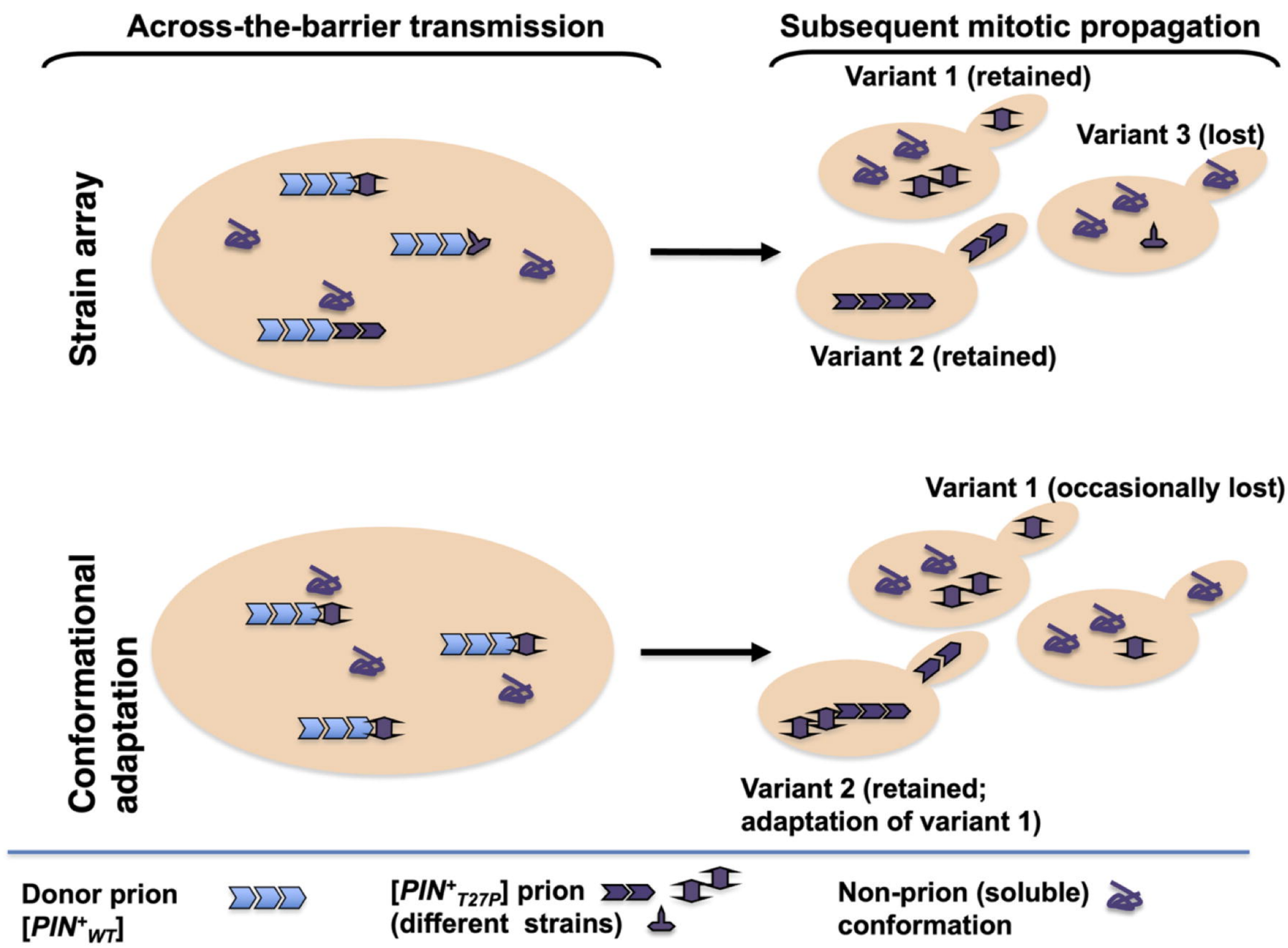
Across-the-barrier transmission
Subsequent mitotic propagation
Strain array
Variant 1 (retained)
Variant 3 (lost)
Variant 2 (retained)
Conformational adaptation
Variant 1 (occasionally lost)
Variant 2 (retained; adaptation of variant 1)
Donor prion [PIN+WT]
[PIN+T27P] prion (different strains)
Non-prion (soluble) conformation